Department of Human Biology
Division of Biomedical Engineering
University of Cape Town

A Novel Cough Aerosol Sampling Device for Sputum-Scarce Individuals with Tuberculosis

by

Ra'eesah Ismail
ISMRAE003

SUBMITTED TO THE UNIVERSITY OF CAPE TOWN
In Fulfilment of the requirements for the Degree:
MSc Biomedical Engineering by Dissertation

Faculty of Health Sciences
UNIVERSITY OF CAPE TOWN

February 10, 2025

Supervisors: Professor Sudesh Sivarasu &
Professor Keertan Dheda

Declaration

I, Ra'eesah Ismail, hereby declare that the work on which this dissertation is based is my original work (except where acknowledgements indicate otherwise) and that neither the whole work nor any part of it has been, is being, or is to be submitted for another degree in this or any other university.

I empower the university to reproduce for the purpose of research either the whole or any portion of the contents in any manner whatsoever.

Name: Ra'eesah Ismail

Signature: Signed by candidate

Date: 15 November 2023

Acknowledgements

In the Name of the Most High, the Most Merciful, without Whom nothing is possible,

They say it takes a village, and I couldn't agree more.

This thesis belongs to each and every mentor, colleague, relative and friend who has supported me in this long journey. There were many days which were not easy, and I would like to thank all of you for the words of encouragement, affirmation, technical advice and shoulder to cry on. Thank you to the NRF-DAAD for accepting me into the program & enabling this research.

Specifically, I would like to thank my supervisor, Prof. Sudesh Sivarasu. It has been an absolute honor working in your lab, I have learnt so much. No doubt, your no-nonsense approach to this work has been challenging. Without it, I would not have achieved half as much as we have. Thank you for teaching me invaluable lessons. Most importantly, thank you for showing me my strengths, albeit through a notorious backhanded compliment. Your support, guidance and mentorship mean so much.

To Prof. Keertan Dheda, thank you for your advice and passion for this research. Your ideas and experience truly shaped the vision of this project. Thank you for believing in my ability to make it a reality.

To Dr. Shameem Jaumdally, you have been an integral part of this research from its inception, seeing it through until the very end. I cannot thank you enough for all your guidance and the hours spent testing (and re-testing). Your enthusiasm and determination towards this work has allowed me to believe that we could conquer it. Thank you for everything.

To the incredible team at Centro Piaggio especially Prof. di Maria and Dr. Montemurro – thank you for your engaged insight and guidance. *Grazie Mille* for your perseverance in electrospinning in the heart of an Italian Summer, not an easy feat.

Mom, without you none of this would be possible. You push me to never give up and you do everything in your power to ensure I can achieve what I set my mind to. You are both the carrot and the stick – exactly what I needed when this task seemed insurmountable. Thank you for the nights with lots of tea and coffee but no sleep. I can never repay you.

Dad, thank you for being there for me no matter what, for always allowing me an escape route, knowing full well that I would never take it. You always know to say exactly what I need to hear. Thank you for your advice and enthusiasm towards this work.

Taareeq, you are my biggest cheerleader and I thank you for constantly reminding me who I am. I believe I can do anything, because you believe I can. Thank you for helping to build this device (literally). It is as much yours as it is mine.

To my Dada, who taught me the value of education. I wish that you could have read this. Thank you for your investment in my studies, talking to you about this project led me to many technical breakthroughs. You were one of the most intelligent people I was blessed to know.

To the rest of my family, you have walked this path with me from the very beginning. Your contributions to this degree are invaluable. Your motivation, confidence and support has pushed me more than you know. I truly hope that I can make you proud.

To my colleagues and friends who have been there for the writing dates, brainstorming sessions, listening to complaints, procrastination coffee, video calls while I write and removing supports off prototypes at 2am. I am so lucky to have you. Thank you.

Abstract

Introduction In 2021, there were 10.6 million tuberculosis cases worldwide, with 1.6 million deaths. Bacterial infection occurs when aerosol droplets enter the respiratory tract and travel to the lungs, causing pulmonary disease. If untreated, the disease has a 50% mortality rate. TB diagnostics require a sputum sample to conduct tests to confirm the presence of *M.tb* but more than 15% of patients have difficulty producing this sample. A cough aerosol sampling system (CASS) can collect aerosol droplet samples for testing when sputum sampling is not possible. These systems rely on inertial impaction whereby particles are sorted based on their diameter. Thus, CASS also offers information regarding the infectivity of the patient based on their expelled aerosol sizes. This is because smaller respiratory droplets can travel to the smallest structures of the lung and are more likely to cause infection. CASS is a useful technology in field sampling in place of sputum sampling. However current systems are bulky, heavy and not optimised for field testing in resource limited settings – which this project aims to address.

Methods & Materials The methodology included designing and developing a physical prototype of a novel miniaturised cough aerosol sampling system (Mini CASS). This device was designed in subsystems, namely the impaction cascade, pump system, mask part and casing. All subsystems followed a rapid prototyping approach characterised by multiple design iterations. The impaction cascade design was guided by Marple and Liu's methodology (1976). This included testing various impaction substrates. Furthermore, it was optimised by computational fluid dynamics. The entire design was evaluated against a set of predefined needs criteria developed through identification of inadequacies in current devices. Verification testing at the Medical Devices Lab (University of Cape Town) included confirmation of the aerosol size fractionation capacity of the cascade impactor. Validation testing was conducted at the Centre for Lung Infection and Immunity (Groote Schuur Hospital) to confirm the ability of Mini CASS to collect culturable bioaerosols (*M. smegmatis*).

Results & Discussion A partially disposable, portable and miniaturised CASS was built with a weight and size of less than 1 kg & 40 cm^2 respectively. Results of *in-silico* and verification testing have confirmed the ability of the device to perform size fractionation with at least a 30% efficiency per stage. The device successfully collected nebulised *M. smegmatis* & *M. bovis*. Culture confirmation of the bacteria proves this as a viable impactor with at least 3 colony forming units on each stage, comparable to current CASS systems.

Conclusion The final Mini CASS prototype exhibited favourable characteristics of being lightweight and easily portable. It fared well in tests conducted to assess viability, proving its capability to collect bioaerosol samples for culture from coughing. It exhibited the ability to fractionate aerosol samples to provide a semi-quantitative measure of infectiousness with known particle sizes and efficiencies. This proof-of-concept device shows CASS technology can be optimised for use in the clinical setting, thereby enabling it to become a more powerful sampling and research tool. The lightweight, easy to use technology has the potential for use at home or temporary sampling sites.

Contents

List of Figures

List of Tables

List of Acronyms

AC	Alternating Current
BCG	Bacillus Calmette-Guérin
CAD	Computer Aided Design
CASS	Cough Aerosol Sampling System
CFD	Computational Fluid Dynamics
CFM	Cubic feet per minute
CLII	Centre for Lung Infection & Immunity
DC	Direct Current
FDM	Fused Deposition Modelling
FMEA	Failure Modes and Effects Analysis
GEP	Good Engineering Practice
HBC	High Burden Country
HIV	Human Immunodeficiency Virus
IGRA	Interferon Gamma Release Assay
IGRA	Interferon Gamma Release Assay
LPM	Litres per minute
M. smegmatis	*Mycobacterium smegmatis*
M.tb	*Mycobacterium tuberculosis*
MDI	Metered Dose Inhaler
MDI	Metered Dose Inhaler
NAAT	Nucleic Acid Amplification Test
NSP	Nozzle Spacing Parameter
PAA	Poly Acrylic Acid
PCR	Polymerase Chain Reaction
PLA	Polylactic Acid
PoI	Patient of Interest
PSD	Particle Size Distribution
PVA	Polyvinyl Alcohol
RMD	Rapid Molecular Diagnostics
RPM	Revolutions per minute
SSM	Sputum Smear Microscopy
TB	Tuberculosis
TST	Tuberculin Skin Test
UCT	University of Cape Town
ZN	Ziehl-Neelsen

Symbols and Units

A	Amperes
C	Cunningham slip correction factor
D_{50}	Diameter with 50% collection efficiency
E	Collection efficiency
Re	Reynolds number
Stk	Stokes number
V	Volts
V_0	Average nozzle exit velocity
Q	Volumetric flowrate
μ	Micron
σ	Standard deviation
ρ	Density

1 Introduction

1.1 Background to study

In 2021, there were approximately 10.6 million TB cases worldwide, with 1.6 million deaths. Two thirds of these global TB cases are found in high burden countries (HBCs) of which South Africa is one. The country accounts for almost 3% of TB cases worldwide (South African Department of Health, 2023). The incidence rate in SA in 2018 was 737 positive TB cases in every 100 000 people (Ayles et al., 2022).

Tuberculosis is a bacterial illness caused by infection by *Mycobacterium tuberculosis (M.tb)*. The disease is transmitted via the air by means of droplet nuclei which contain the mycobacteria. Infection occurs when these droplets enter and travel down the respiratory tract to reach the lungs, causing pulmonary disease. The disease can spread to other body parts causing extrapulmonary TB, such as the brain, kidneys and spine (Sakundarno et al., 2009). TB is preventable via vaccination and can be treated with antibiotics. However, if untreated, the disease has a 50% mortality rate (Bagcchi, 2023).

Tuberculosis diagnostics includes acquiring sputum samples and conducting tests to confirm the presence of *M.tb* This is the gold standard of diagnosis in developing countries. However, more than 15% of patients have difficulty producing a sputum sample (Sakundarno et al., 2009). People with Human Immunodeficiency Virus (HIV) specifically have trouble producing the adequate sputum sample volume of 1 ml. Almost 60% of all TB-infected individuals in SA in 2018 were co-infected with HIV (Ayles et al., 2022).

In such circumstances where an adequate sputum sample cannot be acquired, a cough aerosol sampling system (CASS) can be used. These devices collect bioaerosol samples for diagnostic testing. This form of sampling can also offer information regarding the infectivity of the patient based on the aerosol sizes. The basis of this is that smaller respiratory droplets can flow easily into the alveoli, the smallest structures of the lung (Jones-López et al., 2013). This quality could provide insight into people who may be highly infectious, informing where community testing should be concentrated.

However, CASS technology requires bulky and heavy machinery such as a cascade impactor, drum a vacuum pump. This renders the procedure more complicated than the collection of a sputum sample (Fennelly et al., 2004). This technology has not been designed or optimised for a clinical and low-resource settings, hindering its potential for use in the sample acquisition environment.

1.2 Project Rationale

CASS technology could be optimised for use in low-resource setting and mass sampling in order to overcome the limitations of sputum sampling. This project seeks to develop such a device which could be used by patients who are suspected to have TB, especially those who struggle to expel sputum.

Using the heuristics of cascade impaction based on inertial settling (Marple & Liu, 1974) and previous experiments conducted on infectivity (Fennelly, 2020) a more suitable CASS could be designed. This technology could be a stepping stone towards a simpler and more comfortable sampling process for TB in clinics. Furthermore, it could be a beneficial tool in terms of identifying TB hotspots in communities, especially in countries with high incidence of the disease. Thus, enabling concerned parties to pinpoint where testing should occur next, and subsequently increasing the chances of community case finding. Lastly, it could aid in understanding the epidemiological characteristics of TB by coupling infectivity with physical symptoms, geography and socio-economic conditions.

1.3 Research Question

The research question posed for this study is:

"Can a miniaturised cough aerosol sampling device be designed, optimised and tested to collect & size fractionate aerosol samples from sputum-scarce tuberculosis patients for diagnosis?"

1.4 Aim

The aim of this project is thus to design, develop and test a miniaturised cough aerosol sampling system (Mini CASS) which can collect & size fractionate bioaerosols for diagnostic applications.

1.5 Objectives

1. To develop a miniaturised cough aerosol sampling system that is portable & partly disposable for *M.tb* sample collection purposes.
2. To optimise the Mini CASS device designs by utilising computational fluid dynamics & evaluating various substrates for particle collection.
3. To test if the device successfully fractionates particles into two distinct size ranges reflecting greater & lesser degrees of infectivity.
4. To test if the device can collect viable and culturable mycobacteria. Furthermore, to compare the efficiency of this device against that of current CASS technology.

1.6 Project Scope & Limitations

The scope of this project included the design, development and testing of a cascade impaction device and the ancillary equipment required. The final prototype is a proof-of-concept device. Tests were conducted *in silico* and *in vitro*. The design and testing utilised equipment available at the medical devices lab at UCT (Division of Biomedical Engineering), Centre for Lung Infection and Immunity (UCT) and Centro E. Piaggio (Department of Information Engineering, University of Pisa). The device was not manufactured in a facility with a South African Health Products Regulatory Authority (SAHPRA) medical device establishment licence. As such, human trials were not conducted as part of the validation for the outcomes of this study.

1.7 Dissertation Overview

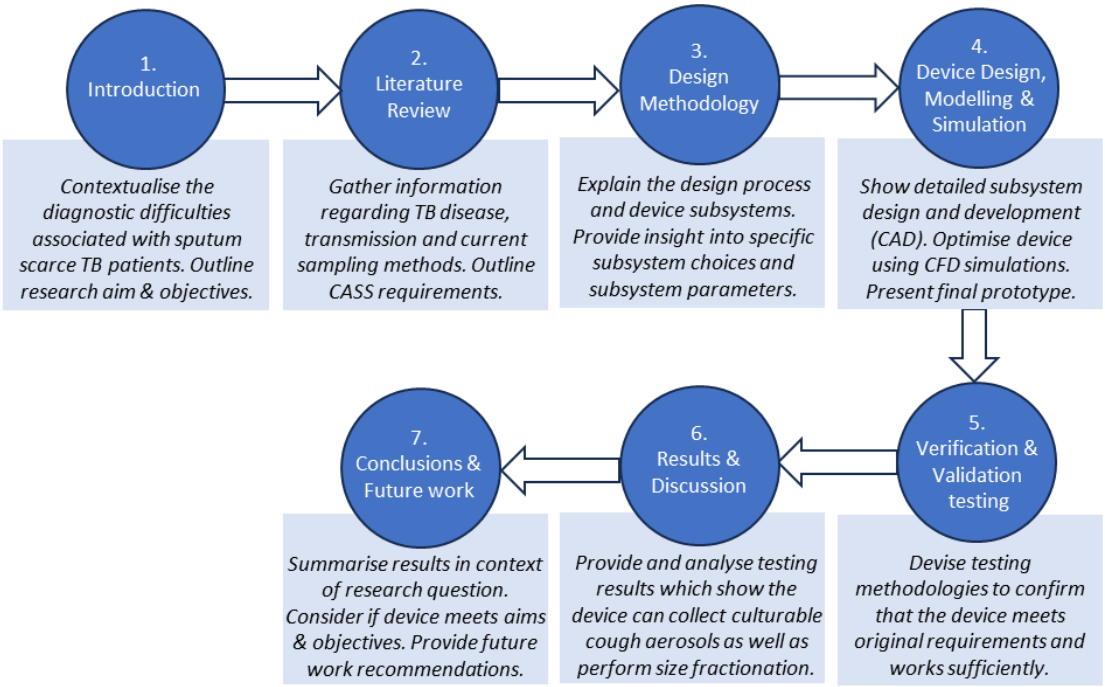

Figure 1-1: Dissertation Outline

2 Literature Review

2.1 Disease State Analysis

2.1.1 History of tuberculosis

The earliest documented cases of tuberculosis as known today were hypothesised to be 20 millennia ago in East Africa. However, the earliest instances can be traced back to remains found in Egypt only 5 centuries ago. The disease reached the western world only in the 19th century, which then saw itself in the throes of tuberculosis epidemics (Daniel, 2006). These epidemics resulted in approximately 900 fatalities per 100 000 in Europe and North America (Sakamoto, 2012).

In 1882, the bacteria that causes the disease was identified by Dr. Robert Koch as *Mycobacterium tuberculosis.* Koch postulated that tuberculosis (TB) was characterised by human-to-human transmission and that it could only be contracted through contact with a sick person or animal. These discoveries informed efforts to eradicate tuberculosis disease. As a result of the finding, the tuberculin skin test was developed by Charles Mantoux in 1910. This test uses a subdermal reaction to diagnose the latent case of the infection, it is still used today in many countries (Cambau & Drancourt, 2014). Shortly after this development in 1920 the far less virulent subculture of *M.tb* was discovered, *Mycobacterium bovis*. Subsequently, *M. bovis* was developed into a successful vaccine by 1924. It is dubbed Bacille Calmette Guerin, after the scientists who discovered it, Leon Charles Albert Calmette and Camille Guerin.

The next 30 years saw tuberculosis disease rates radically decline in the western world as a result of mass vaccination campaigns (Sakula, 1983). Today, the BCG vaccine is more commonly used in developing countries who still suffer from a major burden of TB. TB disease rates remained high towards the end of the 20th century. It is also an opportunistic infection, resulting in increased risk of infection in people with weakened immune systems. This means that people living with Human Immunodeficiency Virus (HIV) are particularly susceptible. Thus, as the HIV pandemic raged on so did TB. There were 10 million infections worldwide by 2018, but mortality rates had declined by 42% from 2000 (WHO, 2019).

Before COVID-19, tuberculosis was named the leading cause of death from a single infectious agent in the modern world (WHO, 2019). Many countries noted a significant impact of the coronavirus pandemic on healthcare services as well as the reduction in availability of TB services. As a result, reported incidences of TB declined by 18%. This can be attributed to mass underreporting and missed diagnoses due to interruptions in public health surveillance efforts focused on TB (Falzon et al., 2023).

Consequently, the post-pandemic era has seen a rise in cases, undoing years of work towards eradicating the disease. The number of people living with TB worldwide rose from 10.1 million in 2020 to 10.6

million in 2021. New instances of the disease per 100 000 also increased by 3.6%, in contrast to the reassuring 2% decline which was experienced for much of the past 20 years. Approximately 10 million people contract TB worldwide annually, which results in 1.5 million fatalities (WHO, 2022). The number of infections per year has been rising since 2021. According to the World Health Organization, TB has most likely once again become the infectious disease with most fatalities worldwide since the decline of the Coronavirus pandemic (WHO, 2024)

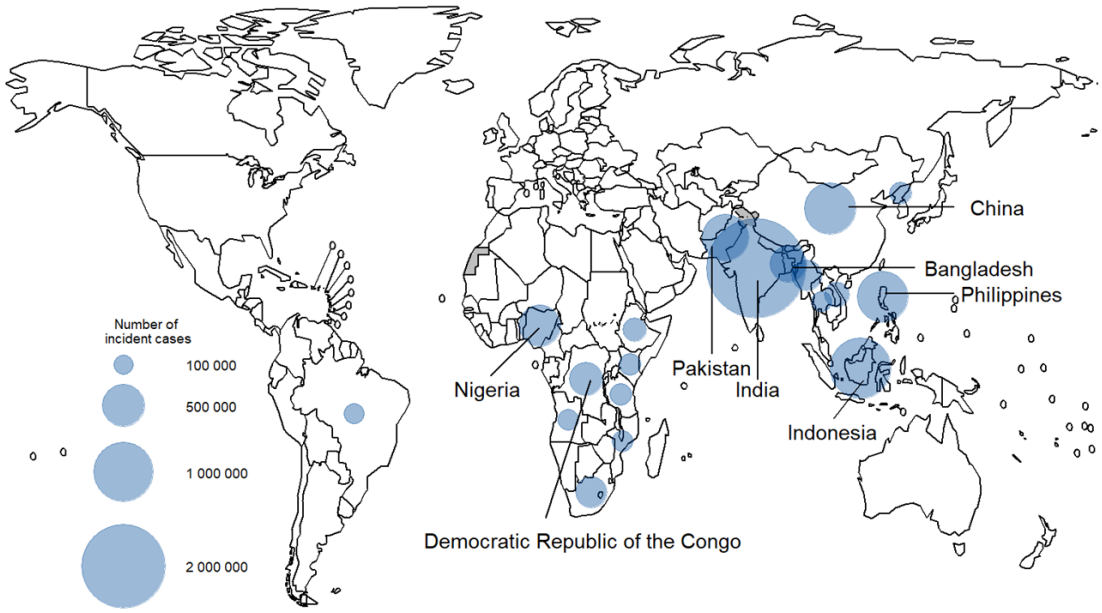

Figure 2-1: Estimated TB incidence in 2022 (WHO, 2023)

The disproportionate distribution of infection is also key to understanding the dynamics of the global TB pandemic. Figure 2-1 refers to the number of new occurrences of TB in countries with more than 100 000 incident cases (WHO, 2023). More than two thirds of all new active tuberculosis cases in the world are found in 8 high burden countries (HBCs). These countries include India, Indonesia, China, the Philippines, Pakistan, Nigeria, Bangladesh and the Democratic Republic of the Congo (DRC). South Africa was part of this group in 2021 but has subsequently been removed. It is still considered in the 30 countries contributing to more than 80% of cases worldwide (WHO, 2023 & WHO, 2021).

South Africa suffers from a staggering number of infections. According to the first national TB prevalence survey completed in 2018, the country accounted for 3% of all active infections, around the globe. Approximately 450 000 people in SA contract active TB yearly, with fatal outcomes standing at 89 000. The South African context is also characterised by high incidence rates of HIV infection, approximately 7.7 million cases in a population of 59 million (Akullian et al., 2021). Subsequently, two thirds of tuberculosis patients in SA are living with HIV (Ayles et al., 2022). South Africa is therefore an HBC & on the WHO's global TB watchlist, firstly for having some of the highest number of active

TB cases per capita. Secondly, for the rates of HIV & TB coinfection and thirdly for the prevalence of Multidrug- or Rifampicin-Resistant TB (MDR/RR-TB) in the country as shown in Figure 2-2.

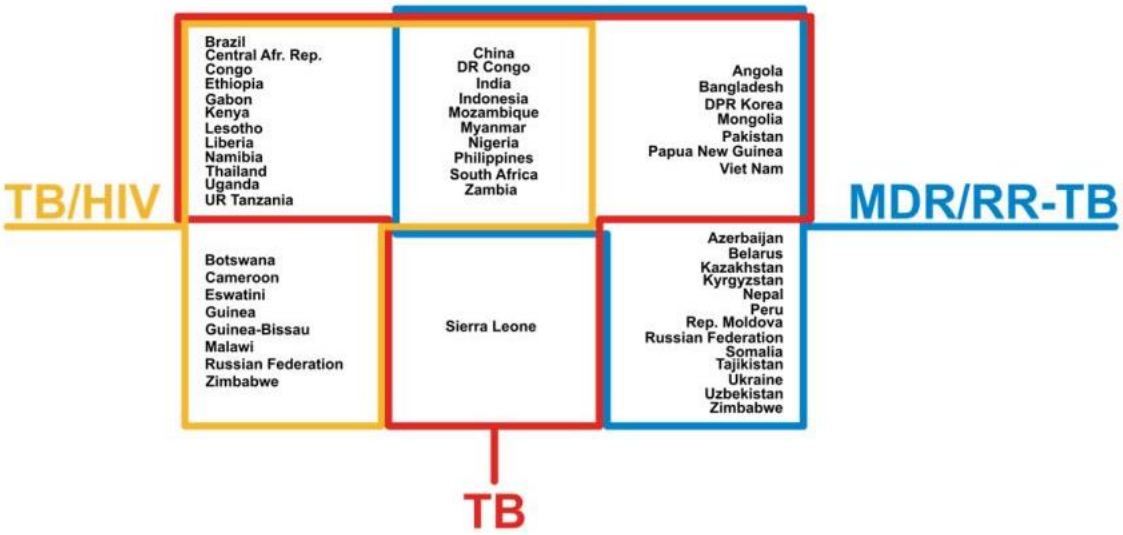

Figure 2-2: Global HBC lists for TB, TB/HIV & MDR/RR-TB for 2021-2025 (WHO, 2022)

2.1.2 Disease State

Tuberculosis disease exists in two states, namely 'latent' and 'active'. The former case is constituted by infection with *Mycobacterium tuberculosis*, called latent tuberculosis infection or LTBI (Bussi & Gutierrez, 2019). People who contract LTBI do not experience any clinical symptoms of tuberculosis. Furthermore, no radiological or microbiological evidence of the disease is present in these cases. About one third of the world's population is infected by LTBI. Approximately 5% of LTBI cases advance into the active disease (Lee, 2016).

The risk of acquiring the active disease from latent infection is increased for people with compromised immune systems such as those living with HIV or diabetes. Socio-economic factors such as lack of nutrition and substance abuse also contribute to susceptibility (Centre for Disease Control, 2019). The disease progression to MDR/RR-TB can be seen a consequence of poverty and limited availability of treatment as well as non-compliance to medications (Alsayed & Gunosewoyo, 2023).

When the disease primarily affects the lungs, it is known as pulmonary TB. Symptoms include chest pain, coughing, night sweats and shortness of breath. Other forms of TB manifest in the kidneys, bones, brain and lymphatic fluid – these are known as extrapulmonary TB (Storla et al., 2008). The disease can be prevented by vaccination. It is curable with antibiotics but without treatment has a mortality rate of 50% (World Health Organisation, 2022). Patients can have subclinical or clinical TB, whereby the former state refers to a disease manifestation with no clinical symptoms (Teo et al., 2024).

2.1.3 Mechanism of TB infection

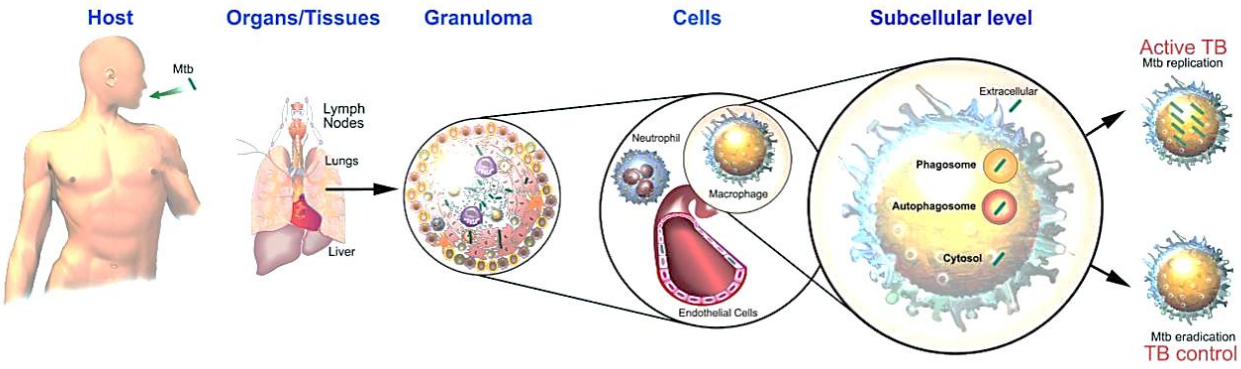

Figure 2-3: Infection of Host by Mycobacterium tuberculosis (Bussi & Gutierrez, 2019)

For infection to occur there must be a bacterial source. In the case of community transmission this would be an infected person. The infected person must have active tuberculosis and expel infectious droplets from their respiratory system to actually transmit the disease. *M.tb* is aerosolised via coughing or sneezing as infectious particles called droplet nuclei. The aerosol droplets consist of *M.tb* in sputum covered by a layer of phlegm. The actual bacillus has a typical length of between 2 and 4µm, with a width between 0.2 and 0.5µm. The droplet nuclei may contain one or more organisms (Wurie et al., 2016).

These droplet nuclei will either stay suspended in the air for some time or enter the oral or nasal cavities of a healthy individual via inhalation. Other entry sites include mucosal membranes, damaged dermal layers and the digestive system (Maison, 2022). The particles will travel through the upper to the lower respiratory tract. If the aerosolised particles are small enough, the droplets can travel through the lungs into alveolar sacs (Bussi & Gutierrez, 2019).

As an immune response, the body generates an organised structure including - but not limited to - macrophages, epithelial cells and lymphocytes around the rod-shaped bacteria. This structure is known as a granuloma. It is used as a defence against infection but is not always effective against *M.tb*, which survives within its walls. The bacteria can lay dormant indefinitely, with reactivation occurring in less than 10% of cases. While the exact cause is not always known, reactivation is often spurred on by events of immunodepression (Silva Miranda et al., 2012).

Once active, the bacteria will break free from the granuloma and disseminate into the cytosol. At this point, the patient has developed active pulmonary TB. Thereafter, it can spread to other parts of the body and become extrapulmonary. The body will employ many other defence strategies on both the immunological and cellular levels to control the infection. If unsuccessful against the bacteria's evasion mechanisms, bacterial replication will occur, and the disease will progress (Bussi & Gutierrez, 2019).

2.2 Transmission & Infectiousness

2.2.1 Transmission

As stated previously, transmission can occur when an infected individual coughs, sneezes or sings in the proximity of a susceptible person. The bacteria which were present in the lungs of the sick person are transferred to the healthy individual via inhalation as shown in Figure 2-4. Exposure to the infectious agent will result in latent infection or the active form of the disease. This can end in recovery, sickness, or in some cases fatality (van Seventer & Hochberg, 2017).

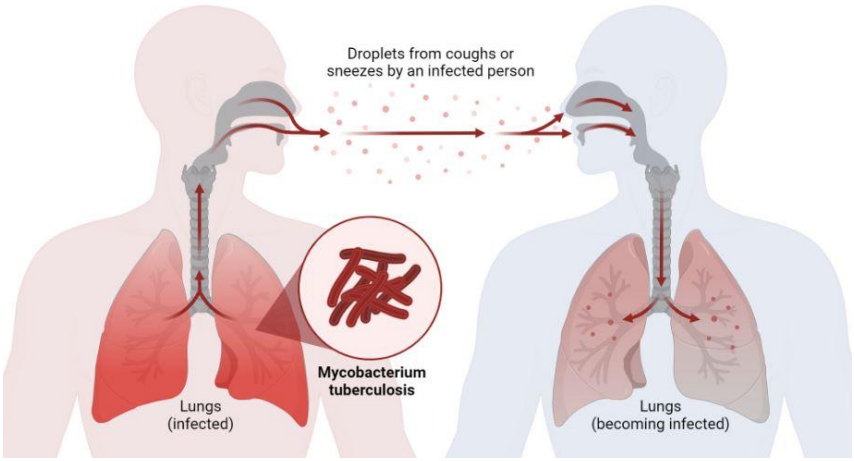

Figure 2-4: TB Transmission through Coughing/Sneezing (BioRender, 2022)

Three main factors influence the likelihood of disease transmission from infected to uninfected individuals (Centre for Disease Control, 2019):

1) Contact time
2) Frequency of contact
3) Proximity

While the initial assumption for the disease was that of homogenous transmission, studies have shown that this is not the case. It is known that a disproportionality exists in which a small group of individuals transmit the disease to many healthy individuals. An empirical 20/80 rule has been adopted when describing many communicable diseases, including TB – this assumes that 80% of secondary infections are caused by 20% of a primary infected population. These instances are referred to as 'super-spreader' events (Stein, 2011).

With regards to TB, some studies have shown that as little as 8% of community infections were transmitted within households. While these contacts sometimes account for as much as 20% of transmission, non-repeated contacts can account for almost 80% of infections (McCreesh & White, 2018).

Unpredictable transmission patterns mean a complex landscape with regards to targeted contact tracing. It is understood that contact tracing in households and repeated contacts provides little value when identifying infections in a community setting. (Melsew et al., 2019). Thus, focus on transmission heterogeneity and super-spreader events is required to increase chances of detecting TB cases in a community

Practically speaking, identifying potential super-spreaders and pooling resources around contact tracing could be of immense value. In this way, the detection capability of tuberculosis transmission within communities could increase. To accomplish this, the mechanisms of super-spreading events need to be detailed. At present the reason for this is not well understood. However, super-spreaders can be characterised by having a high level or long period of infectiousness. The second characteristic is having many contacts. With regards to the former characteristic, there is a 'critical' need for a means to identify superspreaders (McCreesh & White, 2018). This enlists the design and development of technologies which can provide information on how infectious a person is.

2.2.2 Characterising infectivity

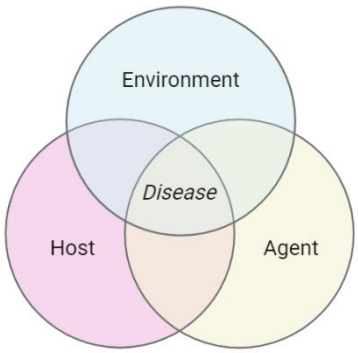

Figure 2-5: Epidemiological triad model for infectious disease causation (Adapted from Sniezko,1974)

The epidemiological triad of infectious disease causation (Figure 2-5) can be used to describe communicable diseases such as TB (Snieszko, 1974). This models infection as a relationship between three aspects. This includes an agent or pathogen which in this case is *Mycobacterium tuberculosis*. Secondly, a host which exhibits some degree of susceptibility. Susceptibility is the resistance towards the infection based on genetic makeup, previous exposure/vaccination status. The third aspect is the environment, which can differ in physical, social and cultural characteristics (van Seventer & Hochberg, 2017).

As described, transmission and epidemiological disease causation are both multi-faceted and complex as there are many aspects to consider during exposure to the agent. As a means of simplification, we can exploit a single parameter to better understand a specific part of the infection landscape. One such vital parameter in the context of this research is infectivity.

Infectivity is the likelihood of host infection following a host-agent interaction. In cases of highly communicable and respiratory diseases, certain physical characteristics may be used a measure of infectivity or infectiousness. Infectivity can be related to the quantity of aerosol droplets released in a coughing episode and the average diameter of these droplets (Melsew et al., 2019). It has also been deduced that the generation of culturable cough impacts from these droplets is a very good indicator of disease transmission ability (Fennelly, 2020). A single droplet on a plate is assumed to be one colony forming unit (CFU). Once the sample has been cultured, the number of CFU's on each stage can be counted. This provides a quantitative measure of how many infectious droplets a person expels, which can be compared to average readings for relative infectivity.

Differences in this transmissive capability can be largely accounted for by the characteristics of a patient's cough. Research shows that smaller droplets can reach the alveolar sacs of the lungs more easily, increasing the chances of pulmonary TB (Fennelly et al., 2004). Therefore, an infected individual who emits high volumes of smaller droplet nuclei is more infectious than someone emitting larger droplets. Literature shows that cough aerosols naturally emitted by people with TB are generally characterised by particle diameters between 0.65 and 10 microns (Fennelly, 2020).

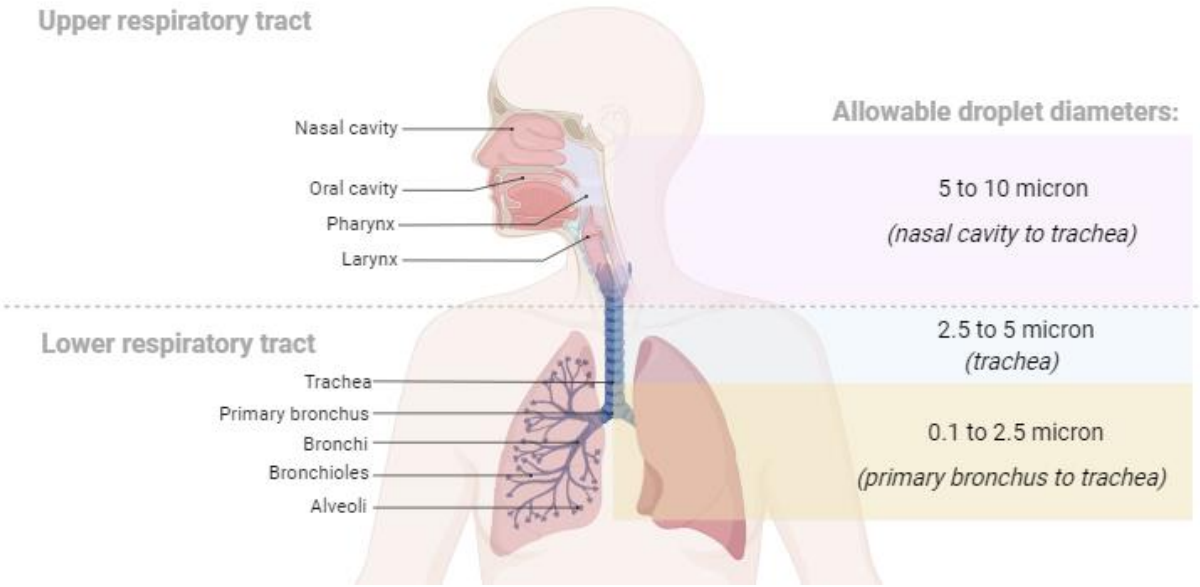

Figure 2-6: Allowable Droplet Diameters in Human Respiratory Tract (Adapted at Biorender.com from Guzman, 2021)

Figure 2-6 describes the allowable droplet diameters at various points in the respiratory tract. Particles between 10 and 5µm are less likely to enter the primary bronchus, meaning these particle sizes would describe a situation of lower infectivity. Particles with diameters between 2.5 and 5µm are representative of higher infectivity. The smallest emitted particles, between 0.1 and 2.5µm are thus the most likely to cause pulmonary TB. Literature also suggests that *Mycobacterium tuberculosis* is emitted at the highest

concentrations in the cough aerosol size range 2 - 3.5µm (Patterson et al., 2018). It should be considered that this bacterial load will also play a role in infectivity and that the minimum cough aerosol size is generally 0.65µm. Thus, the size range of highest infectivity can be adjusted to between 0.65 and 3.5µm.

2.2.3 Sampling Technologies

Sampling technology varies depending on the form of TB which is being tested. The latent form of tuberculosis is commonly diagnosed using a tuberculin skin test (TST) or interferon gamma release assays (IGRA). These are limited in that they do not provide information about active TB (Piccazzo et al., 2014). In South Africa, an estimated 84% of the population have latent TB (Adams et al., 2015). Hence, tests such as TST do not provide valuable information in countries where there is already a high burden of latent TB.

The diagnostic process for active TB is quite different and varies greatly depending on resource availability. A combination of tests can also be employed depending on specific patient characteristics. The gold standard for diagnosis is via culture confirmation (Chen et al., 2012). This requires a sputum sample to be acquired and prepared. Sputum is collected by requesting a patient to cough. A deep cough is required to ensure sufficient sample collection, which must originate from the lung and contains *M.tb* covered in phlegm.

This sputum sample can be used in sputum smear microscopy (SSM), a cost-effective method for TB testing (Sakundarno et al., 2009). Samples are prepared on glass slides and a Ziehl-Neelsen (ZN) stain is applied to them. Ziehl-Neelsen staining exploits the property of acid-fast bacteria (AFB) using a combination of stains and counterstains. From this, it can be discerned if the sample contains mycobacteria, which are acid-fast. ZN staining is utilised in developing countries due to its rapidity and practicality (Chen et al., 2012). For sputum, cultures of the sample are also prepared to confirm infection and antibiotic resistance which can take up to 6 weeks (Pfyffer & Wittwer, 2012).

A serological sample can be acquired and tested relatively easily but results in false negatives often due to high variability. On the other hand, sputum samples can be used for Nucleic-Acid Amplification Testing or Rapid Polymerase Chain Reaction (rPCR) is used to test for the presence of *M.tb* genetic material. This method takes only a couple of hours and exhibits high sensitivity but proves costly for widescale use in low resource settings (Mugenyi et al., 2024). Furthermore, chest x-rays are often used as a diagnostic tool in addition to other methods (Van Cleeff et al., 2005).

All sampling & diagnostic methods considered, sputum collection remains the suggested diagnostic protocol in most high burden countries, including South Africa (South African Department of Health, 2023). However, sputum sample collection proves difficult for clinicians, especially when patients are coinfected with HIV. In such cases, it is estimated that 1 of 2 cases TB cases are either people who are smear-negative or sputum-scarce. Previous studies have shown that more than 15% of patients are unable to produce the 1 ml of viable sputum required to perform SSM. This inability can hinder

treatment and diagnosis, increasing the morbidity and fatality rates (Peter et al., 2014). Consequently, more than 1.5 million people worldwide are left without access to efficient diagnostic procedure. This begs the question, what can be done when viable sputum samples cannot be produced?

One such solution is cough aerosol sampling, which utilises the infectious droplet nuclei expelled by patients on natural coughing. This sample is collected simply and non-invasively. It has been proven as an efficient detection method for tuberculosis-causing mycobacteria. Bioaerosols can be easily collected in clinics and show promise specifically in low resource settings (Williams et al., 2020).

Various sampling & diagnostic methods are employed, including modified face masks compatible with Xpert (Cepheid, Sunnyvale, Ca, USA) MTB/RIF testing. Longitudinal studies of such technologies have shown to be at least four times more successful in detection than traditional sputum. This efficiency was also attributed to the ability to collect samples at more than one timepoint as opposed to a single incidence of sputum collection (Williams et al., 2020). These modified collection substrates, 3D-printed polyvinyl alcohol (PVA), are of special interest for use in rapid PCR but not necessarily for culture confirmation.

Bioaerosol sample collection is avidly being researched, with many experimental devices such as electrostatic precipitators and modified impingers. Electrostatic precipitation is a proven effective method but requires high voltages to operate. Furthermore, devices such as these are still in the experimental phase and have not been commercially rolled out (Rufino de Sousa et al., 2019). Some technologies such as impingers make use of catchment fluids and are fully mechanical. These are more suited to low resource settings as well. Bioaerosol captured using these methods is usually viable but they do not offer information on particle size grading (Patterson et al., 2020).

Another means to collect sputum droplets is the cough aerosol sampling system (CASS) using a cascade impaction system. This method is employed more popularly as a research tool to provide information on patient infectivity. These samples are culture compatible as they collected on agar. However, current CASS technology requires bulky machinery such as a metal cascade impactor, drum casing and an industrial vacuum pump. (Fennelly et al., 2004). This renders the procedure far more complicated than the collection of a sputum sample. Furthermore, this procedure and technology has not been adapted well to clinical settings considering the size and material of construction of the devices.

In terms of the compatible diagnostic method, CASS currently employed at various sites in Africa make use of agar as a collection medium, which limits the sample to being used solely for culture. Studies have shown that while culture is the gold standard for diagnostics, GeneXpert (Cepheid, Sunnyvale, Ca, USA) boasts a sensitivity of more than 90% for both metrics (Shah, 2016). As such, samples which are GeneXpert compatible could offer a competitive advantage over SSM considering the wait time and efficiency of the diagnostic test. This would combine the advantages of devices such as the modified face masks with that of CASS (Table 2-1).

Table 2-1: Current TB sampling methods

Sampling method	*Corresponding Diagnostic method*	*Advantages*	*Disadvantages*
Sputum Collection (Fennelly et al., 2012)	SSM, Culture, rPCR	Gold Standard	Not suitable for sputum-scarce patients
Blood (Brett & Humble, 1991)	TB BACTEC (Culture from blood)	Accuracy	Need to draw blood from patient
Tongue swab collection (Wang et al., 2025)	rPCR	Accuracy, easy acquisition	No information on infectiousness
Cough Aerosol Sampling System (Fennelly et al., 2012)	Culture	Sputum – scarce patients accounted for & infectivity	Bulky machinery, cannot use without technician
X- Ray	Physician	Quick results as per physician's prognosis	Time consuming for patients, mostly hospital based
Electrostatic Precipitator (de Sousa et al., 2020)	Culture	Efficient at bioaerosol collection	Non - commercial Expensive to manufacture
Impinger	Culture	Efficient	Liquid sample handling
Modified Face Masks (Williams et al., 2020)	rPCR,	Inexpensive, easy to use	Untested in patients with little to no symptoms. Threshold sample yield unknown.

Considering the current sampling landscape, CASS is the only method which has been used successfully in hospitals as a research tool for sputum collection *and* particle size fractionation (Fennelly, 2020). As such, the cascade impaction technology will be used as a basis for the design of a cough aerosol sampling system in this research.

2.3 Cough Aerosol Sampling Systems

2.3.1 Current systems

Current cough aerosol sampling systems are used mainly as research tools. These take the form of aerosol/bioaerosol sampling devices which may not necessarily be optimised for use as a medical device.

For instance, the CASS used at the Centre for Lung Infection and Immunity makes use of a cascade or Anderson impactor (Fennelly et al., 2004). These cascade impactor systems which are currently available are designed for use in the aerosol drug testing industry. These tests are carried out in very controlled environments with compatible fittings and equipment. Thus, the technologies which are available are not designed for the specific use of bioaerosol sampling in a hospital/clinic setting. Cascade impactors usually operate in the micron and submicron ranges. Cough sampling studies currently employ one or two Andersen cascade impactors arranged in parallel (Fennelly, 2020). Commercial impactors are available in 1, 2 or 6 stage conformations (Tisch Environmental Inc., Cleves, OH, USA).

These current systems are made up of stainless-steel cascade impactor plates interspaced with petri dishes, a stainless-steel drum, industrial vacuum pump and ancillary piping. An example of this setup is shown in Figure 2-7. As shown, the complete device is bulky, difficult to transport and awkward to use.

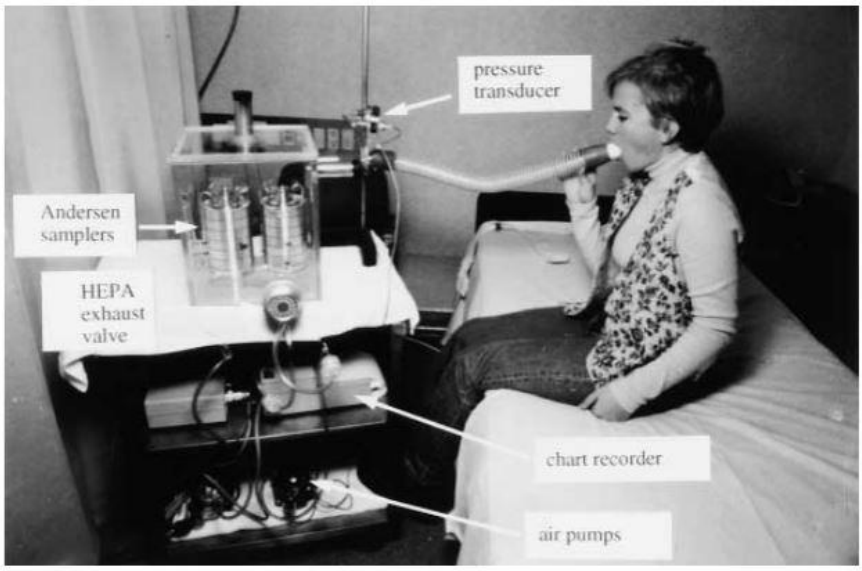

Figure 2-7: Andersen Impactors (from Fennelly et al., 2004)

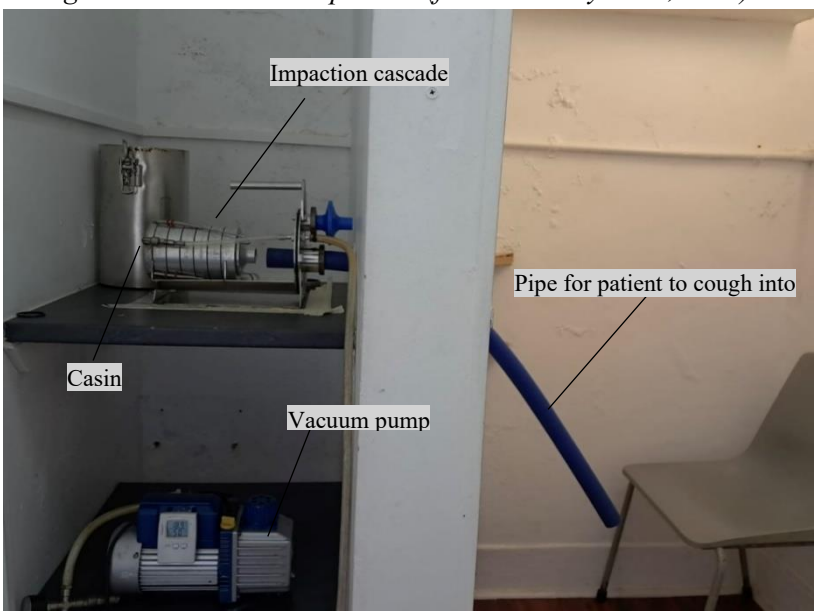

Figure 2-8 is an example of a typical CASS testing facility at an active TB community case finding site

Figure 2-8: CASS testing facility at Brooklyn Chest Hospital, Cape Town

in Cape Town, South Africa. Here, the patient will sit in the cubicle with a modified wall for the device to sit behind. A 1m long pipe is connected to the device through the wall. Patients and technicians/nurses sit opposite sides during testing. The device is also not airtight or closed off completely, hence the chamber is negatively pressurised to capture any residual microbes.

2.3.2 Limitations of Current CASS technologies

Limitations of current CASS technology include issues with detecting low bacterial loads. This is affected by low cough volumes (Jones-López et al., 2013). Furthermore, ideal size fractionation is difficult since the particles of interest are in close range of one another. Systems which are reusable can be sterilised using thermal or chemical methods, but this requires a stringent decontamination protocol and added infrastructure. This in turn, reduces the number of screenings which can be done over a single site visit. *M.tb* are also fastidious bacteria so the conditions for bacterial collection and storage need to managed appropriately to ensure viability for culture.

The equipment used at the Centre for Lung Infection and Immunity (University of Cape Town) will be used as the basis for evaluation of current systems. This device is set up and standardised according to general practice as described by seminal works in the field (Fennelly, 2004). Furthermore, the same systems are in place in active TB case finding studies in Zambia (ZAMBART, Lusaka) and Zimbabwe (Biomedical Research & Training Institute, Harare) (Theron et al., 2020) (Esmail et al.). However, in discussions with principal investigators involved in these studies it was found that quality control of these sites was particularly difficult considering the lack of standardised protocol for equipment setup in these tests.

The physical impaction cascade is made up of 6 stages of stainless-steel cylindrical nozzle plates, each weighing approximately 200g. The nozzles are arranged with 6 corresponding agar plates which need to be prepared in a sterile environment. Each stage corresponds to a specific d_{50} value such as 0.65, 1.1, 2.1, 3.3, 4.7 and 7μm. Commercially available impactors are available in 6 or 8 stages. This is because these systems are commonly used in quantitative air sampling and inhaler testing where more particle size ranges are important. For the purposes of separating particles into rough size ranges for more semi quantitative research, fewer stages are required since there is a simplified approach of more/less infectious. This would also increase yield per plate, subsequently increasing the chances of culturing the bacteria, at least.

This system is placed in a casing, also stainless steel, which is approximately 40cm in length and 20cm in diameter. The casing is not airtight and merely provides a connection for the 1m long rubber tubing,

with a thickness of 0.5cm. This pipe is not connected to any other part of the system, i.e. it needs to be reconnected every time the system is used. The distance between the pipe and impaction cascade is maintained at 3cm as far as possible. No formal connections are in place to ensure the gap between the pipe and cascade is maintained consistently between tests run using the same system, or across different locations with different users.

A large single stage vacuum pump pulls the air throughout the system. This pump weighs 7kg, is noisy and has no carrying handle or casing. It also does not incorporate a switch and turns on as soon as it is connected to power, meaning the user needs to be near the power source to operate the device. This also means less control is possible over sampling times if the power source is further away from the device.

All these factors contribute to hindering cascade impactors from becoming a ubiquitous technology in bioaerosol sampling and epidemiological research. These practical issues are important when considering low resource settings with short and under-staffed skilled personnel. Improvements on aspects such as the weight, portability and size of the device are important to consider.

2.3.3 Cascade Impaction Theory

Cascade impactors are based on the fluid dynamic principle of inertial impaction. The theory of inertial impaction relates to the property of an aerosol particle in a fluid which causes it to move in a straight line due to the inertia it possesses. It will continue to move in this direction until such a point that the fluid around it encounters some obstacle (Golovin & Putnam, 1962). The particle will either flow around the obstacle in fluid aerosol streams or collide with it.

Impaction takes place when particles in an air stream have a high enough inertial momentum to overcome the fluid drag force. Particles with less inertia (and less mass) will continue on the airstream. This would continue until such a point where they impact on a plate at a later stage in the cascade, i.e. cascade impaction. Each stage is designed to cause impaction of a particle size range by manipulating the velocity of the airstream. This is accomplished by altering the diameter (W) of the orifice which the

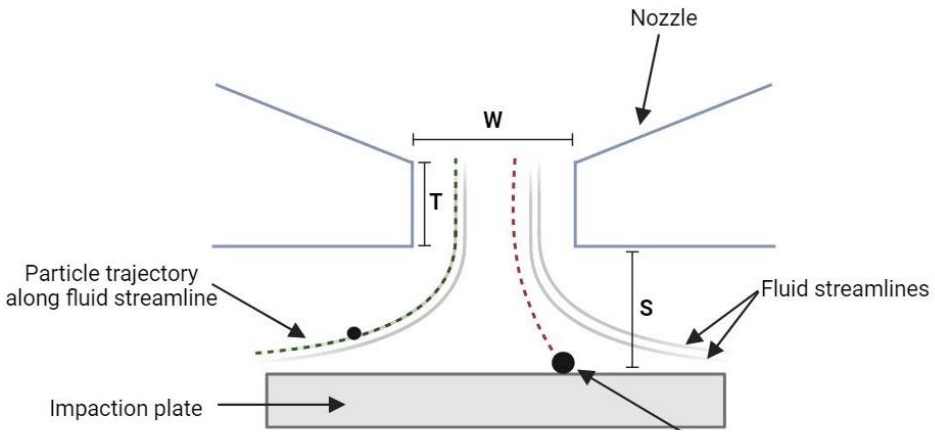

Figure 2-9: Cross section through a cascade impaction stage (Adapted from Marple & Willeke 1976)

airstream passes through, called the nozzle or throat (Marple & Willeke, 1976). The throat length is denoted by 'T' and the distance from the jet exit to the impaction plate by 'S'.

2.3.4 Stokes number

To discern whether a particle will undergo inertial impaction or not, the stokes number (Stk) must be calculated. It is an indicator of the stopping distance of the particle to an obstacle at a characteristic length in the device. Particles with Stk < 1 tend to stay on fluid streamline paths while particles with Stk > 1 will not be able to continue on a fluid streamline following changes in direction, thus resulting in inertial impaction on a plate (Finlay, 2001). The Stokes number can be calculated based on the following equation (Marple & Liu, 1974):

$$Stk = \frac{C_{dp} {d_p}^2 \rho_p V_0}{9\mu W} \qquad \textit{Equation 2-1}$$

Where C_{dp} is the Cunningham slip correction factor, d_p is the particle diameter (μm), ρ_p is the density of the particle (g/m^3), V_0 is the average nozzle velocity (m/s), μ is the absolute gas viscosity (Pa.s) and W is the nozzle diameter (m).

2.3.5 Reynolds number

The Reynolds number is a useful dimensionless parameter in fluid dynamics as it describes the relationship between the inertial and viscous forces of the fluid under consideration (Kaneda et al., 2021) This number provides information of the flow regime in the device. As the inertial force increases, so does the Reynolds number, generating a turbulent flow. A Reynolds number below 2000 refers to a laminar flow, while values more than 3500 correlate to turbulent flows (Kothandaraman & Rudramoorthy, 2013). Increased turbulence also results in higher particle losses within the device which is unfavourable in terms of cascade impactors.

For the purposes of cascade impactor, the Reynolds number should be understood as the flow regime is an integral part of the collection efficiency of the device, specifically for very low or high values. The ideal scenario would be to control for these types of impacts on collection efficiency by minimising the effect of the Reynolds number. According to previous experiments, it was found that this effect is in fact minimised for values where 500<Re<3000 (Marple & Liu, 1974). The formula below describes the Reynolds number in the context of a closed path or pipe (Romay & García-Ruiz, 2023).

$$Re = \frac{4\rho_g Q}{\pi n \mu D} \qquad \textit{Equation 2-2}$$

Where ρ_g refers to the gas density (g/m^3), D is the nozzle diameter (m) and μ is the absolute gas viscosity (Pa.s). Here, Q refers to the volumetric flowrate through the impactor & n is the number of nozzles

2.3.6 Average nozzle exit velocity

In order to calculate the Reynolds number for the stage, the average nozzle exit velocity must also be deduced. This value is calculated by the following formulae where Q refers to the total volumetric flowrate and n is the number of nozzles, D is the nozzle diameter.

$$V_0 = \frac{4Q}{n\pi D^2} \qquad \textit{Equation 2-3}$$

2.3.7 Jet-to-Plate Distance

Jet to plate distance is the difference in height between the nozzle and the impaction plates (i.e. the surface of the agar)

2.3.8 Pressure drop in the impaction region

Pressure drop along the entire device is an important consideration especially when considering fewer stages than traditional CASS. The pressure drop for a specific stage is assumed to be equal to the dynamic pressure of the jet through the nozzle (Marple & Willeke, 1976). This is described as:

$$P_2 = P_1 - \frac{1}{2}\rho {V_0}^2 \qquad \textit{Equation 2-4}$$

P_1 refers to the static pressure at the inlet of the stage and P_2 is the static pressure at the nozzle.

2.3.9 Cunningham slip correction factor

The Cunningham slip correction factor (C) accounts for discontinuities which arise in scenarios where the size of aerosol particles in a fluid tend towards the mean free path of gas molecules (Gussman, 1969). Effectively accounting for drag effects on small particles. It is described by the following equation (Wahi & Liu, 1971):

$$C = 1 + \frac{0.163}{D_p P_2} + \frac{0.0549}{D_p P_2} exp(-6.66\ D_p P_2) \qquad \textit{Equation 2-5}$$

2.3.10 Cross flow

Cross flow refers to the fluid dynamics scenario in which fluid streamlines run in non-parallel directions to each other. This can impact the collection efficiency of the device since interference between streams can increase particle bounce. Cross flow can be decreased by designing the shell to minimize sharp turns and edges on the internal face of the shell.

2.3.11 Impaction Efficiency

Impaction efficiency is also an important measure to account for during the design and simulation of this device. Threshold efficiencies for each stage must be determined. The efficiency is given as:

$$E = \frac{number\ of\ particles\ arriving\ by\ impaction}{number\ of\ particles\ geometrically\ incident\ on\ plate} \qquad \textit{Equation 2-6}$$

This theoretical value does not account for particle bounce or rebound, which is an important consideration in real terms. That being said, it can be used as a measure of collection efficiency if it is assumed that particles which impact on the plate do not rebound, i.e. every particle which hits the plate stays impacted (Vincent, 1995). For the purposes of this research this value could be used as a measure of efficiency in the *in-silico* testing stage of the device. It does not hold much merit in physical testing unless direct inspection using real time analysis of particle impaction mechanics can be conducted.

2.3.12 Collection efficiency

Collection efficiency is the most vital aspect of cascade impactor design and optimisation (Marple & Liu, 1974; Marple et al., 1973; Marple & Willeke, 1976). It amalgamates all previously mentioned qualities, serving as the measure of how accurately the cascade impactor operates. The "cut point" is the term used to describe the size or diameter for which 50% of particles will report to the filtrate. This means that there is an equal probability of a particle reporting to the over- or underflow during a separation step. This cut-size is termed d_{50} (Svarovsy & Thew, 1992).

A collection efficiency curve can be used to illustrate how many particles of a specific size are collected on the impaction plate, including the d_{50}. An example of such a curve is shown in Figure 2-10. These (cumulative) curves are characterized by a distinct S-shape (Nakayama, 2000). After constructing the cumulative efficiency curve a line can be drawn from the y-axis to the curve at 50% efficiency. At this point another line can be constructed towards the x-axis. The corresponding diameter on the x-axis is the d_{50} value.

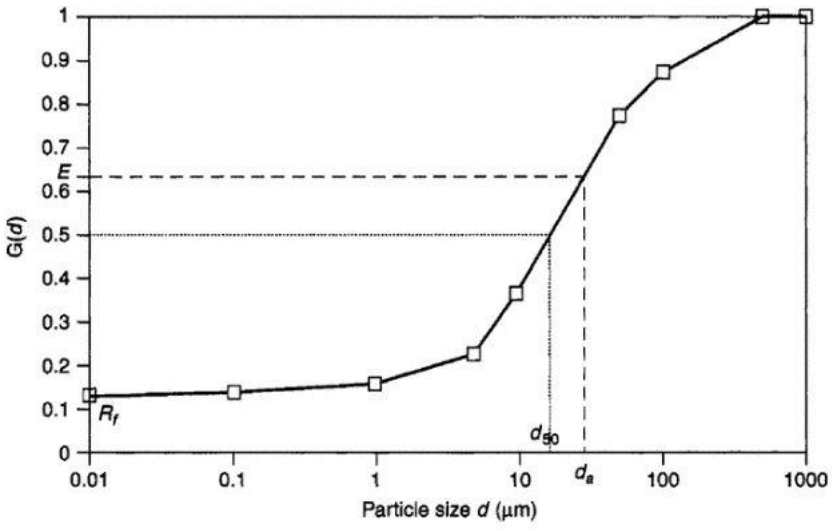

Figure 2-10: Sample Collection Efficiency Curve

3 Design Methodology

3.1 Design, Development & Testing Methodology Overview

Chapters 3, 4 and 5 deal with the design, development and testing of the Mini CASS. This process can be described by 3 distinct stages namely prototype development, design optimisation and device evaluation, shown in Figure 3-1. Prototype development is the physical device design, modelling and building (chapter 4) of the device. This also includes the substrate design and development for the impaction plates (chapter 5). The development and optimisation stages are intertwined in that concepts are designed and tested iteratively.

The final prototype has gone through multiple design changes which were informed by CFD simulation tests (for the physical device) and physical tests (for the substrate). Once the device design was frozen and the prototype finalised, device evaluation could be carried out. This comprised the design verification & validation testing (chapter 6). These are two distinct tests, the first of which verifies that the device can fractionate particle sizes into two distinct size categories. After this, the ability of the device to collect a viable (culturable) simulated cough aerosol is tested. These results can be compared to the same tests carried out on the conventional CASS.

A subsystem design approach was adopted such that the device was split into components characterised by different functions. These were chosen according to components that current commercial cascade impaction systems have. Each subsystem had its own set of requirements and design considerations. The four main components are the:

- Impaction Cascade
- Casing
- Vacuum pump
- Mask

The integration of commercially available components was considered, so as to reduce reliance on specific manufacturing, especially for the 3D printed parts of this device. Commercially available components were utilised where necessary, like petri dishes and the vacuum pump itself. Cases and enclosures were designed to fit the equipment they house. The cascade impaction system is custom designed, not lending itself very well to being integrated with more commercial parts at this juncture. The mask part, however, could present an opportunity for replacement with mass manufactured components. This will be further discussed in Section 3.4, ‘Mask Design Considerations’.

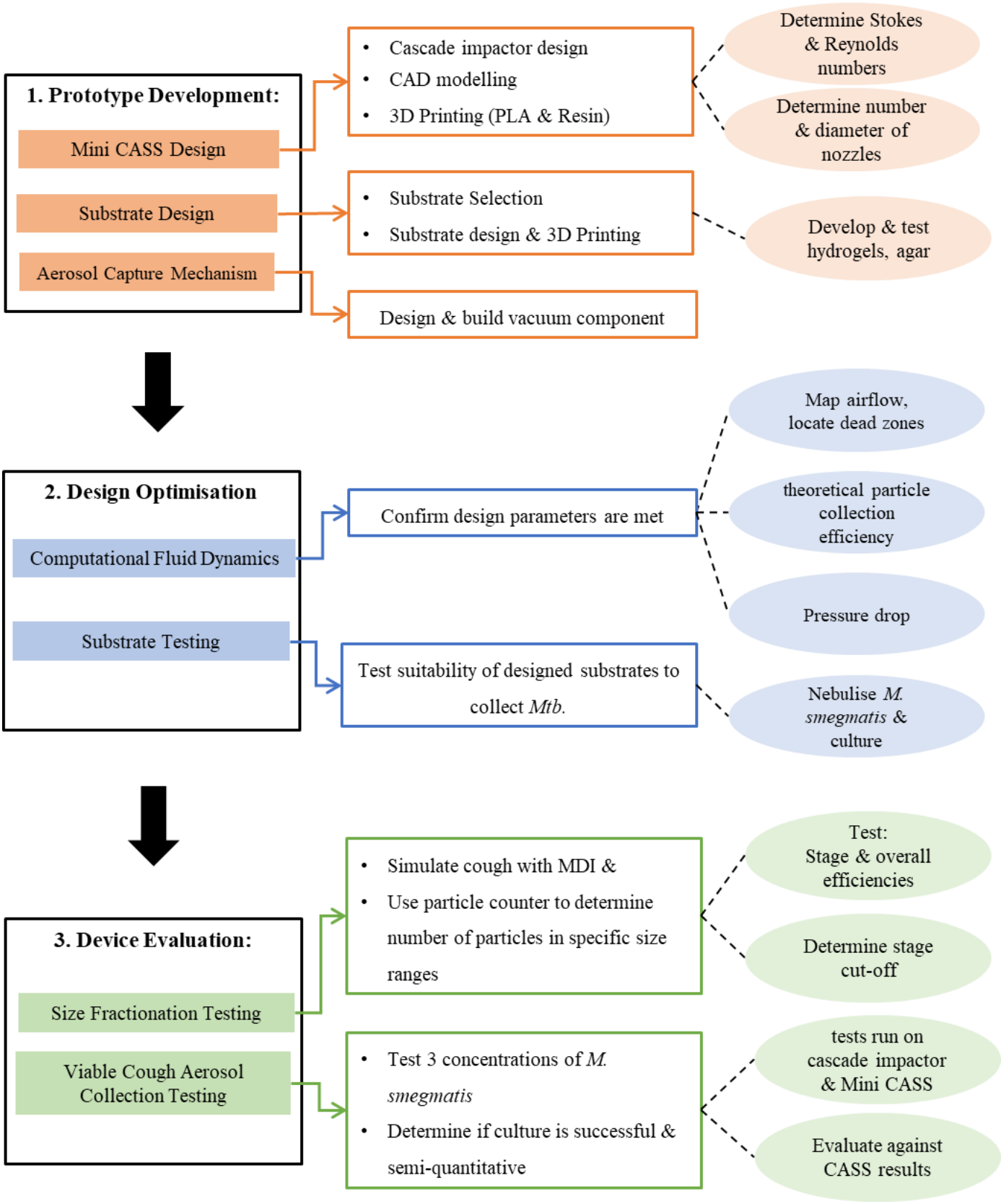

Figure 3-1: Design, development and testing overview

3.2 Device Requirements

The needs criteria describe the qualities the proposed device needs to have to address the issues identified in the review stage. They effectively form the basis for the device requirements (Yock, 2015). The needs criteria were divided into compulsory and supplementary categories. The former category refers to the requirements which must be met for the device to be deemed satisfactory. The latter category refers to qualities that are not necessarily compulsory but would enhance the design. Compulsory device requirements include that the device must have the ability to:

1. Collect culturable cough aerosol samples
2. Fractionate particles collected based on two distinct particle diameters (*d*)
3. Be easily operated by persons older than 18
4. Be handheld
5. Be portable

Supplementary criteria include that the device could:

6. Be single use & disposable
7. Be manufactured 'inexpensively'

These requirements were translated into design parameters with corresponding acceptable limits or design quantities. This serves as the framework that Mini CASS was developed against. Practical design parameters and defined constraints are listed in Table 3-1. The relevant subsystems making up the device and their corresponding functions are described in Table 3-2.

Table 3-1: Device Parameters & Constraints

Requirement	Design Parameter	Acceptable threshold
1	Impaction plates which can successfully culture *M.tb*	< 3 colonies of *M. smegmatis* cultured
2	Capture particles in desired particle size categories	> 50% collection efficiency per stage
3	Simple setup & operation – minimise setup time	Setup time < 5 minutes
4	Device size	Diameter < 15cm, length < 20cm
5	Total weight	< 1 kg
6	Disposable parts & compartmentalized design	3D printed parts
7	3D printed parts	3D printed PLA (FDM)

3.1 Device Subsystems

Table 3-2: Subsystems, relevant components & functions

Subsystem	Components	Function
Impaction Cascade	Nozzle plates	Diverts particles into designated size groups
	Impaction plates	Collects particles for culture
Casing	Housing	Covers & stabilises impaction cascade
	Impactor outlet piping	Connects impactor to outlet filter
Vacuum Pump	Vacuum pump (and enclosure)	Provides constant flowrate and vacuum
	Outlet filter	Ensures no particulate matter or liquid enters pump & traps residual bioaerosol.
	Pump inlet & outlet tubes	Connects casing to pump and exhaust
	Power cord	Connects pump to power source
Mask	Mask	Interface between patient & device
	Tubing	Connects mask to impactor inlet

3.2 Cascade Impactor Design Methodology

The most vital aspect of the Mini CASS - in terms of design - is the impaction cascade. The design of the device was based on the method outlined for impactor design (Marple & Willeke, 1976). This procedure is based on previous experimental and theoretical work is a seminal paper in the field, with continued popularity in the last decade (Demokritou et al., 2002; Grinshpun et al., 2005; Romay & García-Ruiz, 2023). This is an iterative process which uses the Stokes, Reynolds and Cunningham numbers to design a nozzle plate for a specified particle size, d_{50}. This process, as described by Marple and Willeke (1976) is outlined in Figure 3-2.

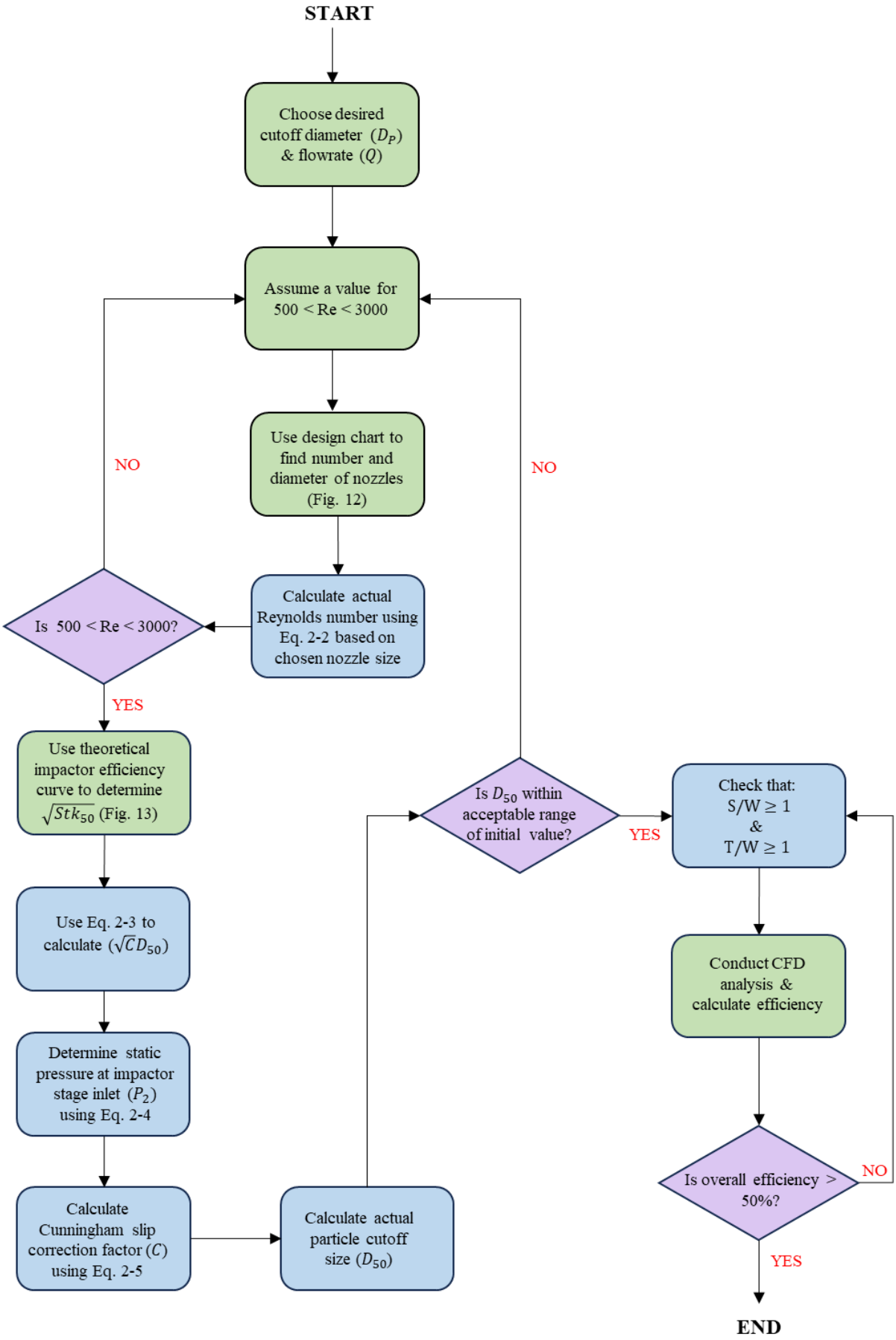

Figure 3-2: Algorithm for cascade impactor design (Adapted from Marple & Willeke, 1976)

3.2.1 Design Considerations

Commercially available CASS devices usually have 8 or 10 stages. It is also common that two devices are arranged in parallel to increase collection. The stages and mock impaction plates of a 6 stage Andersen impactor are shown in Figure 3-3. This means that, excluding pre-filtration, an impactor comprises up to 10 levels of particle size fractionation for a 10 stage impactor. Typically, nozzle quantity increases while size decreases as the cut-point gets smaller. The particles collected in impaction systems can range from 0.1 to 25 micron (Demokritou et al., 2002). This is attributed to the fact that cascade impaction systems were conventionally designed to collect aerosolised suspensions air samples.

The aim of Mini CASS was to reduce the bulkiness and weight of the technology. Considering its use in a clinical setting as a sample collection tool, these many stages of particle size fractionation could be unnecessary. There was a decision to be made regarding the number of stages which would be beneficial in Mini CASS. The purpose of a device such as this is two-fold. Firstly, to capture culturable *M.tb* of any size. Secondly, to separate these particles into distinct categories which correlate to 'more' and 'less' infectious. Considering this, two stages would be sufficient, with the first one indicating lower infectivity and the second, higher. This would also minimise the resource requirement of additional impaction plates for more stages. Furthermore, if infectivity was not the concern but rather culture confirmation of *M.tb*, either one of the samples could be used in place of a sputum sample. The next consideration was therefore, what these distinct ranges are and what would the relevant cutoff diameters be.

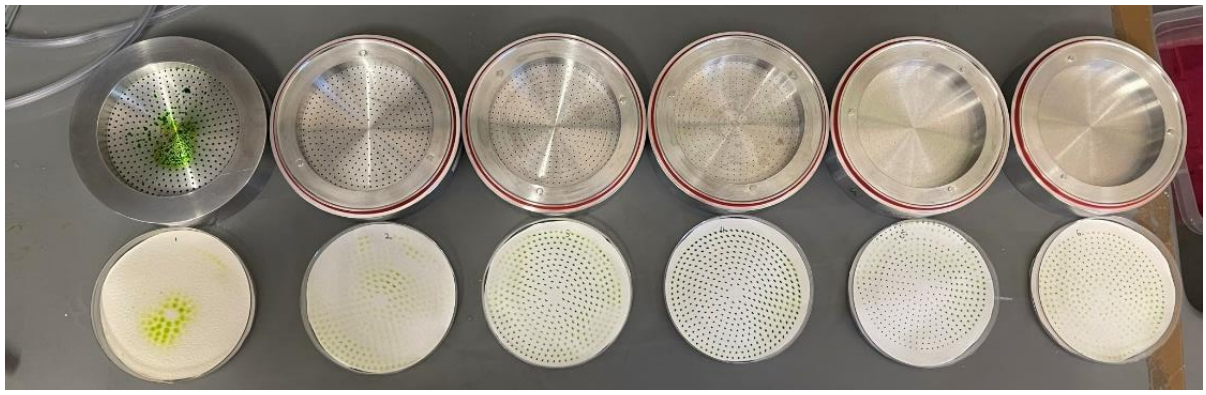

Figure 3-3: Unstacked 6-stage cascade impactor with impaction plates

Since only two stages would be used, these would need to cover the entire particle distribution of a characteristic cough. Consideration was taken that the particle counter used to evaluate the device (Lighthouse Handheld 3016) also measures in discreet size ranges. As shown in Figure 3-4, the ranges that were chosen for design were a compromise of the TB transmission, particle counter and highest infectivity ranges. Stage 2 includes both particles of high infectivity and those which would most likely be trapped in the trachea. This is because the modal range of 2 – 3.5µm falls here (Patterson et al., 2018). It was thus reasoned that if the device was being used purely for sample acquisition, the probability of obtaining a positive sample would be higher than if this range was left out (i.e. only 0.65 – 2.5µm).

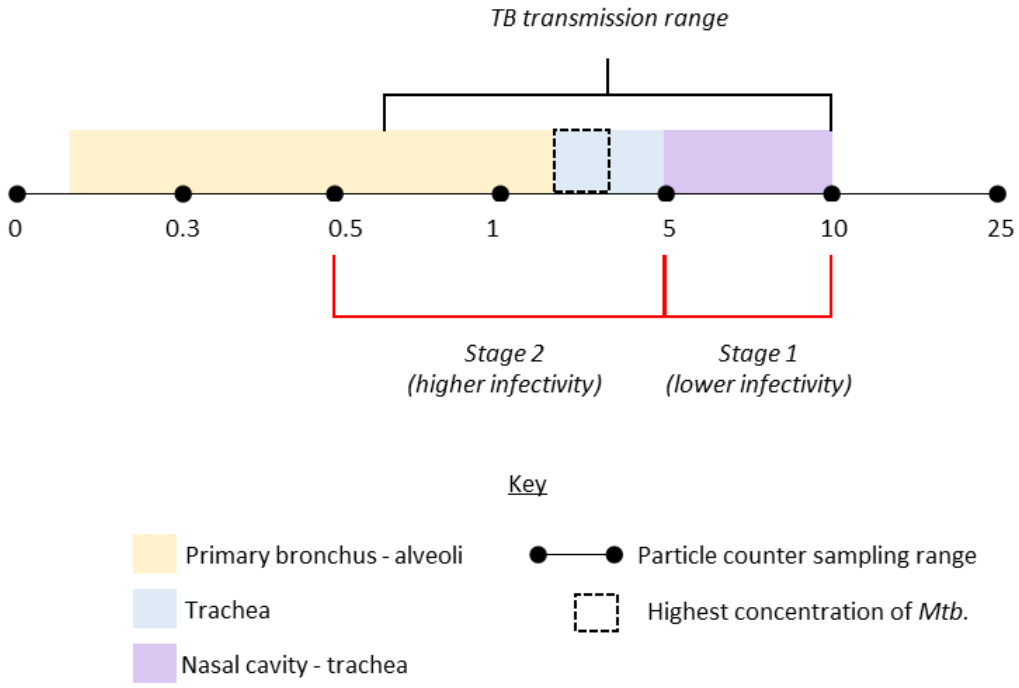

Figure 3-4: Mini CASS stage design considerations

Stage 1 was designed to capture particles with diameters between 10 and 5µm, while stage 2 would capture particles from 5 to 0.5µm. These ranges also fit well within the particle counter sampling ranges, making them suitable for verification testing. The designed cut-point or d_{50} for each stage is therefore 5 and 0.5µm for stage 1 and 2 respectively.

In terms of the design process, some considerations were made regarding general design choices. For instance, between Re values 500 and 3000 the sharpest cut efficiencies can be achieved and thus the design was modelled with this condition in mind (Marple & Willeke, 1976). Round nozzles were chosen over rectangular slots. This was to create a device comparable to the current cascade impactor, which has round nozzles. A round nozzle is also more conducive to the distribution of bacteria into their colony forming units (CFU's) for enumeration.

The design chart for round impactors was used to determine nozzle quantities and sizes (Figure 3-5). A Reynolds number of 3000 was initially assumed as this produced a more favourable combination. For example, for a cutoff diameter of 5µm at a flowrate of 20l/min can be considered with two different Reynolds numbers. At 3000, the nozzle size is 0.565 cm and between 1 or 2 nozzles are recommended. At 500, 25 nozzles at a diameter of 0.224 cm are recommended. Since the prototypes would be manufactured on 3D printer, it was decided that larger nozzle sizes are preferable since they would be more accurately achieved by fused deposition model printing. Smaller nozzles could be subject to less favourable resolutions, resulting in nozzles with inaccurate diameters which could affect the stage cut point.

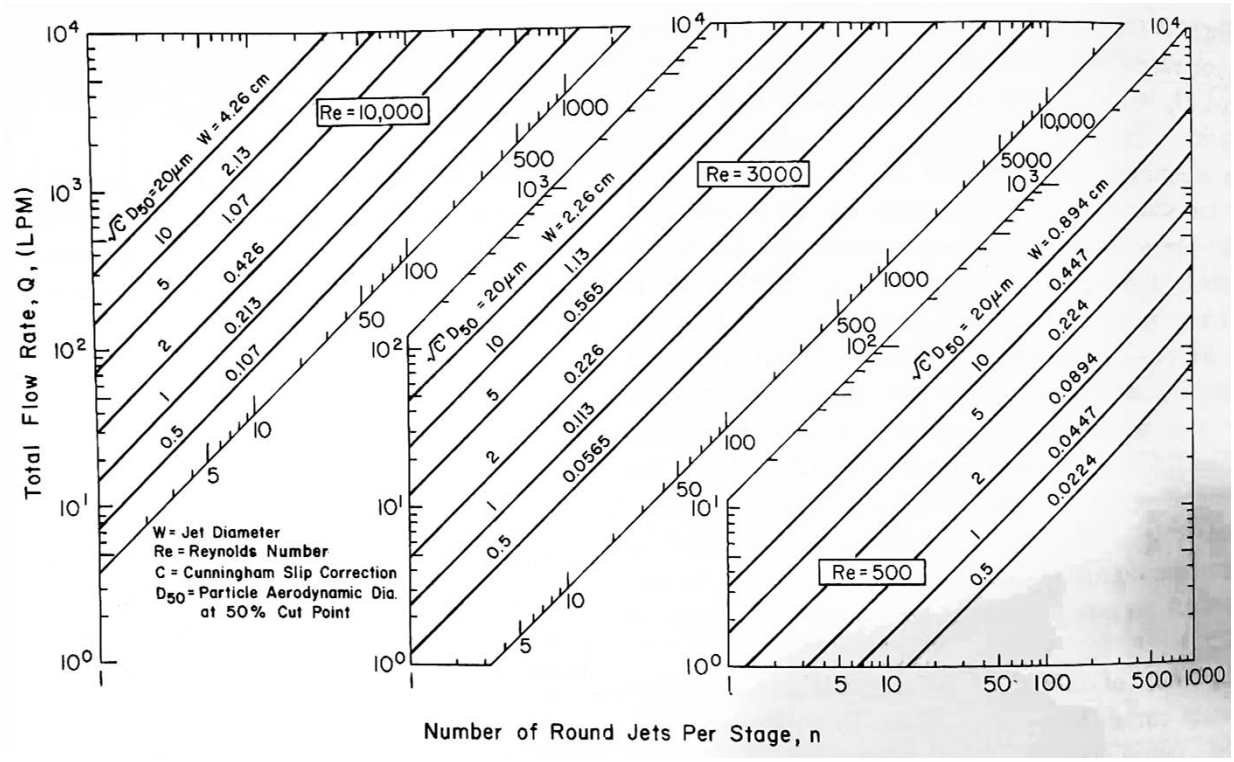

Figure 3-5: Design chart for round impactors (Marple & Willeke, 1976)

The same procedure followed for the 0.5µm cutoff diameter where at a Reynolds number of 500, 300 nozzles of 0.0224 cm were required. For a Reynolds number of 3000, less than 20 nozzles of 0.0565 cm were required. Once again, the resolution of FDM printers at such small diameters would struggle to achieve accurate results. Furthermore, with only two stages the pressure drop would not be very high, which could result in particle buildup at the entrance to these small nozzles.

The next step was to calculate the actual Reynolds number using Equation 2-2. The Reynolds number for stage 1 was calculated to be 1560 and 1170 for stage 2. These are both acceptable as they sit between 500 and 3000. Equation 2-2 was rearranged and used as defined by Marple and Willeke (1976) to form Equation 3-1.

$$Re = \frac{4\rho_g Q}{\pi n \mu D} \qquad \textit{Equation 3-1}$$

The next step was to use the theoretical impactor efficiency curve (Figure 3-6) to determine $\sqrt{Stk_{50}}$. This is the square root of the stokes number for the cutoff particle diameter. Once this is determined, the value of $\sqrt{C}D_{50}$ can be calculated by rearranging Equation 2-1 to make it the subject of the formula.

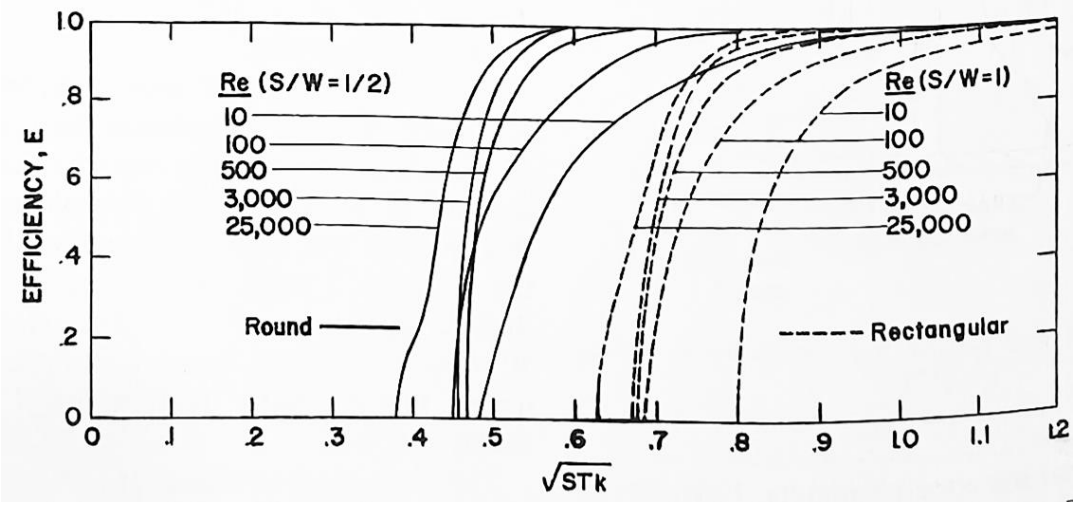

Figure 3-6: Theoretical impactor efficiency curves for rectangular & round impactors at T/W = 1 (Marple & Willeke, 1976)

The pressure in the impaction region had to be determined using Equation 2-4 so that the Cunningham slip correction factor could be calculated by Equation 2-5. This value can be substituted into the value obtained for $\sqrt{C}D_{50}$ to finally obtain the cutoff particle size. In the case of this research, the two cutoff particle sizes of interest are 5 and 0.5µm.

The above process was followed to obtain an initial estimate of the cutoff diameters. Excel was used to compute the relevant values. Subsequently, iterative methods such as 'goal seek' were used to monitor how changing the diameter or number of nozzles could obtain a more favourable nozzle plate configuration. Therefore, the final design outputs for the nozzle plates are not only resultant of the design procedure laid out, but also considering iterations carried out afterwards to inch closer to the ideal cut points. Cutoff particle sizes were deemed satisfactory if found to be within 5% error of the goal cutoff diameters.

3.2.1 Assumptions For Nozzle Plate Design

Certain bulk fluid values were required for the mathematical modelling. These were kept consistent across the different calculations. For instance, the gas density of exhaled breath at 34°C was assumed to be 1.15 kg/m^3 as found in literature (Gao & Niu, 2006). The absolute gas viscosity was taken to be 1.895 x 10^{-5} (Kanoğlu & Çengel, 2020). The number of nozzles was 3 and 20 for stages 1 and 2 respectively.

Other general assumptions for this design included that the aerosolised particles are 100% water, with a density of 1000 kg/m^3. It was assumed that the particles would be suspended in air, which has a gas density and viscosity of 1.15 kg/m^3 and 1.802 x 10^{-5} km/m-s respectively. The volumetric flowrate was used as 20 l/min, determined via experimental confirmation from the current CASS setup (Fennelly et al., 2004).

3.3 Pump Design Considerations

The efficiency of a cascade impactor is also heavily reliant on the operating flowrate of the pump used. In general, 6-stage cascade impactors require a 28.3 L/min flowrate and ultimate vacuum of 60 kPa which is supplied by an industrial pump. These pumps have brushed motors which require a lubricating oil for operation.

In an attempt to reduce the bulkiness of the device it was imperative to change the pump which is currently used. This is not usually a big consideration in cascade impactor design. For the purposes of this project the goal was to source a vacuum pump which could achieve a flowrate of 28.3 l/min with a maximum pressure of -60 kPa. The pump which was acquired (HLVP10, Kamoer®) is capable of a 20 l/min flowrate at a maximum vacuum of -50 kPa. This pump is brushless, requiring no oil. It has a reduced weight of 450g. The design flowrate for the cascade impactor was therefore 20l/min.

The pump was sourced and connected to a power cord with a transformer. Once this connection was tested the pump enclosure was built. The purpose of the enclosure was to house and stabilise the pump. It also had to serve to transport the vacuum pump and this was incorporated into the design. Another important consideration in this design was user-friendliness and practical placement of tubing inlets and wiring etc.

3.4 Mask Design Considerations

The mask part is the only component in the device which interfaces with the patient directly. The design was therefore driven by creating a comfortable and visually pleasing object. The purpose of this part of the device is to act as a conduit between the mouth and the device itself. This part was necessitated through the discussions with technicians involved with CASS sampling. Practically speaking, coughing into a pipe with a diameter smaller than the mouth is more difficult that coughing freely, into a mask for instance.

While the design of this part is included in the final product, there is an alternative design which could be explored which includes replacing this part with a KN95 mask and adapter insert to pierce the mask and connect the inlet tube. This would reduce the amount of 3D printed objects required in the design. Furthermore, masks are already designed to fit snugly on a patients face, while reducing the spread of pathogens because of the filtration material. This can be explored in future work as an improvement.

3.5 Casing Design Considerations

The casing for the impaction cascade effectively serves to stabilise the device and to contain any spillage or leaks from the device. Furthermore, it plays a large role in fulfilling the easy-to-use aspect of the device. This is through the size and shape as well as through the locking mechanism. A newer design requirement in the case of this handheld CASS device is that more importance is placed on fixing the impaction cascade to the casing so that the device is not moved out of place when used. This would also solve the issue of varying distances from the inlet tubing which is encountered in current CASS sampling. Thus, a major aspect of this part was the design of the fastening, fixing and locking mechanisms.

4 Physical Device Design, Modelling & Simulation

This chapter deals with the final prototype and the subsystems which were developed thereof. The requirements and parameters outlined in Chapter 3 guided the prototype development. Specific verification tests were conducted on each subsystem to confirm this, taking into account that the final design was a product of many iterations. Some notable iterations in each system are highlighted in this chapter to contextualise the final design. Once the design specifications for each subsystem were satisfied, the design was considered final. Following this, risks in the prototype were considered as part of following the guidelines of Good Engineering Practice (GEP). This took the form of a Failure Modes and Effects Analysis (FMEA). This is a practical and relevant way of identifying and addressing operational risks. It is also a means to institute "risk-based thinking" in compliance with ISO 9001 (Quality Management) and ISO 13485 (Medical Devices). Areas of concern were identified and relevant mitigation routes (design changes etc.) were employed.

The final Mini CASS device incorporated the 3D printed components, including the impaction cascade, pump system, casing and mask part. Most of the prototype was constructed from 3D printed materials such as PLA (Polylactic Acid) and synthetic resin.

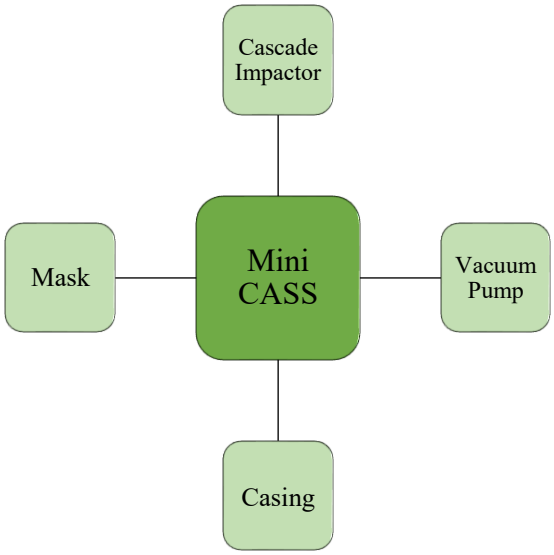

Figure 4-1: Mini CASS Subsystem Overview

4.1 Cascade Impactor Design

The purpose of the impaction cascade is to capture and separate the particles into two size ranges (0.5 to 5µm and 5 to 10µm). This subsystem was designed using the process outlined by Marple and Willeke (1976). The parameters used for these calculations are found in Table 4-1. Detailed sample calculations can be found in Appendix A. The resultant impaction cascade consisted of 4 main components which included the 2 nozzle plates and 2 impaction plates

Table 4-1: Summary of design input parameters

Parameter	Value
Volumetric Flowrate	20 l/min
Pump Vacuum	-51 kPa
Absolute Gas Viscosity	1.802 x 10^{-5} km/m-s
Gas Density	1.15 kg/m^3
Particle Density	1000 kg/m^3
Static Pressure at Inlet	55 kPa
Stage 1 D_{50}	5µm
Stage 2 D_{50}	0.5µm

4.1.1 Nozzle plates

The purpose of the nozzle plate in a cascade impactor is to facilitate the separation of aerosol particles by size at a specific stage. Furthermore, it usually performs the dual function of housing the impaction plate for the previous stage. For example, it serves as the platform for the petri dishes to be positioned and fixed on. This design is advantageous in that it conserves space in the cascade. Both of these purposes influenced the design of these plates. The nozzle plates are practically identical with the exception of the number and size of nozzles on the upper surface which distinguish plate 1 and 2. Due to this, the general nozzle design will be outlined using plate 1 as the exemplar.

The nozzle sizes were calculated using the procedure laid out by Marple & Liu (Marple et al., 1973), one of the primary publications outlining cascade impactor design methods still used today. Microsoft Excel was used as a computing tool for iterative calculations. According to the findings of this paper, impaction efficiency on a plate is influenced mainly by the jet Reynolds number and to a lesser extent the jet-to-plate distance. The third factor, which is of lesser consequence is the impactor throat length (Marple et al., 1973). These are the factors which were heeded specifically in nozzle plate design. The nozzle plate itself was designed to create the pathway for the cough aerosol to flow through. This required that each nozzle plate fit snugly into the next to reduce particle losses in the system.

It should be noted that the figures in this section with single nozzles are from earlier stages in the design process. At first, a single nozzle approach was adopted but this showed to be less favourable in preliminary flow simulations of general flow in the device. Subsequently, a multi-nozzle approach was decided on. The issues regarding to the physical design of the nozzle plate remain relevant whether single or multi nozzle.

For example, the initial plate design included a small ledge on which the petri dishes would be placed (shown in Figure 4-3). This is very similar to conventional cascade impactors. However, when flow simulations were conducted this ‘step down’ design contributed to a significant amount of particle bounce. This reduces the number of particles contacting with the plate. This effect is shown in the cross section of a nozzle plate in Figure 4-2.

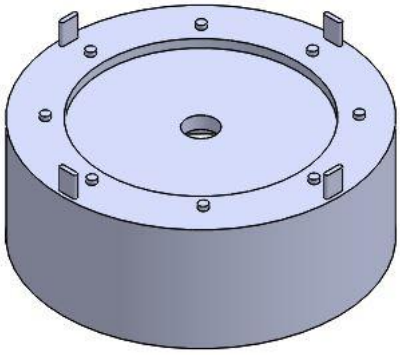

Figure 4-3: Nozzle Plate Design 1

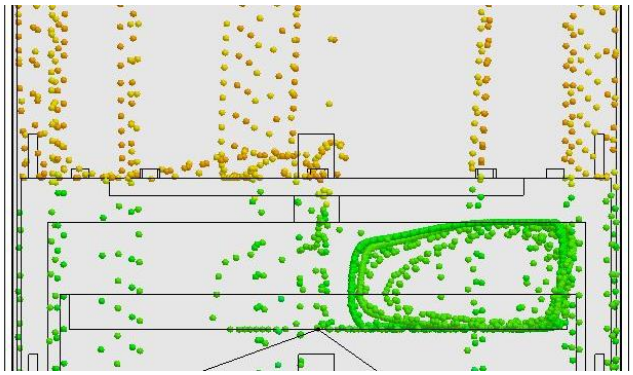

Figure 4-2: Particle bounce due to 'step down' design

To minimise these adverse effects the ‘step down’ design was converted to incorporate a gradient. This would minimise bounce and guide the particles into the next stage. Particle entrapment in the system would be reduced. The first iteration of the nozzle plate was approximately 2cm in height, which was based off the flatter nozzle plates in commercial CASS. However, with a reduction in total system size and only two impaction stages it was likely that a taller nozzle plate would be required to maintain the desired flow pattern. As such, after noting the cross flow in the first iterations the distance between the nozzle and impaction plates (S) was increased in 0.5cm steps to decrease formation of dead zones. As changes were made, particle studies were re-run and the results inspected to refine the design. The height differential would be adopted in the nozzle plates, i.e. a taller nozzle plate.

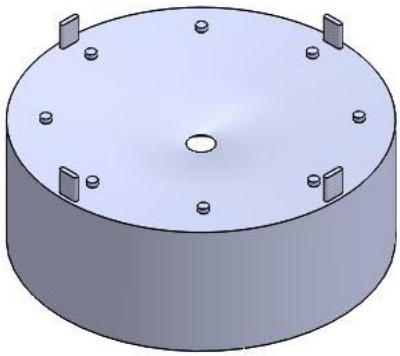

Figure 4-5: Nozzle plate design 2

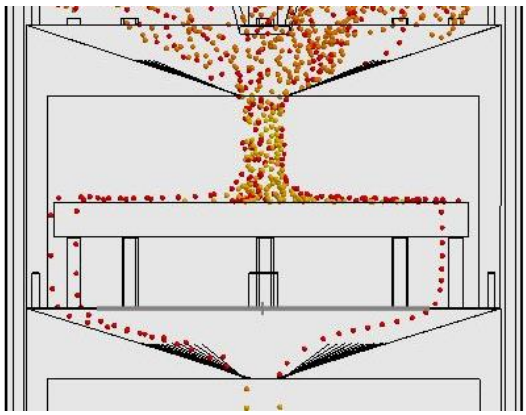

Figure 4-4: Preferred flow with nozzle plate design 2

Another aspect of the nozzle plate which had to be considered was how the petri dish could be secured in place. Initially small circular projections were designed on which the dish could rest (as shown in Figure 4-4). However, on prototyping it was found that this design did not allow for secure positioning. Slippage of the impaction plate results in inefficiencies in the impaction system. This was also a concern noted in current CASS technologies, which employ some form of gluing agent to the plate to ensure non-slippage. To solve this, this design needed to ensure a secured plate. A redesign was conducted in which the plate could sit more snugly so as to mechanically fix the plate without requiring extra steps.

The nozzle plates were also originally printed on fused deposition modelling (FDM) printers, but the thin seats at the top were incompatible with the supports required – resulting in a poor print. For this reason, a resin print was conducted using the FormLabs 2 Clear Resin. The resolution of this printer is as high as 150µm, making it a good choice for smaller nozzle sizes such as those required for stage 2.

An airtight system was required, so design considerations for this had to be made. To achieve this an interlocking plate-to-plate system was implemented. This made use of an extruded ring at the top of each nozzle plate which fit snugly into the seat at the base of the previous plate. The fit and tolerance of this part of the device was particularly important considering the usability and setup time required. Thus, this mechanism was designed to be assembled by a simply stacking the plates on top of each other. The plates were also labelled with a '1' and '2' to indicate the order in which they should be stacked (stage 1 should be closest to the device inlet). The final nozzle plate design is shown in Figure 4-6.

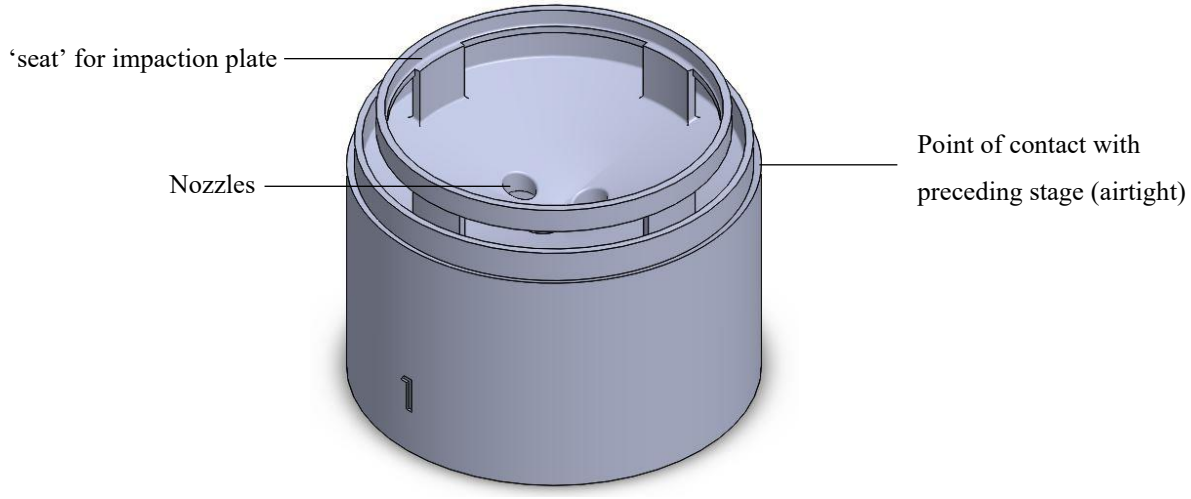

Figure 4-6: Final nozzle plate design

As stated previously the differences between plates 1 and 2 can be seen on the upper surface of the objects. Furthermore, the throat length (T) differs for each. This is because the design constraint of T/W > 1 was to be satisfied. As such, smaller nozzles will have a thinner nozzle plate (like stage 2) and larger 'T' values will suffice for larger nozzles. T/W ratios are also not of much significance in terms of the cutoff diameter of the nozzle plate (Marple & Willeke, 1976).

The S/W ratio has more of an effect on the cutoff diameter and was examined in slightly more detail. The aim was to design the nozzle plates with an S/W ratio of 1 and discern the theoretical cut points. An S/W ratio of ≥ 1 is generally acceptable for round nozzle impactors (Marple & Willeke, 1976).

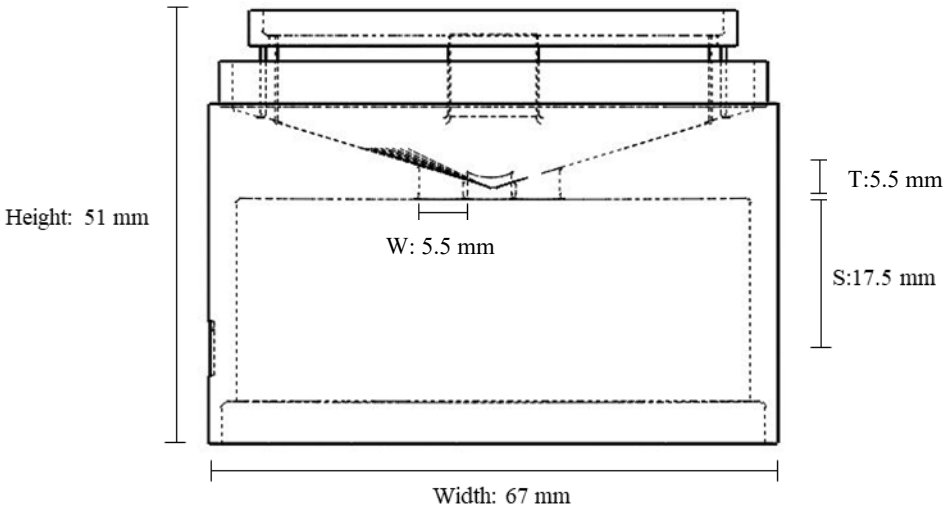

Figure 4-7: Cross Section of nozzle plate 1

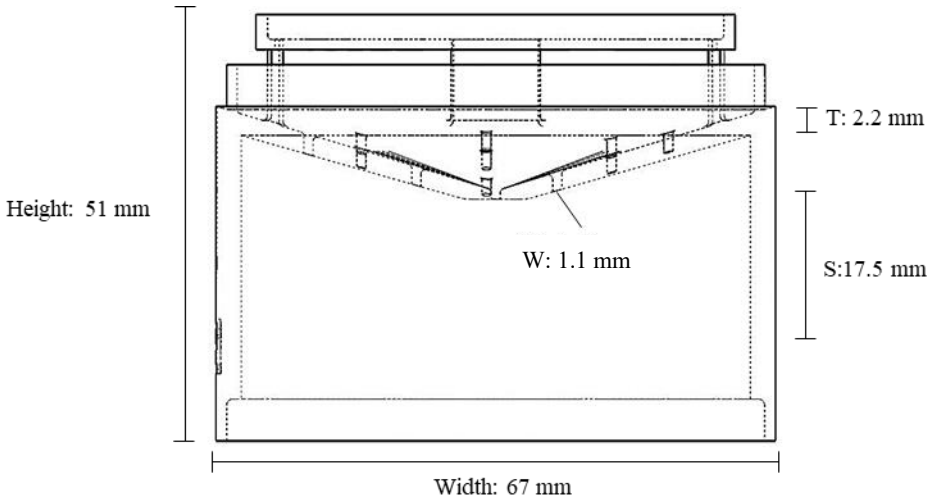

Figure 4-8: Cross Section of nozzle plate 2

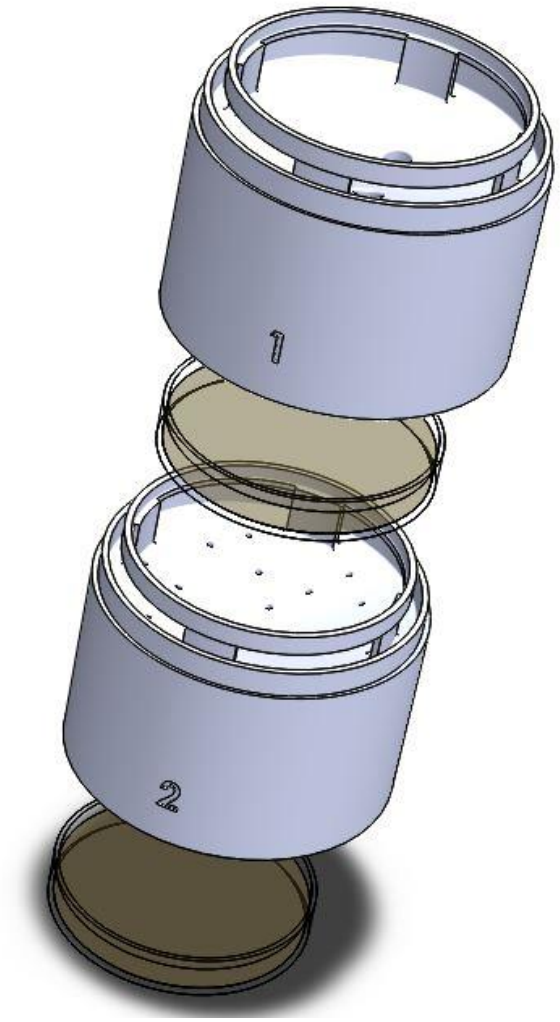

Figure 4-9: Arrangement of nozzle & impaction plates in the impaction cascade

4.1.2 Nozzle Sizing & Arrangement

The size and quantity of nozzles on the plate were designed using the process outlined in Chapter 3. While nozzle arrangement does not have a significant effect on the collection efficiency, research has shown that randomly arranged nozzle exhibit more similar efficiencies (consistency) than other more structured arrangements (Kwon et al., 2002). It was thus decided that the nozzles would be arranged randomly around the plate. Nozzle spacing becomes more apparent at cut points larger than 5µm, hence for this design the nozzle spacing parameter (NSP) was not of much importance (Romay & García-Ruiz, 2023). The NSP is also used to minimise spray through the nozzle. Spray refers to flow that is not contained to the airstreams through the nozzle on impaction very well. This causes lowered efficiency. However, in this instance a more spread-out impaction could be beneficial in that colonies would be more discrete and easier to count.

The design variables for the nozzles were first calculated as described previously. These values served as initial guesses for flow simulation. Flow simulations were performed iteratively to maximise the particle recovery on each stage. This was conducted by leaving one stage's nozzle diameter unchanged and changing the other. The design parameters which had to be satisfied included that the retention efficiency for each stage had to be maximised. The design parameters for the nozzle plates can be found in Table 4-2 below.

Table 4-2: Nozzle plate design outputs

Parameter	**Stage 1**	**Stage 2**
Nozzle diameter (W)	0.55 cm	0.11 cm
Nozzle quantity	3	20
Distance between each nozzle	0.80 cm	0.60 cm
T	0.55 cm	0.22 cm
S	1.75 cm	1.75 cm
T/W	1	2
S/W	3.18	15.9
S/W ≥ 1 ?	YES	YES
T/W ≥ 1?	YES	YES

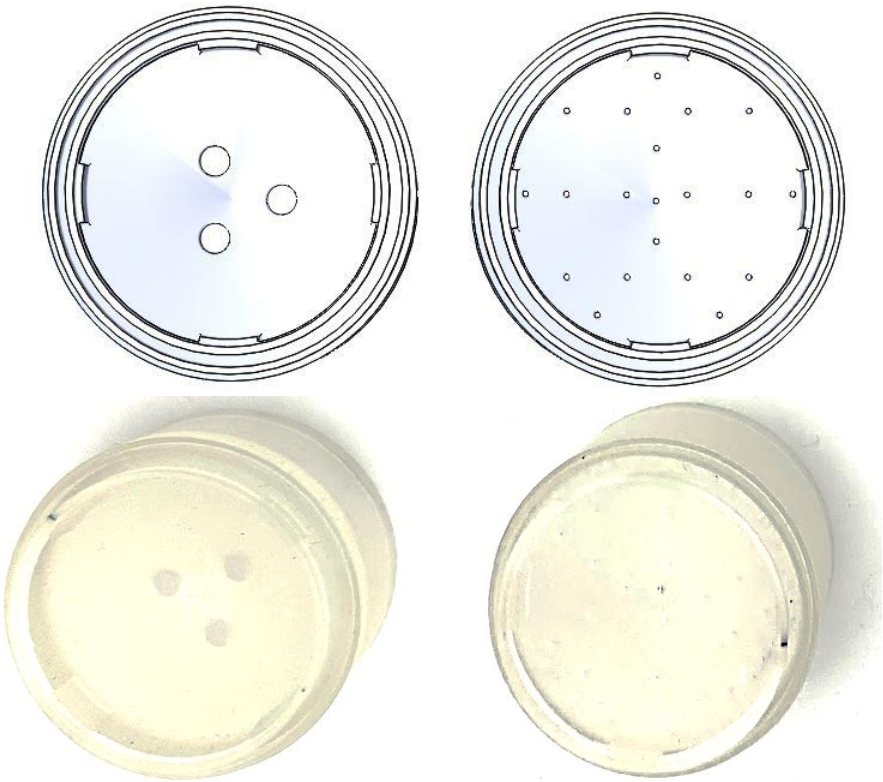

Figure 4-10: Rendered and actual nozzle plates for stage 1 (left) & stage 2 (right)

4.1.3 Impaction Substrate

The impaction plate refers to the part of the cascade which holds the sample. The most crucial aspect of the impaction plate is the substrate chosen. Cascade impactors used for clinical research traditionally use petri dishes filled with agar as the collection surface for sampling (Fennelly, 2020). This is because using agar prepared with Middlebrook 7H10 and 7H11 media helps to grow fastidious bacteria such as *M.tb* as well as increases the chances of detection. It is also the current gold standard medium for culture.

In the redesign of this system, it would be advantageous for the device to include a substrate which is compatible with Nucleic Acid Amplification Testing (NAAT). Therefore, various substrates for sample collection were considered. In searching for the ideal substrate certain qualities needed to be prioritized. This included that the material needed to:

- be biocompatible with *M. tuberculosis* such that the microbes can be collected and cultured off this substrate
- be non-toxic (biosafe)
- be prepared in a disc like formation (easy to insert and remove)
- be stable at room temperature (over a 24h period)
- withstand humidity from coughing
- be *either* soluble in water for culture preparation & rPCR or compatible *with both* methods

The chemical composition of the material itself was an important consideration for the listed reasons. However, since the impaction plates would interact with the bioaerosol on a microbiological level an investigation was conducted into how the chemical and physical surface properties of certain materials could be exploited to increase material capture.

A material property of particular interest is hydrophilicity/hydrophobicity and how this affects the bacterial adherence to a surface. Considering that agar is a universally favourable material for bacterial adhesion & growth, the fact that it is also hydrophilic (Qiao et al., 2019) should not be discounted. While there exist many different properties which could be prioritised for applications such as this, the interplay between hydrophilicity and bacterial adhesion is one of particular interest. It should be noted that research has shown in some cases bacteria (*Escherichia coli, Bacillus sp*.) adhere more readily to hydrophilic structures, while in others – hydrophobic ones (Sutthiwanjampa et al., 2023).

One specific material has garnered attention for this very application. Polyvinyl alcohol (PVA) has exhibited the ability to collect *M.tb* laden bioaerosols for rPCR analysis in clinical settings. Furthermore, it has been reported to be as effective as conventional methods in collecting live *M.tb* organisms via cough aerosol sampling (Williams et al., 2020). PVA also possesses an advantage over agar in that it can be manufactured and stored well in advance while agar plates need to be poured within a couple of hours of use to prevent contamination and desiccation. PVA would be more favourable for use in a

medical device such as Mini CASS as it lends itself to mass production, portability and simpler sample handling. It is non-toxic to humans and bacterial species. It is in fact a hydrophilic material as well, but the correlation between this and its ability to collect *M.tb* has not been well researched. Furthermore, while showing promise in terms of capturing bacterial genetic material, the viability of samples collected on a PVA substrate is not as well documented for this purpose. It was thus decided to assess the suitability of this interesting material for capturing aerosol for culture.

Once the material had been chosen, another aspect came into play – how would this be produced and why? Various methods were researched, beginning with 3D printing as done in previous studies (Williams et al., 2020). Taking this investigation a step further though, it was decided that a consideration of the physical surface properties could be advantageous as well.

Over and above hydrophilicity, another aspect was considered, the impact of an increased surface area on the collection efficiency of a material. This is something that agar in its current form is not easily combined with. Agar is produced by pouring liquid agar into a petri dish and allowing it to set at room temperature. Due to the low melting point it does not lend itself to many different production methods. PVA is a more versatile material in this sense and can be produced by various other methods. One such method which is also known for increased surface area, is electrospinning (Mamun et al., 2021).

Electrospun materials are commonly used as scaffolds in biomedical applications. This is due to their biocompatibility and stability for the intended duration and type of use. There is also the added benefit of being able to combine desired qualities of different materials in one blend (Chen et al., 2021). Electrospun materials are also implemented in filtration systems due to the favourable surface-to-volume ratio (Mamun et al., 2021).

It was thus decided to investigate the applicability of PVA as an impaction substrate (as opposed to agar) in Mini CASS due to its chemical properties. While many other materials could be used, PVA has shown to be promising for precisely the applications of this research. The substrate would be produced in a variety of forms to investigate the influence on physical surface properties on viable bioaerosol collection:

1. A 3D printed version of PVA
2. An electrospun version of PVA
3. A cast PVA disk
4. Agar (control)

The methods included firstly designing a CAD model of the impaction disk on SolidWorks and printing the material (200°C) A fused deposition modelling (FDM) Ender 3 S1 Pro 3D printer (Centro E. Piaggio, University of Pisa) was used to produce the sample from IdroVANISH™ PVA filament shown in Figure 4-11. The product was a 2mm thick disk with a diameter of 40mm (Figure 4-12).

The aim was to second substrate was an electrospun nanofibre mat of mixed PVA/PAA. This entailed considering possible blends, ratios and solvents. This is because PVA alone is so hydrophilic that it dissociates almost immediately on contact with water, especially an electrospun mat which is typically quite thin. Furthermore, electrospinning parameters were varied to obtain the optimal settings for process. The final product was made from a mixture of PVA and Polyacrylic Acid (PAA) of 6 w/v% in water. PAA was used as it is commonly mixed with PAA and provides the thermostability PVA lacks in such low concentrations (Park et al., 2010). For the actual electrospinning a 10 ml syringe was used on a flowrate of 1 ml/h. The voltage was slowly amped up in 30-minute increments to 45000 V and left for 4 hours.

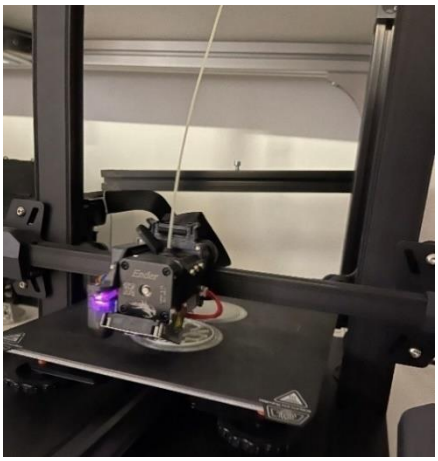

Figure 4-11: 3D printing PVA inserts

Figure 4-12: 3D printed PVA substrate

The ambient temperature was a major concern with regards to electrospinning as this research was conducted in Summer at the University of Pisa. The ideal temperature for electrospinning is below 21°C with low humidity to obtain a successful mat. After some failed iterations a suitable mat was produced as shown in Figure 4-13 and Figure 4-14. The mat thickness was approximately 2mm.

Figure 4-14: Electrospun mat after 4 hours

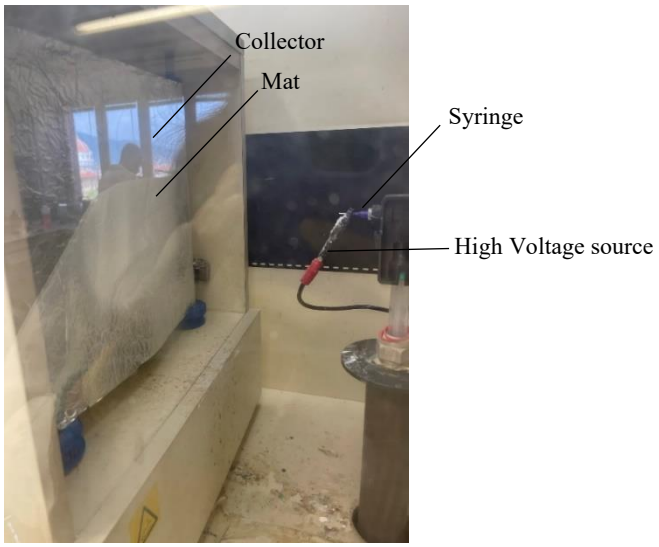

Figure 4-13: Electrospinning setup

The third substrate was created using the same solution prepared for electrospinning but instead using a petri dish as a mould and pouring a 2mm layer into it. As such, it was effectively cast. The petri was left to dry overnight and removed cured the same way the electrospun mat was.

Figure 4-15: Cast PVA/PAA

Figure 4-16: Electrospun & Cast materials post curing

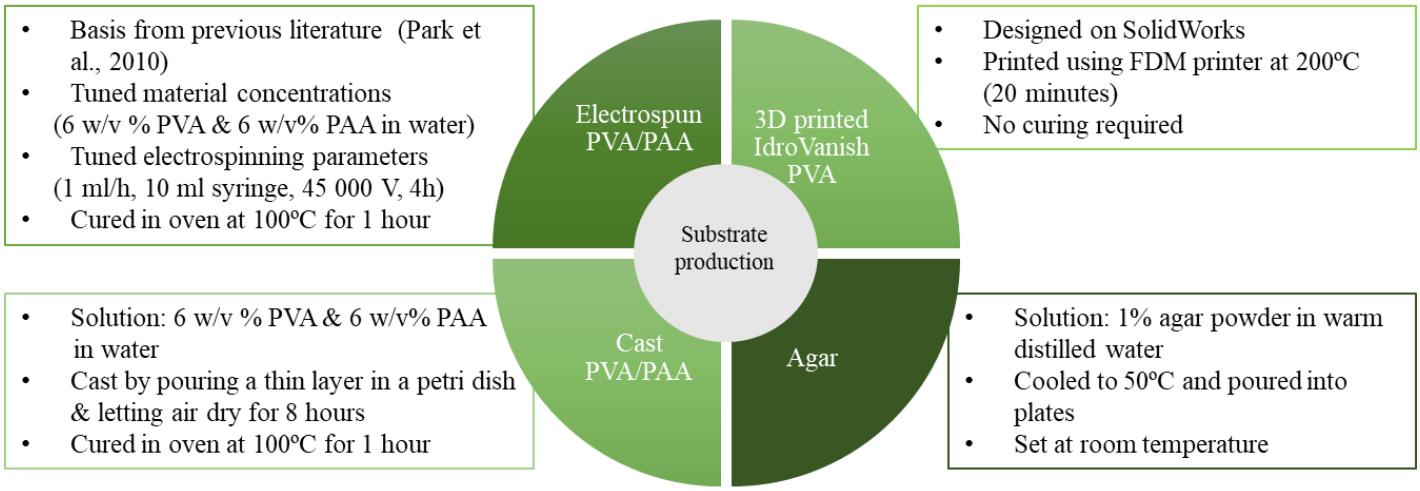

Figure 4-17: Summary of substrate production

Once the substrates were produced, they were assessed in terms of ease of production, where the electrospun mat and cast PVA/PAA blends were ranked as slightly more difficult to manufacture since the solution needed to be mixed well for 30 minutes before use. The 3D printed version is easily manufactured as well as the agar. In terms of being stable in water the electrospun PVA/PAA blends were stable after 1 day in water. This was most likely due to the properties of PAA. The 3D printed version is easily dissolved in water. Agar is soluble in water but that is not applicable since bacteria will be cultured on the agar itself. Figures 4-20 and 4-21 show the stability of the electrospun mat after 12 and 24 hours in water respectively.

The surface area was increased for the electrospun and 3D printed PVA. The cast version and agar both have the minimum surface area due to the smooth texture. Another consideration was how to keep the bacteria alive during the sampling process. When collecting bacteria for rPCR the most important aspect is to collect the genetic material of the bacteria. This type of diagnostic test is based on detection of

DNA/RNA and thus it makes no difference if the specimen are alive or not. However, when collecting bacteria with the intention of culturing them, they need to be living (and stay alive) in order for them to replicate.

Thus, the final and most important substrate test was to determine if these materials could successfully capture *M. smeg* for culture. To do this, an *M. Smeg* solution of 1000 CFU/ml was nebulised on each substrate. The nebuliser was run for 30 seconds each time with the substrate placed 15cm from the nebuliser outlet.

The plates were left to incubate for approximately 48 hours (the average culture time for *M. smeg*) with a check for colony formation every 12 hours. None of the plates aside from the 3D printed PVA successfully were able to culture the bacteria. Comparing the quantity of the colonies produced to that grown on agar, it is evident that the viability on PVA/PAA and PVA alone is substantially less than on agar. This would most likely impact the outcomes of testing the device itself if PVA substrates were to be used in the design.

Ultimately, the reduced culture yield was too high to jeopardize the sampling success of the device. Consequently, it was decided that agar would be used as the impaction substrate of choice (this is currently used in CASS procedures).

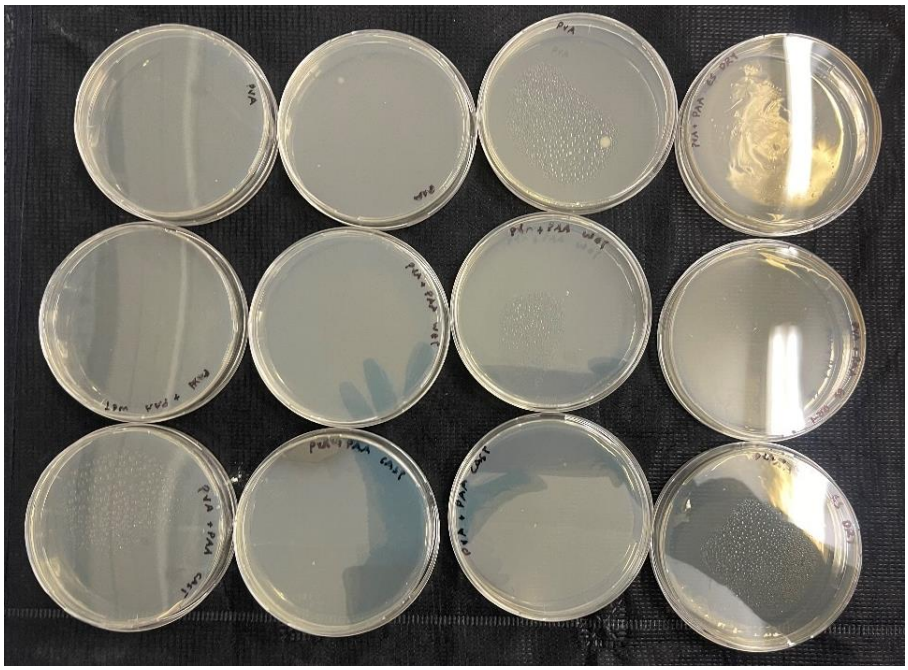

Figure 4-18: M. smegmatis culture results for various PVA substrates

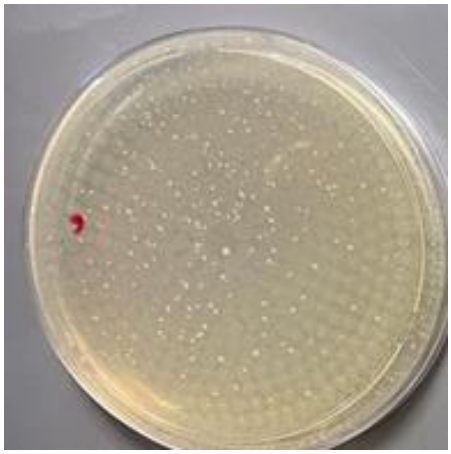

Figure 4-19: M. smeg culture on agar

Table 4-3: Experimental substrate testing results

Substrate	Ease of production of homogenous mat	Stable in water	Surface area increased (compared to current PVA design)	*M. Smegmatis* cultured successfully
Electrospun mat PVA/PAA	Medium	Yes	Yes (maximised)	No
Cast PVA/PAA	Medium	Yes	No	No
3D printed PVA	Easy	Type dependent	Yes	Yes
Agar (Middlebrook treated)	Easy	N/A	No	Yes

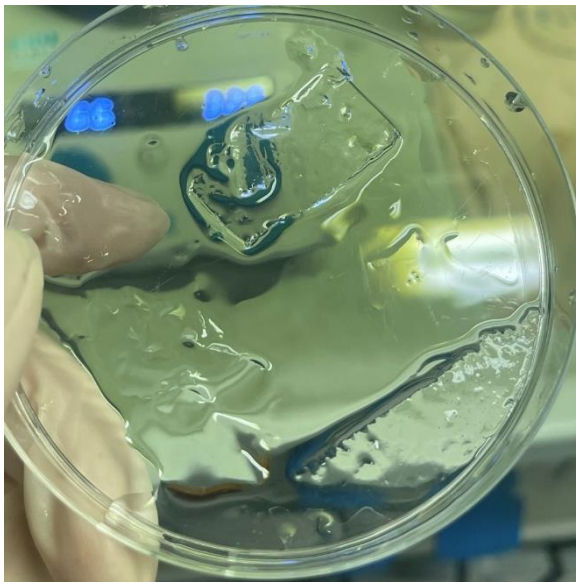

Figure 4-21: Electrospun mat after 24h in water

Figure 4-20: Electrospun mat after 12 hours in water

4.1.4 Impaction Plates

Petri dishes (Falcon® 50mm x 9mm) were used as the impaction plates, as is done with conventional CASS devices. They are clear plastic, sterile plates. Prior to use in the device, they are filled with an agar containing MH9 broth specifically to aid in culture of *M.tb*

Earlier versions of the impaction plate were modelled according to a standard lab petri dish with a diameter of 60 mm and a height of 15 mm. The agar was modelled at the standard thickness of 2 cm. While the impaction plate includes the petri dish and agar, the impaction surface itself is only the face of the agar contacting with the fluid. Taking this into consideration, specific surface parameters were used to model the different material characteristics in this subsystem. SolidWorks Flow Simulation has

three surface characteristics settings with regards to particle studies. These are ‘absorption’, ‘ideal reflection’ and ‘reflection’. For the last option, the tangential and horizontal vectors of reflection can be specified. For the agar surface, ideal absorption was assumed. All other wall conditions in the device were set to ideal reflection. This type of reflection was assumed considering that the reflection would vary from particle to particle.

When simulations were conducted it was noticed that particles that did not immediately impact on the agar surface would experience a bounce-back effect. Particles would be following a streamline around a petri dish but would become trapped between the wall and the agar, ultimately causing losses in the system. This was effectively caused by the height difference between the agar layer and the walls of the petri dish.

To remedy this, the studies were re-conducted with a 4cm thick agar layer to determine if this had influence on the particle losses in this area. As a result, fewer particles were trapped in this manner. Ideally, there should be no height differential between the agar surface and the petri dish wall. Practical considerations included that these dishes need to be sealed during culturing according to biosafety protocol. It is thus suggested that as thick a layer of agar as possible is set by the lab technicians when preparing the dishes for Mini CASS. This would aid in maximum particle recovery on the plates.

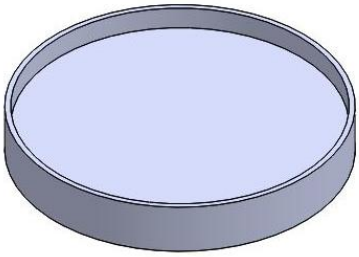

Figure 4-23: Petri design 1

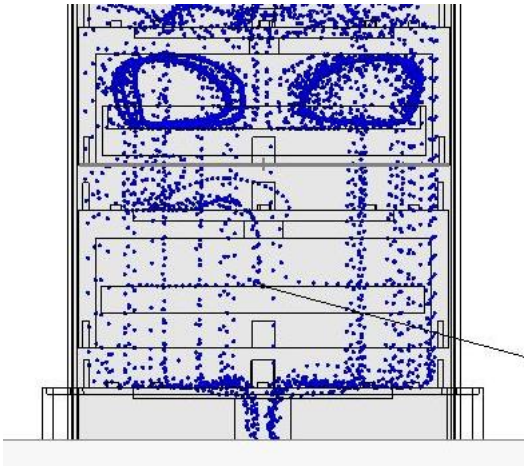

Figure 4-22: Simulated particle interaction with impaction surface

Subsequent particle studies highlighted the issue of particle stagnation, resulting in dead zones above the impaction plate. The cause of this appeared to be that the particles which did not impact the plate were caught on the lip of the petri dish. This resulted in a vortex forming which also reduced the number of particles being carried into the next stage.

Table 4-4: Impaction Cascade Functions & Components

Component	Function
Nozzle Plate 1	Change trajectory for particles with $d > 5\mu m$
Nozzle Plate 2	Change trajectory for particles with $d > 0.5\mu m$
Impaction Plate 1	Collect particles with $d > 5\mu m$
Impaction Plate 2	Collect particles with $d > 0.5\mu m$

4.2 Casing Design

The 'casing' refers to the parts of the device that the patient/user sees and may also personally handle. The aims in the design of this subsystem were to create parts which were easy to use, simple and sturdy. The device also needed to be fully closed off from the external environment by means of this subsystem. The casing design is also linked to the impaction cascade as it houses the second impaction plate, attached to the baseplate. Since the Mini CASS device would be used for field testing there needs to be thought into the aesthetics in this subsystem. Patients need to feel comfortable enough to complete the sampling procedure and not be intimidated by it. This applies to the mask part as well in the 'Mask & Tubing Design' section.

The system was composed of a bottle-like casing which interlocked with the baseplate. The bottle was inspired by the shape and size of a regular drinking bottle, something which is easy to hold and feels/looks familiar. This bottle went through a couple of iterations in conjunction with flow simulations in order to determine the ideal size and shape required. Some design choices regarding the general shape of the bottle will become more apparent in the 'Flow Simulation' section. These parts were also 3D printed with the top section of the baseplate being printed in resin & combined. This was because the ring for the second impaction plate sits on the baseplate. The baseplate also was designed to have much less open space internally so that it was a bit heavier than the hollow bottle. This aimed to help with balance and aligning the bottle straight up if it is held during use. The bottle would be held in the upright position in line with the chest if used in this manner. This subsystem, when closed is 201 cm x 72 cm with a weight of 226g.

An important aspect of this subsystem is the interlocking nature of the bottle and baseplate. These were designed in conjunction with each other. The final bottle and baseplate are shown below with the twist and lock mechanism which fixes the top part of the device to the bottom into place even if the device is rotated 180º.

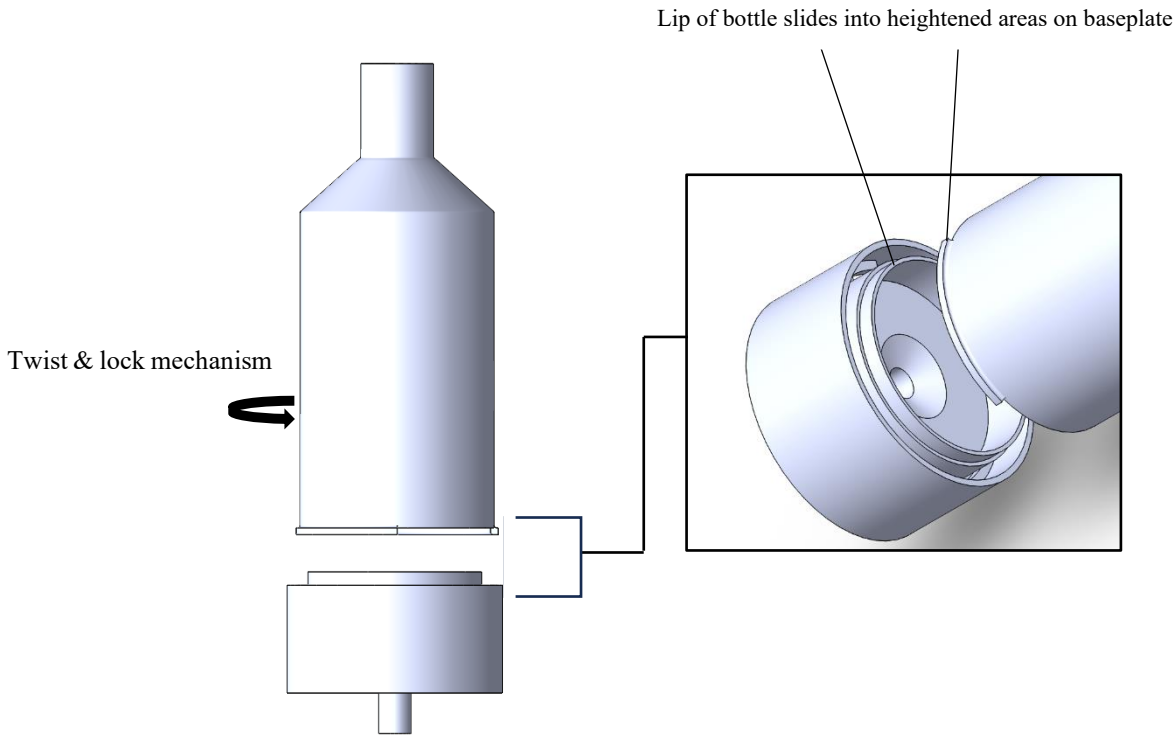

Table 4-5: Casing Components & Functions

Component	Function
Bottle	Enclose the impaction cascade
	Stabilise impaction cascade & fix in vertical direction
Baseplate	Fix casing to a base, weight distribution, attachment for impaction plate 2

Figure 4-24: 3D printed casing, baseplate & nozzle plates

4.3 Pump System Design

The main design requirement for the pump system in the Mini CASS design was that it needed to provide the same vacuum as the pump system used in conventional CASS. This was determined to be 28.3 l/min. Furthermore, in complying with aim of minimising the bulky and heavy current design, the pump system had to weigh less than 1 kg and be smaller than 20 cm x 20 cm x 20 cm. Finding a relatively small vacuum pump which could provide a flow of more than 20l/min at the desired pressure proved to be challenging. However, after considering available options the HLVP10 pump (Kamoer Fluid Tech Shanghai Co., Ltd., China) was chosen as it was the closest to the specified pump specifications. The pump specifications are as follows:

Table 4-6: Summary of pump specifications

Parameter	Value/type
Motor	DC Brushless
Achieved flowrate	≥20L/min
Negative pressure	≤ -58 kPa
Noise	< 70 dB
Weight	450g
Allowable temperature & humidity	0ºC-50ºC (relative humidity < 80%)

Figure 4-25: Kamoer HLVP10 Vacuum Pump

In designing the enclosure, the aim was to create a casing which is portable and lightweight. The design incorporated space for the pump, tubing inlet/outlets and power inlet. The enclosure itself was 3D printed in PLA in two parts. The case should be able to be opened if necessary but was fixed by screws to ensure the pump is covered during operation and transportation. A rocker switch was used as these are easy to operate and are not prone to breakage since there is no spring involved. The pump was attached to the side of the enclosure wall with foam inserts at friction points to reduce movement when

operational. A heat sink was considered but on running the pump for 20 minutes no significant heat was generated and it was decided that this addition was not necessary. This enclosure was 13cm x 21cm and weighed 779g (See Appendix B).

The pump was connected as shown in Figure 4-26. This specific pump can be speed controlled but for the applications of this device this was not necessary since varying the speed and flowrate of the pump could affect the cut point of each stage. Hence, as instructed in the specification sheets the pump was connected to always operate at full speed.

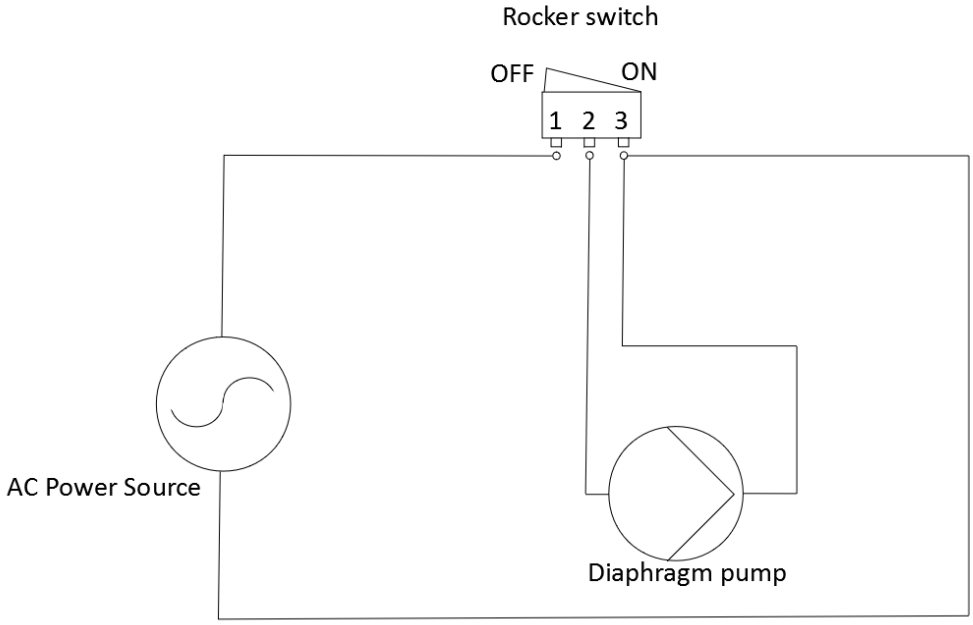

Figure 4-26: Vacuum pump circuitry

The power cable is a standard AC laptop charger which can be connected and disconnected easily for transportation and in case of breakage. The entire electronic system (including the power cabling and transformer) could have been incorporated into the pump enclosure, but this modular design approach was adopted for replaceability of parts while also aiming to reduce bulkiness of the pump housing.

A pump outlet filter needed to be added ahead of the pump to ensure that no particles entered the pump to escape into ambient air. This entailed certain requirements such as pressure drop, pore size and feed conditions. Pressure drop was one of the most important considerations since the pump would be connected upstream of the pump. The filter that was chosen needed to provide relatively low resistance, i.e. the pressure drop over the filter. This is because the pump power should not be compromised such that the effective vacuum is reduced considerably. Furthermore, the filter should remove particles as

small as 0.05µm at a high efficiency considering that re-aerosolising infectious bacteria and viruses is a biohazard. The two most important constraints were thus pressure drop and filtration limits. Pump system components are outlined in Table 4-7.

A Finite High Efficiency Disposable In-Line Filter (Parker Hannifin, USA) was suitable for this system. The IDN-6G filter was chosen based on its applicability to air sampling applications, specifically vacuum and gas impurities. This design also lends itself to moisture removal, which is necessary to protect the pump. This filter is small and lightweight with a width of 3.5 cm, which is advantageous considering the aim of de-bulking the device. It has an allowable pore size of 0.01 micron at 99% efficiency which ensures that bacteria such as *M.tb* will be captured in the filter. It has a maximum allowable pressure of 690 kPa, much higher than operating pressure of the system of -58 kPa. Furthermore, the allowable flowrate is 106 LPM, with the 20 LPM system flowrate well within these limits. The disposability of the filter is also favourable since no maintenance will need to be conducted, instead the filter can be removed and replaced without the risk of contamination from filtered germs. The pressure drop was experimentally checked by setting up the entire device and adding the filter inline. The pressure change is 2 kPa when the filter is added. The effective vacuum supplied is thus 56 kPa.

Figure 4-27: Parker Hannifin Finite Filter 1DN-6G

Table 4-7: Pump System Components

Component	Function
Vacuum Pump	Provide negative pressure to induce constant flow of particles
Rocker Switch	Allow pump to be switched on and off
Internal Wiring	Connect pump to power source and switch
Mounted Jack	Easily connect and disconnect pump to power cable
Power Cable	Connect pump system to power outlet
Inlet filter	Remove particulate matter and moisture ahead of pump
Enclosure	Secure pump and reduce movement when operational. Allow pump to be easily transportable. Mount connections.

Figure 4-28: Assembled pump casing

4.4 Mask Part & Tubing Design

The purpose of the mask was to be the interface between the user and the device. This is one of the areas in current CASS which does not garner much attention but plays a big role in usability of the device. The mask allows for the patient to cough into a space without needing to aim for the orifice of a pipe allow for better usability. The mask was manufactured out of PLA, with KN95 material trimmings as well as an elastic band to fasten the mask over the head. The mask shape was modelled against the contours of the face to create a comfortable and snug fit, minimising gaps.

Figure 4-29: Mask design version 1

The initial designs of the mask were created to discern the best fit and sizing of the mask. Version 1 was of an acceptable size, but the shape was not optimised to the face when tested on a mannequin. It also placed pressure on the nose. This would be an issue in terms of a universal fit as well. The points of incongruity were noted and informed the second version of the design. The approach to design here was that instead of increasing the number of contours on the mask, certain contour were removed entirely. The theory behind this was that instead of trying to match a certain face shape a more universal design could be achieved. For example, the nose contour was left out completely. Ventilation slots were also

added to increase breathability in the mask. These were covered with KN95 material to reduce the spillage of bacteria from the mask. Table 4-8 details the mask part components.

Essentially, version 2 was designed with comfort of the user in mind Figure 4-30. An insert was created for attachment to the tubing (shown in Figure 4-31) which creates a more airtight pathway during sample collection. An elasticated strap can also be added to the design for ease of use, depending on patient preference.

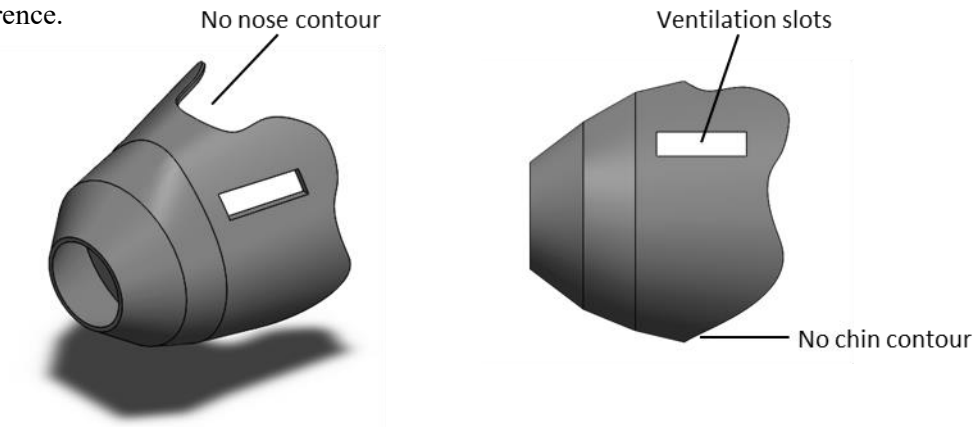

Figure 4-30: Mask design version 2

Figure 4-31: Final mask design

The piping in the device was chosen based on function and connection requirements. Silicon tubing (inner diameter: 1.4cm, thickness 0.4 cm size) was used to connect the pump to the device. Connecting the mask to the impaction cascade is medical grade corrugated aerosol tubing, which is used in ventilator applications etc. This was fit for purpose considering the flexibility and strength of the material. It is also easily replaced if need be. Lastly, ancillary connections were created to fit on either side of the corrugated tubing so as to easily connect and disconnect components. These were 3D printed from PLA.

The whole device as described was evaluated by a Failure Modes and Effects Analysis (FMEA) which is detailed in Appendix C.

Table 4-8: Mask part & tubing component summary

Component	Function
Mask Part	Creates closed space for patient to cough into
Pump Inlet Tube	Connects impaction cascade to the pump
Pump Outlet Tube	Connects to pump outlet, the
Mask-tubing connector	Connect pump to power source and switch
Tubing-bottle connector	Easily connect and disconnect pump to power cable

4.5 Flow Simulation

Once the individual components of the device were designed, they were combined in assembly to confirm the general fit of the components in the device. Once this was confirmed a fluid simulation was conducted. There were three main purposes of the fluid simulation including:

- Confirmation of generally acceptable flow regimes in regions of interest
- Confirmation of interstage and overall pressure drop across the device
- Particle studies to obtain the simulated d_{50} and collection efficiency curves for each stage

The fluid simulation plugin on SolidWorks was used to conduct in-silico tests in order to optimise the design. In particular, fluid simulation & particle study functionalities were used. These tests were conducted once an initial design was frozen as part of the iterative design process as shown in Figure 4-32. This methodology is the detailed process referred to in Figure 3-2 as 'Conduct CFD analysis and calculate efficiency'.

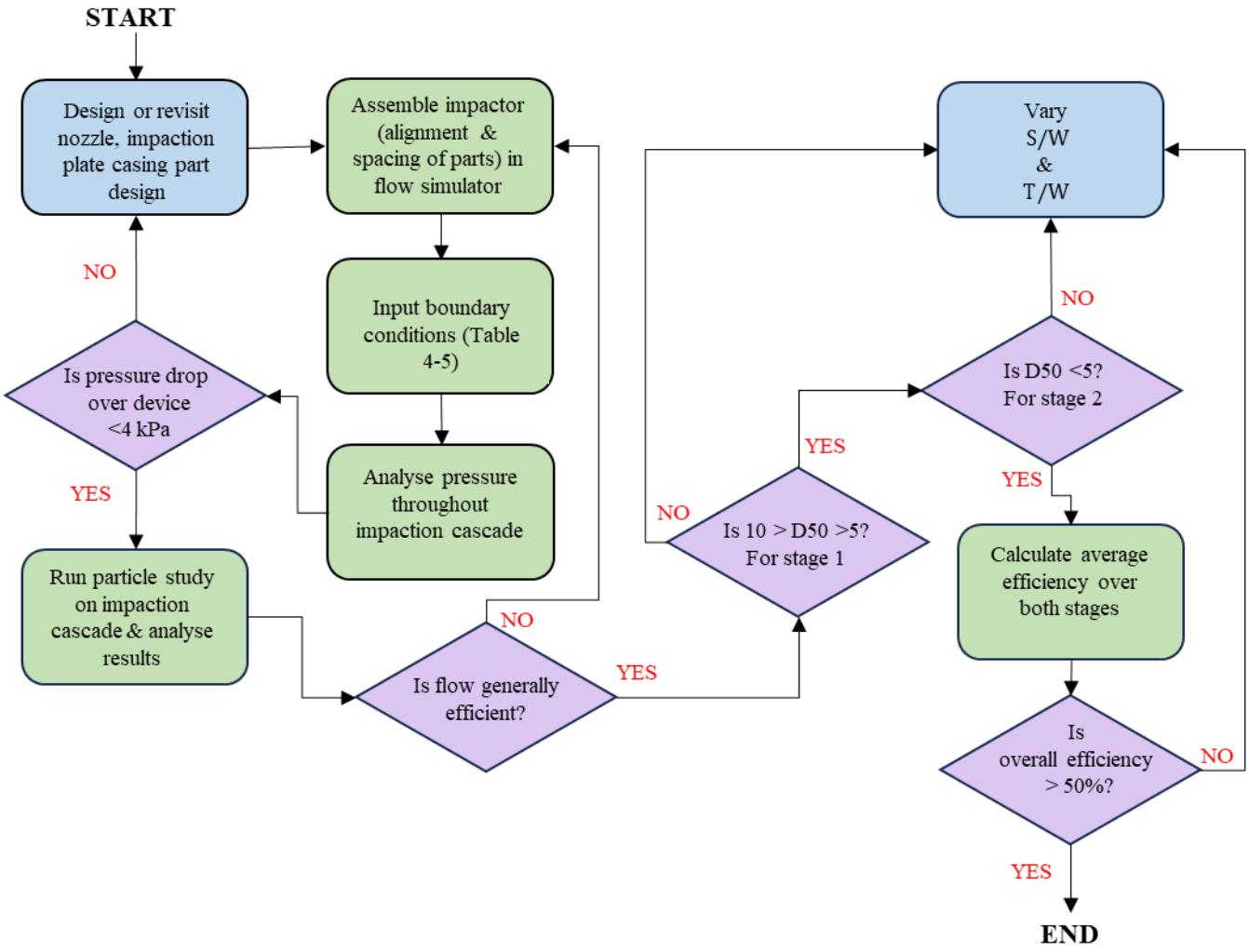

Figure 4-32: Fluid Simulation Approach Algorithm

4.5.1 Study Parameters & Modelling

The impaction cascade was the system of interest for flow studies, this included the nozzle & impaction plates, casing and baseplate. The boundaries for the flow simulation were the inlet lid which would connect to the mask piping and the exit orifice which would connect to the pump inlet filter. The vacuum pump was modelled as an outlet parameter of -55 kPa. This value was informed by experimental tests on the Kamoer Pump. The pressure at the device inlet was assumed to be atmospheric pressure (101.3 kPa). The assumptions and flow simulation parameters used for the flow simulations are found in Table 4-9.

Table 4-9: Summary of Flow Simulation Parameters for the Impaction Cascade

Parameter	Value	Rationale
Inlet volumetric flowrate	20 LPM	From Kamoer pump specification
Outlet pressure	-55 kPa	Experimental deduction
Particle fluid	Water	Cough aerosols can be simplified to be modelled as 100% water
Fluid in device	Air	Feed to the CASS will constitute air & carbon dioxide, simplified to air.
Temperature	293.20 K	Standard temperature
Static Pressure	101325.00 Pa	Standard pressure
Gravitational settings	X & Y t: 0 m/s^2 Z: -9.81 m/s^2	Normal gravitational acceleration
Default wall conditions	Adiabatic wall	Assume no/negligible heat transfer
Mesh generation	Automatic	Sufficiently generated results

In addition to setting up a flow simulation a particle study was enlisted to visualise the flow of particles through the device as well as quantify the number of particles incident on each stage. In this manner *in silico* tests could be run to generate data towards a theoretical collection efficiency curve.

Particle studies were initially conducted to assess if the design of the device was sound and to configure how best to arrange parts in relation to each other (nozzle – impaction plates etc.). The particle size distribution of particles shown were generated using data from literature. The distribution of aerosol diameters in the common cough was used as a basis for the simulation with the assumption of 635 aerosolised particles (Fennelly, 2020; Fennelly et al., 2004). These findings were used to calculate a mass flow rate for each diameter. This mass flow rate could be directly specified in the Flow Simulation Wizard. Particles of sizes 10, 9, 8, 7, 6, 5, 4, 3, 2, 1 and 0.5µm were generated according to the following PSD:

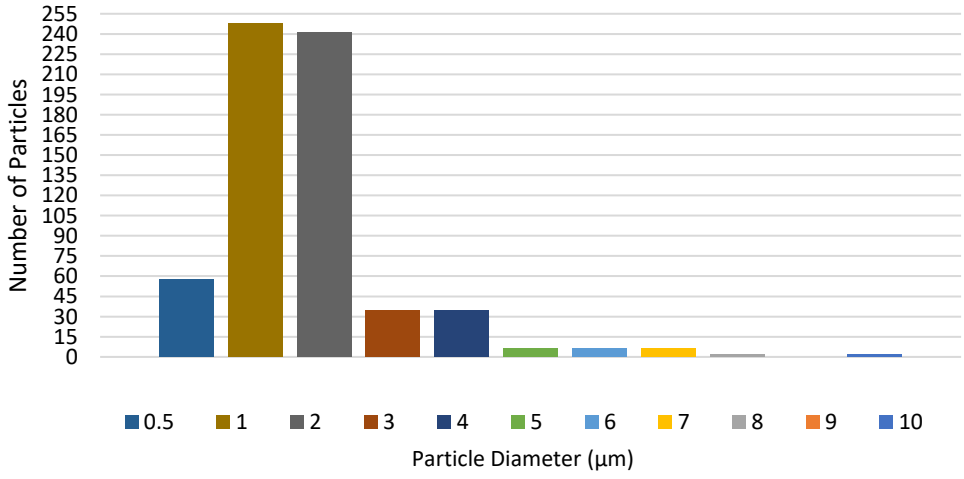

Figure 4-33: Particle Size Distribution for Particle Studies

Particles were injected from the lower surface of the upper lid of the bottle casing in a random arrangement. The particle motion is affected by drag forces, gravity and wall interactions. Cross sectional analysis of the impaction cascade showed the particles following fluid streamlines. These iterations were helpful in assessing general flow.

Over and above this, the particle study was coupled with surface parameter analysis of the impaction plates to analyse the incidence rate of particles at each stage. Further assumptions are required for this tool, including wall conditions. For the purposes of this study the absorbance on the petri dishes (top surface) was set to 1, assuming 100% impaction of particles that are incident on the surface. In reality some degree of particle bounce occurs but this was out of the scope for the initial simulations as more ideal conditions were assumed. All other wall conditions were set to 100% reflection. Practically, these settings simulate an impactor in which if a particle lands on the top surface of the agar, it stays there. If a particle hits any other object in the device it will bounce back. Snapshots from key stages in the design can be found in Appendix A.

4.5.1 General flow & Theoretical Particle Collection efficiency

With regards to the general flow in the device there were some key areas to consider. These included the formation of dead zones or areas where no mixing occurs. Furthermore, ensuring that particles were not leaking into the casing and making sure that some degree of impaction occurs on both stages.

In early flow simulation runs the issue of dead zones became apparent. These are areas resulting in particle entrapment which result in lowered collection efficiencies. This was assumed to be because of the casing shape and the length of the inlet to the first stage. An example of two such occurrences shown below. A significant number of particles become trapped in a loop in the upper portion of the device. This affects the ultimate particle yield in the device as these particles never exit this portion of the device. It was decided that the physical pathway to the first stage should be changed to minimise this effect, similar to what was required for the impaction plates. This entailed creating a longer throat for the particles to flow through before impacting the first stage, which allows the flowrate to slow slightly, decreasing turbulence as well.

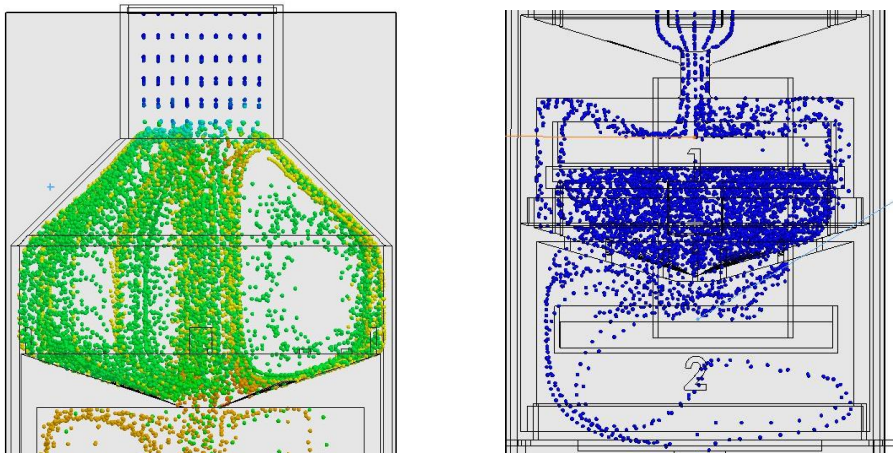

Figure 4-34: Occurrences of particle entrapment in impaction cascade

Another key change that was made in the design process to optimise the flow included altering the S/W ratio. An interplay between the general flow of particles in the device and their respective collection efficiencies exists here. Thus, the particle studies were enlisted to create collection efficiency curves for each stage based on different S/W ratios. Noting this, special care was taken here to confirm that the relationship between the nozzle size and the distance between the nozzle and impaction plate (S/W ratio) was more than 1 as suggested by Marple and Willeke (1976).

Figure 4-35 highlights one of the final flow simulations conducted before the design was frozen. The dead zones at the entrance of the device have been eradicated by means of a longer entry pipe. There seems to be good interaction between particles and both impaction plates. There was a significant amount of pooling between stage 1 and 2. That being said, there was still a significant amount of particle interaction on the second impaction plate. Hence it could have been that particles are not actually stagnating that severely. This could be solved by bettered by altering the S/W ratio of the second plate. However, to properly assess the collection efficiency here the particle study results were analysed while varying said ratio.

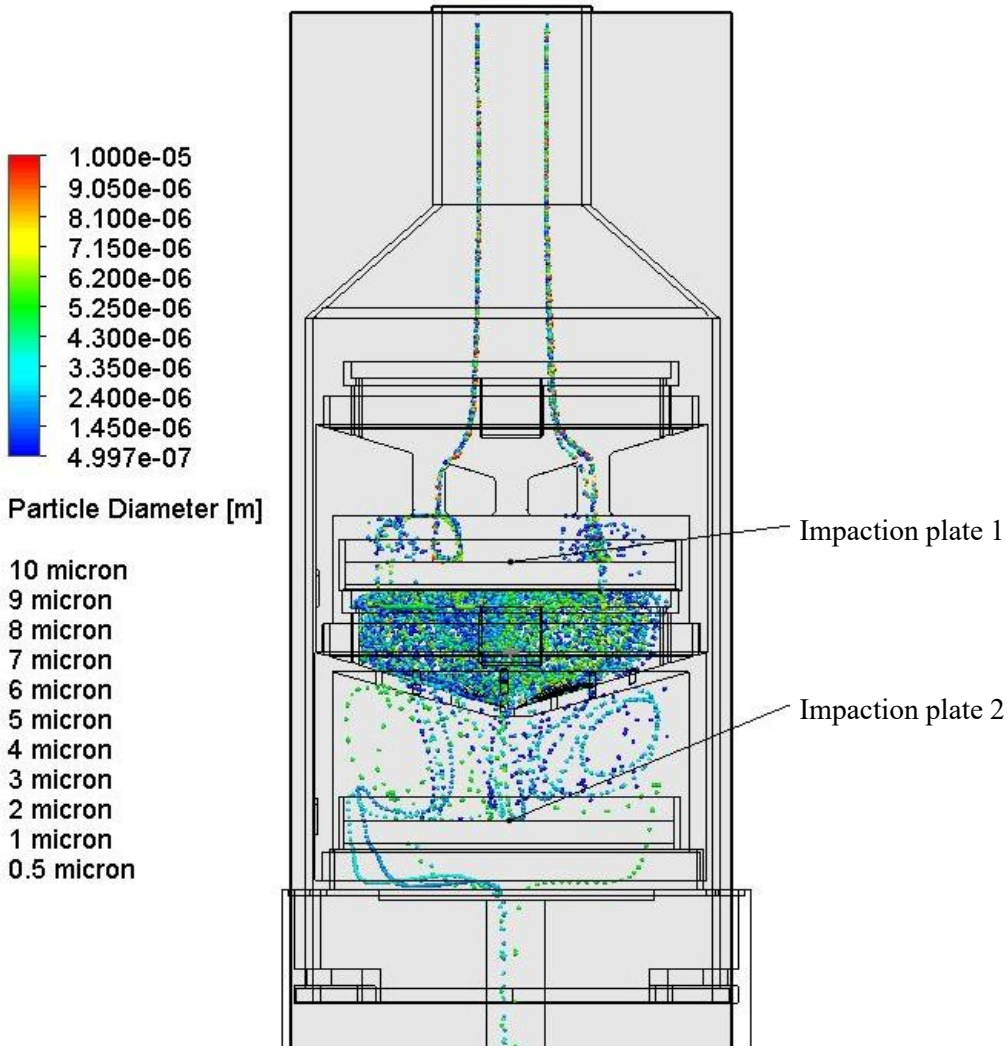

Figure 4-35: reduction of dead zones in impaction cascade

4.5.2 Theoretical Particle Collection Efficiency

The collection efficiency curves shown in Figure 4-36 were generated using the particle counts gathered from the SolidWorks particle studies. General flow to impaction plate 1 indicated that the S/W ratio was sufficient at 3.2. On examination of the produced curve, the collection efficiency increases steadily from 5 to 10µm with a d_{50} of 8µm. While the design d_{50} was 5µm this arrangement would suffice considering the correct range has been achieved by the design. Changing the nozzle plate design at this stage would leave room for the entire range to shift, leading to too little differentiation between stages 1 and 2.

Since the general flow pattern above the second nozzle plate raised concerns, different S/W ratios were chosen and the particle studies were run with these ratios being implemented. Practically, the impaction plate was moved up in certain increments to achieve the different scenarios shown below. The general curve tends less towards the ideal than for stage 1, most likely as a result of the pooling and pressure differentials which exist. It can be deduced that for S/W ratios 8 and 1 more particles with smaller diameters are collected considering that the curves do not start at 0% efficiency where d = 0.5µm. However, there is a sharper gradient at smaller diameters which exists at S/W ratios of 2 and 6.5. This indicates higher collection efficiencies for the particles of interest in stage 2.

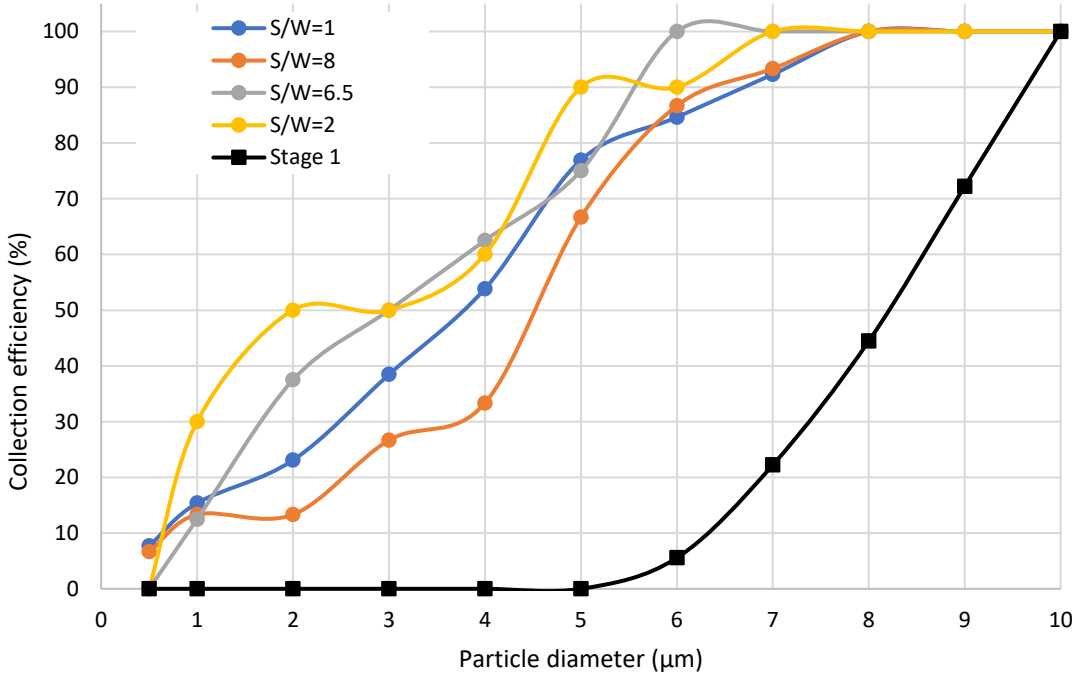

Figure 4-36: Collection Efficiency Curves from Particle Studies

Considering the trends noted in Figure 4-36 were not highly conclusive, it was decided to examine the overall collection efficiencies of the stages. For stage 2, S/W ratios of 2 and 6.5 enabled collection of less than 10 micron. On stage 1, 18 particles were collected. At this juncture, it was important to consider

the original aims of the device, i.e. to collect culturable cough aerosol. It was decided that a higher S/W ratio (8 or more) would be the better choice to ensure that maximum particle collection occurs, so as not to jeopardise the original aim of the device for the second aim of indicating infectivity. As shown in Table 4-2 an S/W ratio of 16 was eventually settled on – which also corresponded to the least backflow and particle entrapment between the nozzle and impaction plates of stage 2.

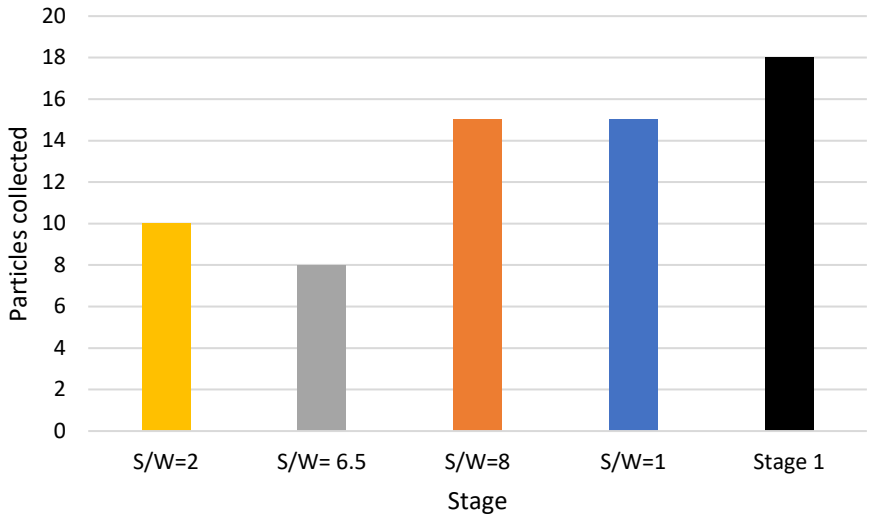

Figure 4-37: Number of particles collected for each stage in flow simulations

4.5.1 Pressure Drop

The pressure changes throughout the device had to be checked to ensure that the design is as airtight as possible. This was the first parameter to be examined. This was because if there were areas of unusual pressure or leaks the overall design would be considered massively flawed. Consequently, other flow simulations would be affected by this. The pressure was analysed by generating a flow simulation with the parameters listed in Table 4-9. Thereafter a cut plot of the pressure was generated by selecting the front plane through the middle of the impactor. The pressure in the system was checked to be in accordance with the initial design constraint of < 4 kPa at 0.4 kPa (Table 4-10.). Furthermore, the average percentage error between the calculated and simulated pressure drop was found to be 27%. Considering the negligible values in pressure drop this is an acceptable percentage error.

Table 4-10: Design vs Simulation Pressure Drop

	Design Pressure Drop (kPa)	**Simulation Results (kPa)**	**% error**
Stage 1	0.0197	<0.058	66%
Stage 2	0.276	<0.348	21%
Total	0.297	<0.405	27%

Since the purpose of the device is to collect bioaerosol, sample containment is very important to minimise the risk of contamination and infection. Analysing the system for leaks and pressure uniformity confirms that the design is sound. The pressure simulation can be found in Figure 4-38. The pressure at the inlet is confirmed to be approximately 55.4 kPa, which is effectively the pump inlet pressure.

There are three important areas to consider in the device. Firstly, confirming the inlet pressure which has been done. Secondly, the at first nozzle plate and second nozzle plate. At the first nozzle plate there is virtually no pressure drop (most likely due to the size of the nozzles). As shown in the magnified cross section (bottom left) there is a more substantial pressure drop across the smaller nozzle sizes (approximately 400 Pa).

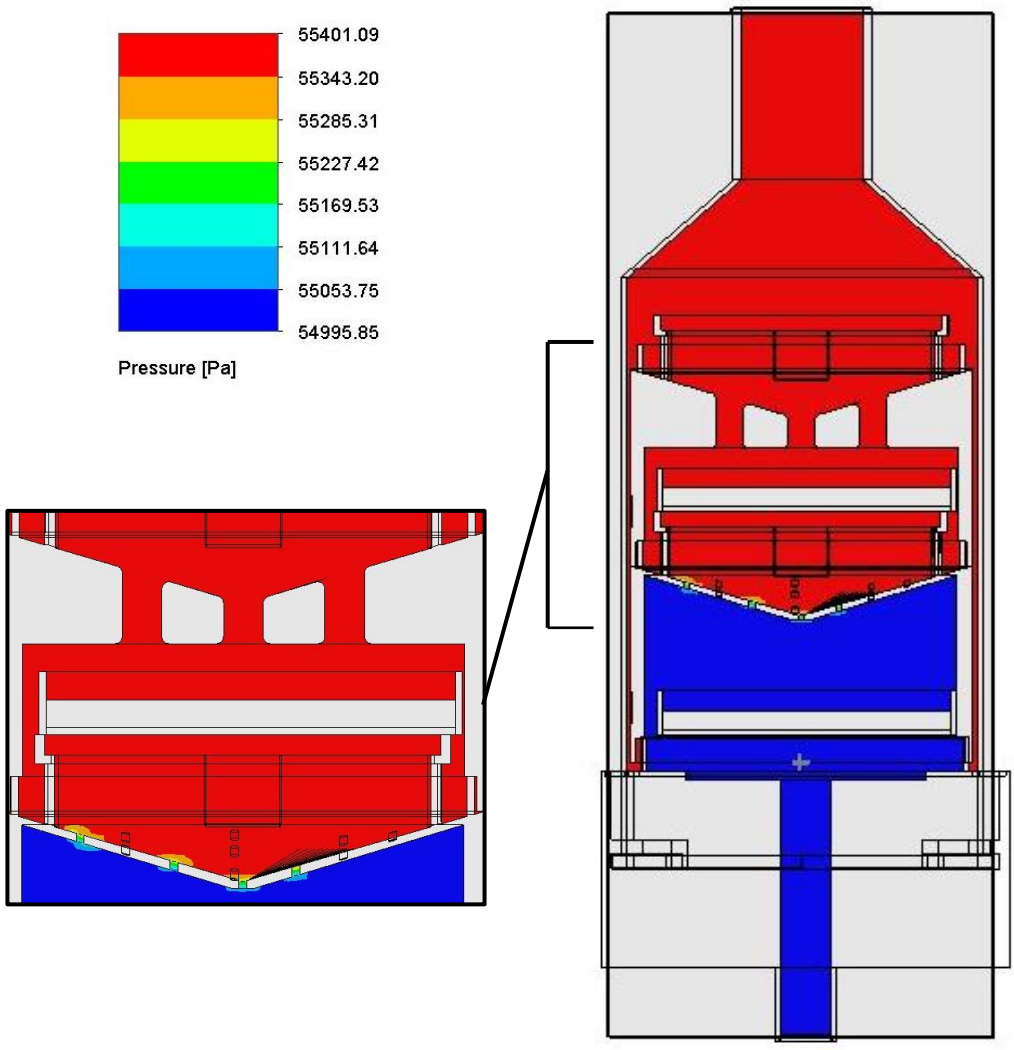

Figure 4-38: Pressure Simulation of Cascade Impactor

4.6 Final Prototype

The final device was produced by combination of all the individually designed subsystems. The full system is assembled by connecting the power cable to the mounted jack on the pump enclosure. Thereafter the impaction cascade is arranged before the bottle is locked in to place. The mask part can then be fastened into the bottle in preparation for use. The fully assembled device weighed 1.0 kg (excluding the power adapter). The time taken to assemble this device was also less than 2 minutes.

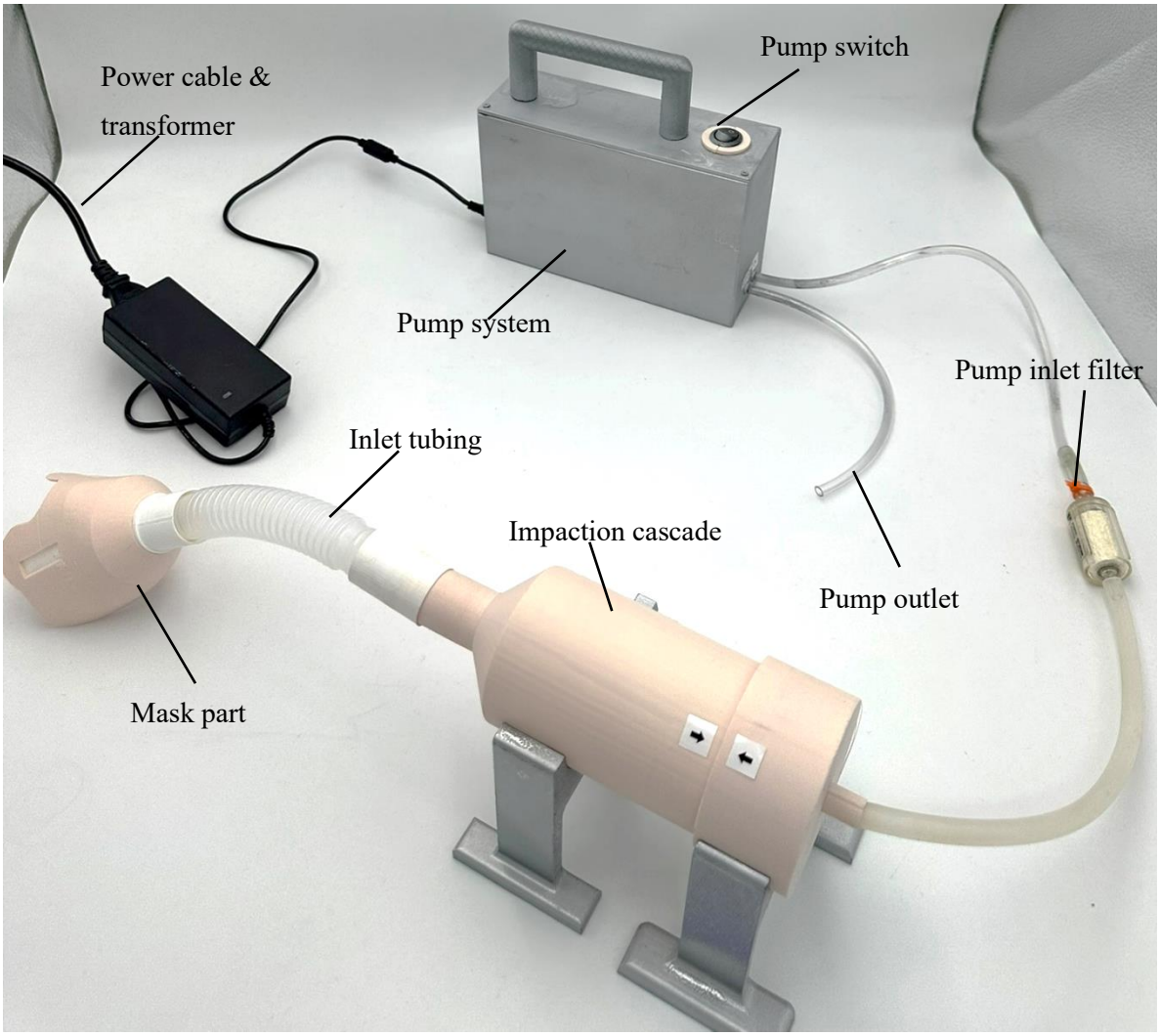

5 Design Verification

The verification stage of the project is a means by which to assess if the device which was built meets the specifications outlined in the device requirements. In the context of this research, this chapter refers to testing aspects specifically pertaining to the design of the device. Simulations informed the device design in the previous chapter. Following on from this physical testing was conducted to confirm that the Mini CASS device works as it was designed. The outcomes for this section can also be compared to that of the simulation. verification testing was focused on 2 main goals:

1. The ability of Mini CASS to fractionate aerosolised particles into two distinct ranges from 10 to 5μm and from 5 to 0.5
2. Confirming that the produced prototype meets the design criteria outlined in the device requirements section.

5.2 5.1 Particle Size Fractionation

5.2.1 Particle Size Fractionation Testing

The purpose of this test is to confirm that the designed device meets the objective of separating the particles entering the device into two size ranges. This, in turn would confirm that the device can assist in making deductions about the infectiousness of the patient. It should be noted that these tests provided no insight into the viability of a sample collected, which will be addressed later in the work. The test was designed to simulate a cough in a reproducible manner so that the number of particles which the device collects on each stage could be monitored. This requires real-time sampling and as such important considerations were made regarding the approach to testing.

5.2.2 Test Considerations

The considerations for this experiment included that the simulated cough needed to be reproducible such that the particles emitted in the experiment exhibit a similar particle size distribution for each run, i.e. consistency was important. Various production methods for aerosol generation were considered including a nebuliser, aerosol spray and asthma inhaler. For the reasons of favourable humidity and relative consistency per spray the asthma pump method was chosen to generate the particles for this test.

A beclomethasone diproprionate metered dose inhaler (Beclate 200μg, Cipla, India) was used to generate the aerosol for this test. This was the aerosol of choice as it was experimentally found to be one of the more consistent forms of aerosol generation. Other options included nebulising medical grade saline and commercial deodorants. However, the former option did not produce high quantities of larger particles such as those with diameters of between 5 & 10μm. In initial tests using the latter method there was very little control over the particle count as this is directly related to actuation force. The asthma inhaler was decided on as it provides a specific dose (200μg of beclomethasone) with every actuation, regardless of force. Furthermore, it is designed to be relatively consistent over the prescribed 200 doses.

To mimic the clinical setting and particle surface interactions, the petri dishes were lined with tissue and paper for the agar height. A thin layer of petroleum jelly was smeared onto the top of the paper to model the surface characteristics of agar.

The pressure in the system also had to be controlled and monitored during this test. The challenge was that the flowrate of the vacuum pump (21 LPM) is much higher than the operating flowrate of that of the particle counter (2.83 LPM). When experimenting with the setup of this test it was found that the particle counter was not measuring if the pump was switched on. It was also postulated that the vacuum from the pump (-58 kPa) could be opposing the vacuum from the particle counter and interfering with the operation. Reducing the pump's vacuum to approximately 3 LPM was considered. However, this would affect the operating flowrate of the device and thus change the particle efficiency curve, so the design of the device would not be verifiable. Also, 3 LPM is much slower than an actual cough (approx. 12 LPM). This would also change the test parameters - resulting in data which is not applicable to verification testing.

Hence the test was designed in such a way that the pump was operational while the aerosolised particles were carried throughout the CASS, and inoperative when the particles neared the particle counter. This would ensure that the two vacuums would not interact with each other while sampling was carried out.

Furthermore, the pressure in the system had to be controlled and monitored using a pressure gauge to ensure that pressure was maintained during the sampling given that the vacuum pump was sampling throughout the process. The pressure calibration test found that the vacuum in the system (with the filter) was maintained at -54kPa with the particle counter switched on. This is 2 kPa lower than the design pressure. The effect of such small changes in pressure on the system was found to be negligible when inputted into the original design algorithm as a check. As such, these discrepancies were considered unavoidable due to the nature of the test, but inconsequential.

5.2.3 Test Methodology

This setup included the full Mini CASS device, the inlet piping, vacuum pump and associated tubes. In addition to this, the Lighthouse Handheld 3016 Particle Counter was used to measure the particles in the exit stream of the device. This device can detect particles with diameters between 0.3 - 25μm. The measurement categories are 0.3, 0.5, 1, 5, 10 and 5μm. The apparatus was arranged as shown in Figure 5-2 with the MDI arranged such that the test could be run as shown in Figure 5-1.

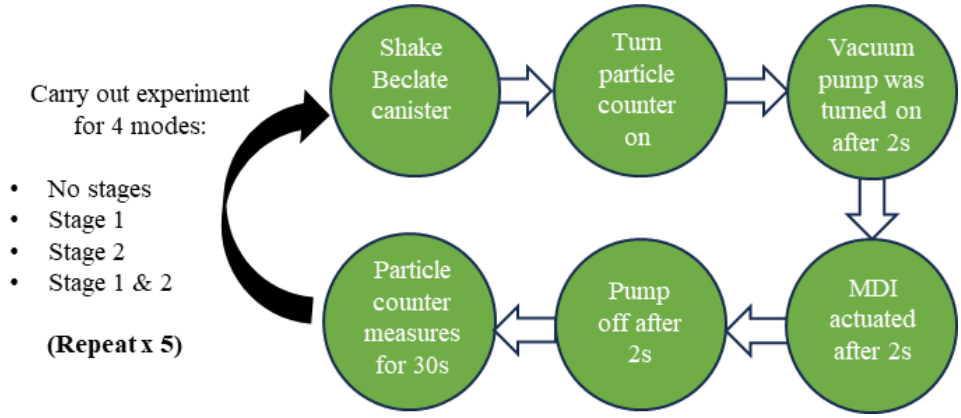

Figure 5-1: Particle size fractionation testing methodology

The duration of the operation of the vacuum pump was experimentally determined in calibration tests. It was found that if the pump was left on for 1 second or 3 seconds there were much fewer particles being reported than at 2 seconds. Thus, it was taken that the optimal sampling time based on the length of pipe and flowrate was 2 seconds. In these 2 seconds the MDI aerosol would flow through until the end of the device. Once the pump was switched off the vacuum from the particle counter at 3 LPM would be sufficient to pull the particles along the remaining pipe length. This 'optimal' sampling time was rechecked for the tests where both stages were installed. This was necessary considering that there is more resistance to flow, and this would mean not all particles may be out of the impaction cascade after 2 seconds. On examination, it was found that the same trend was noticed, 2 seconds was still sufficient for sampling.

There are 4 testing 'modes' referred to in Figure 5-1, these refer to the arrangement of impaction plates and nozzles in the cascade impactor. The configurations were chosen for various reasons. The first mode refers to where no stages or plates are in the impactor. Only the device and casing are used in this mode. This acted as a control for the test. This is because through these tests an average particle count could be established for each particle size range. Using these readings the baseline particle counts could be discerned. This would effectively be used as the basis for the collection efficiency calculations on the assumption that with no other parts in the device, the number of particles in equals the number of particles out.

The second mode constituted placing the first stage and the respective impaction plate into the device. From this the particle collection on stage 1 could be established, The third scenario was the same as the second except instead of the first stage nozzle plate, stage 2's nozzle plate was placed in the device. The fourth scenario emulated the complete use case of the device, where both stages were placed in the casing. Through these modes, various data points could be acquired to create collection efficiency curves and determine cut points for the Mini CASS device. The tests were repeated 5 times to gather enough data points while reducing uncertainty in the sample.

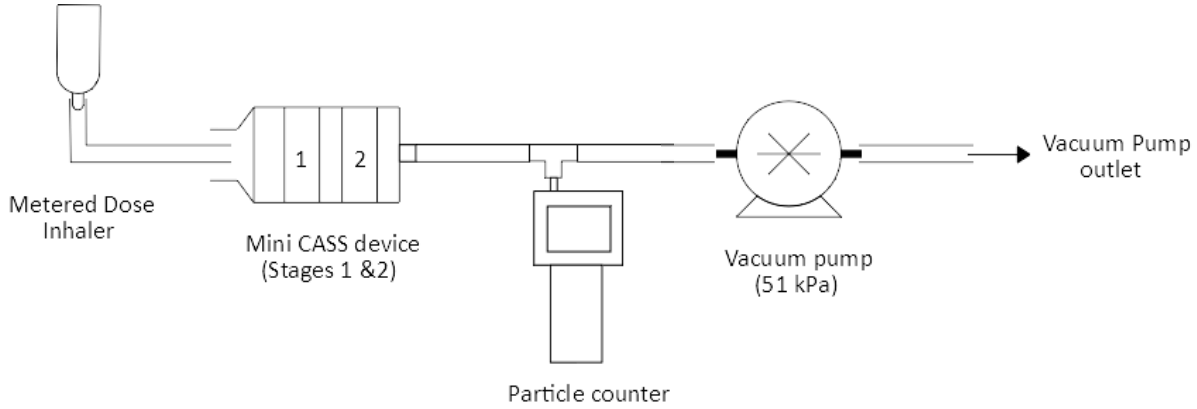

Figure 5-2:Equipment setup for particle size fractionation testing

The particle counter was set to 'differential' count mode. This reflects the number of particles equal to and bigger than the category but smaller than the following category. For example, the 1µm channel describes the number of particles shown with diameters between 1µm and 5µm. The particle counter was recalibrated before every run using the 0.1 CFM purge filter as specified by the manufacturer. The filter was connected and run for 30 seconds. This process was repeated until all particle counts registered as zero. Raw particle count data can be found in Appendix D.

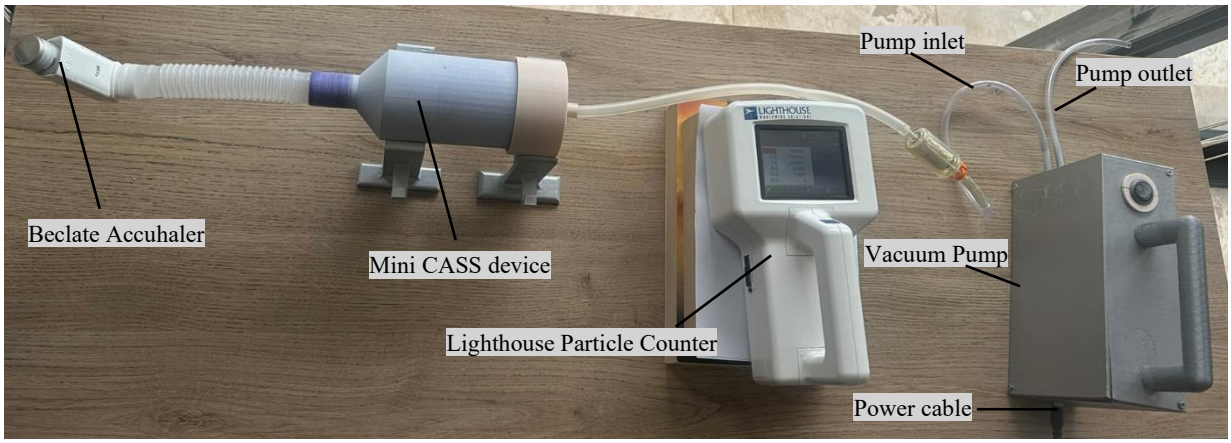

Figure 5-3: Experimental setup for Particle Size Fractionation testing

5.2.4 Testing limitations

Inaccuracies in data collection could be attributed to inconsistencies in a few areas of the testing. This includes the fact that standard deviation in the particle counts is not controlled very easily. While many sources of particle generation were considered this was the method which was the best fit. The standard deviation could be a consequence of the particle counter or the MDI.

5.2.5 Test Results

Table 5-1: Results of Particle Size Fractionation Testing

		0.3 µm	0.5 µm	1.0 µm	5.0 µm	10 µm	25 µm
Control	Number of particles	1258488	1129933	962131	134104	25796	49
	Standard Deviation	128663	115979	105736	32093	10162	27
	% Standard Deviation	10	10	11	24	39	55
Stage 1	Number of particles	940948	827154	688340	89142	14404	17
	Standard Deviation	45644	46264	47565	22796	6024	24
	% Standard Deviation	5	6	7	26	42	144
	Particles retained	317540	302779	273791	44962	11392	33
	% Particle retention	34	37	40	50	79	195
Stage 2	Number of particles	1228898	1129765	993008	188365	44012	126
	Standard Deviation	58208	54626	51020	15735	4101	49
	% Standard Deviation	5	5	5	8	9	39
	Particles retained	29590	168	-30877	-54261	-18216	-77
	% Particle retention	2	0	-3	-40	-71	-155
Stages 1 & 2	Number of particles	592368	515013	410677	25943	1959	9
	Standard Deviation	25143	22839	21675	3545	184	7
	% Standard Deviation	4	4	5	14	9	81
	Particles retained	666120	614920	551454	108161	23837	41
	% Particle retention	53	54	57	81	92	83

Particle retention R of diameter range, d, was calculated according to the following formula:

$$R_d = n_{d,control} - n_{d,run} \qquad \textit{Equation 5-1}$$

Where $n_{control}$ refers to the number of particles in diameter range d in the control run. The number of particles counted in the actual test run are indicated by $n_{d,run}$. The percentage standard deviation vs sample particle size is also exemplified in the error bars shown in Figure 5-4. It is clear that the standard deviation increases with increased particle size. This could be attributed to the fact that as the particle diameters increase, so do the sizes of the ranges in each category. For instance, between 0.3 and 0.5µm there is only a difference of 0.2µm. Conversely, when considering the larger particles, the widest range is between 10 and 25µm – a difference of 15µm. This agrees with the general increase in standard deviation shown over the particle counter measuring ranges. However, it should be noted that the source of this uncertainty is also not known for sure since it could be a result of the MDI or the particle counter.

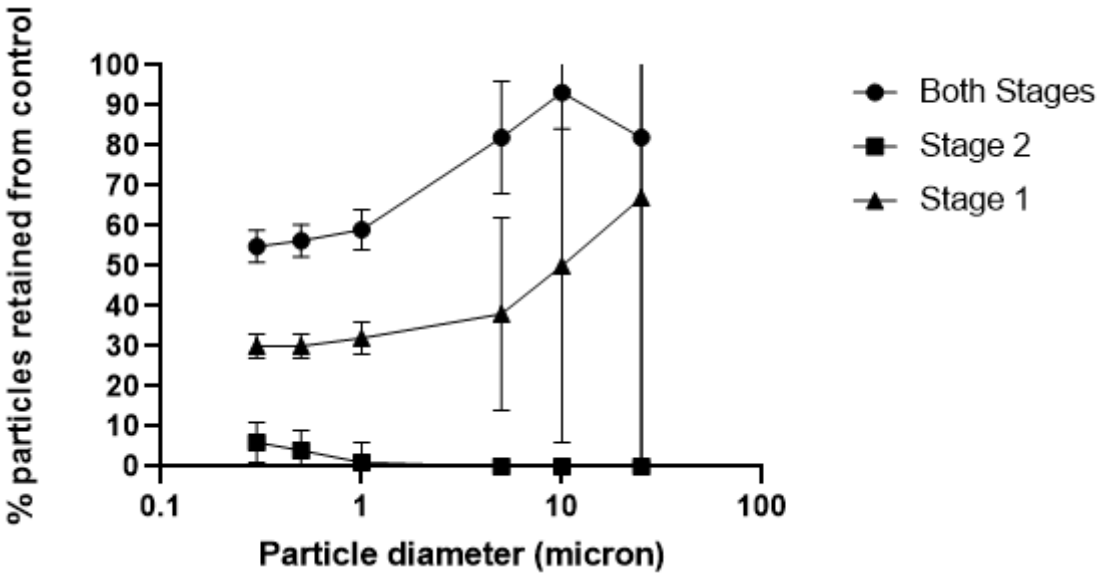

Figure 5-4: Percentage particle retention vs particle size

Figure 5-4: Percentage particle retention vs particle sizeFigure 5-4 describes the particle retention trends for stages 1 and 2 when used in isolation as well as when combined. Particle retention was determined by subtracting the particles collected in these tests from the control tests with no nozzle/impaction plates inside the device.

The verification tests indicate an increasing collection for stage 1 where particles with diameters of 0.3, 0.5 and 1µm are collected at an efficiency of 30%. The curve can be likened to the typical S-shape of an efficiency curve where collection efficiency increases as particle size increases (Marple & Willeke, 1976). Stage 2 exhibited a decreasing collection efficiency as particle size increased, this indicates that the device collected smaller particles on stage 2 – as desired. Particles larger than 1µm in diameter were shown to experience a negative collection efficiency in testing. This implies that there were more particles collected in this test than in the control. This could be attributed to the pooling effect when only stage 2 is used as this incident is not observed in the measurements taken with both stages installed in the device. It is also possible that without stage 1 installed the number of particles in the system exceed the counting threshold of the particle counter. Noting this, negative readings were not included in efficiency calculations.

Considering the fully assembled device, a minimum collection efficiency of 55% is shown for 0.3µm diameter particles. This efficiency is increased to 95% for particle sizes until 10µm. Between 10 and 25µm, collection drops to 82%. Since the margin of error is relatively larger for 25µm readings, these will not be considered in much detail. These are also not of much significance for the purposes of this research which is concerned primarily with respirable particles between 12 and 0.2µm.

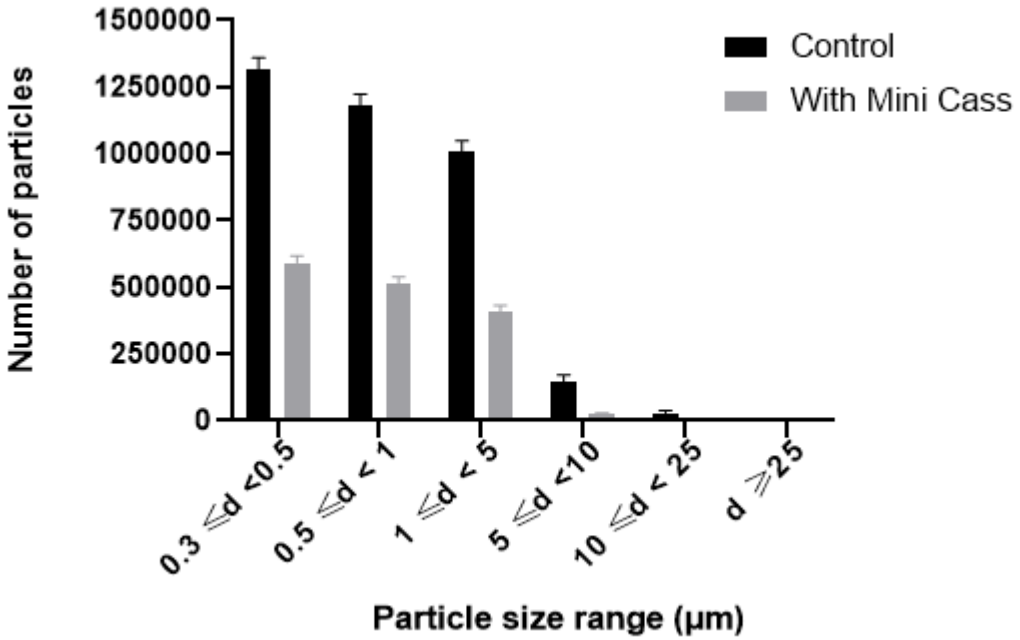

Figure 5-5: Particle counts of control and Mini CASS stages

Figure 5-5 shows the average particle counts in each size range with the fully assembled device (i.e. with both stages 1 and 2 installed). The control particle counts are also shown as a reference. A reduction in particles was noticed in every particle range. This confirms that particles were collected across the stages in the device. The collection efficiency varied from between 53 to 92% as outlined in Table 5-2. The overall collection efficiency of the device was found to be 70%. This proves the ability of the device to collect particles with diameters between 0.3 and 25µm.

Table 5-2: Collection Efficiencies of Mini CASS device

Particle Size (µm)	Collection Efficiency (%)
$0.3 \leq d < 0.5$	53
$0.5 \leq d < 1$	54
$1 \leq d < 5$	57
$5 \leq d < 10$	81
$10 \leq d < 25$	92
$d \geq 25$	83

As per Figure 3-4 in the design methodology section, stage 1 was designed to collect particles between 5 and 10µm. Stage 2 was designed to collect particles between 0.5 and 5µm. There are three particle sampling ranges to examine to determine if these design parameters have been satisfied. Stage 1 is described by the range of $5 \leq d < 10$. Stage 2 falls within two ranges, $0.5 \leq d < 1$ & $1 \leq d < 5$. Considering

this, the overall device collection efficiencies for theoretical stages 1 and 2 are 81% and 56% respectively.

Each stage was also tested independently to discern the particle collection dynamic and actual cutpoint independently of the other. As discussed in the testing limitations section, there are some issues which were considered with this method that may have affected reliability of the results here.

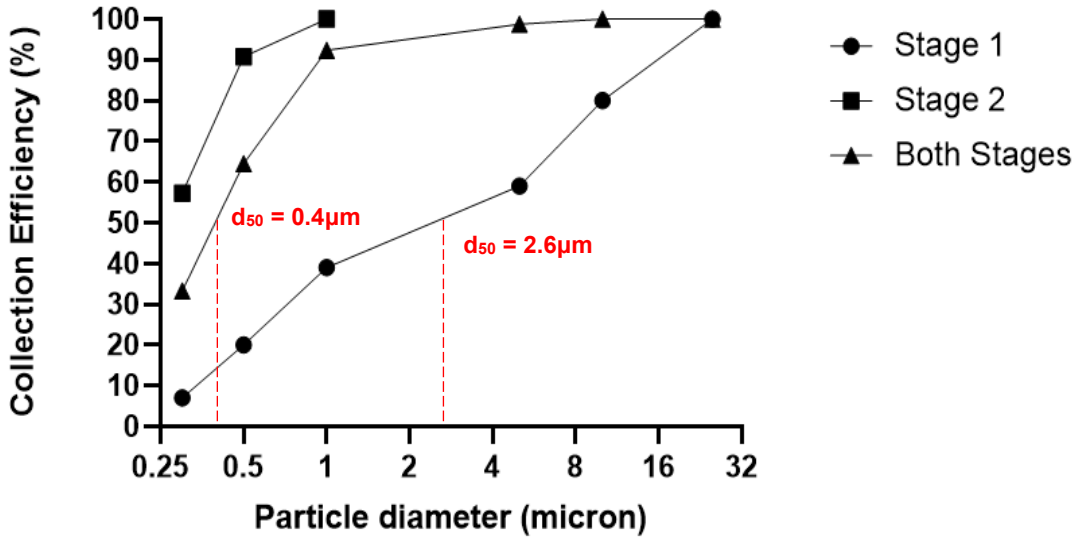

Figure 5-6: Particle collection efficiency curves

Table 5-3: Design vs. Experimental Cut point Diameters

Stage	Designed cut point (as per Figure 3-4)	Corresponding paths (As per Figure 3-4)	Experimental cut point	Corresponding airway (as per Figure 3-4)	Difference
1	10µm>d>5µm	Nasal cavity	10µm>d >2.6µm	Nasal cavity to trachea	1.4µm (28%)
2	5µm >d>0.5µm	Trachea, Primary bronchus to alveoli	2.6µm>d>0.3µm	Primary bronchus to alveoli (some trachea)	0.2µm (40%)

The d_{50} value was acquired from the curve by drawing a horizontal line from 50% efficiency on the y-axis to the curve. At this point a perpendicular was drawn from the curve to the x-axis to determine the d_{50} particle size. The experimentally determined d_{50} (median) diameter for stage 1 was 2.6µm. The designed diameter was approximately 5µm. The d_{50} for the entire device was found to be 0.4µm. The cutoff diameter for stage 2 is less than or equal to 0.3µm as indicated by Figure 5-6. While these diameters deviate from the design they are still be useful in understanding infectivity. Stage 1 still indicates an area of lower infectivity considering the d_{50} falls in the allowable droplet size for the nasal

cavity and tracheal region. Stage 2 indicates a higher infectivity since the d_{50} falls quite comfortably in the allowable droplet size for the alveoli and primary bronchus towards the tracheal region as shown in Figure 2-6.

The deviation from the expected results could be as a consequence of the particle counter detection limits, leaks in the system or insufficiencies in the flow simulation. That being said, the collection ranges are still acceptable in that they correspond to different areas in the respiratory tract, and thus differing infectivity levels. Ideally, further research could aim to improve these results by aiming for a more typical S-curve trend for Stage 2. This could also impact the collection efficiencies more favourably

Requirement	Design Parameter	Acceptable threshold	Achieved value within acceptable limit?
1	Impaction plates which can successfully culture *M.tb*	< 3 colonies of *M. smegmatis* cultured on impaction substrate	Yes. More than 90 colonies cultured on a single agar plate.
2	Capture particles in desired particle size categories	> 50% collection efficiency per stage	Partially. Stage 1 collects particles between 5 & 10µm with 30-50% efficiency. Stage 2 collects particles between 5 and 0.5µm with 28-48% efficiency
3	Simple setup & operation – minimise setup time	Setup time < 5 minutes	Yes. 2 minutes required.
4	Device size (bottle)	Diameter < 15cm, length < 20cm	Partially, device length is 21 cm
5	Total weight	< 1 kg	Yes.
6	Disposable parts & compartmentalized design	3D printed parts	Yes. All parts ahead of vacuum pump 3D printed. Pump can be sterilised for next use and reconnected.
7	3D printed parts	3D printed PLA (FDM)	Disposable parts are 3D printed.

5.3 Device Requirements Verification

Table 4: Summary of device requirements verification test outcomes

6 Design Validation

The validation stage was focused on evaluating the device in a setting which can emulate the practical use case of the technology. These tests are imperative for the assessment of the developed device for real-world applications. The validation tests constituted simulating a cough using mycobacteria (non-hazardous) and culturing these organisms. The outcomes for this included understanding a minimum threshold concentration of bacteria to render sampling successful. Also, understanding the relationship between the vacuum pump and impaction outcomes by testing the device with the pump off. Lastly, comparing the performance of Mini CASS to current commercial CASS technology. The ethics letter for this research (HREC number: 192/2024) can be found in Appendix E.

6.1 Viable Cough Aerosol Testing

Validation of the device constituted lab testing to ensure that the compulsory needs criteria were met. The primary purpose of this test was to determine the ability of the device to collect culturable aerosol particles. The test was designed to confirm that the device 'successfully' collects the cough aerosol. A 'successful' collection in this sense entails that the particles are deposited on the impaction medium in a viable state. A viable state refers to an aerosol droplet which contains live, culturable *Mycobacterium tuberculosis*. Secondary aims of the test included:

- To determine the threshold bacterial concentration for successful culture & compare this to a commercial CASS
- To determine the reliance on the system on the vacuum pump

Essentially, the test protocol was designed to simulate the real, clinical scenario in which the cough aerosol sampling device is used. It was also imperative to control the feed stream concentration to the device so that the capture efficiency could be calculated accurately. In reality this is very difficult to control when the feed stream is a cough from a person. Thus, a cough simulant was chosen instead. It is not practical to aerosolise active mycobacteria as this would risk contamination and increase chances of acquiring TB for those involved in the experiment. As such, suitable alternatives were explored which bore similarities to *M.tb,* specifically mycobacteria. *Mycobacterium smegmatis* was chosen for these experiments due to:

- its likeness to *M.tb* in terms of the bacillus (rod) shape and size;

- it being relatively easy to enumerate – distinct colony formation;
- it takes approximately 3 days to culture, as opposed to *M.tb* – which is a slow growing, fastidious bacterium (can take up to 46 days to culture).

6.2 Solution preparation

The *M. smegmatis* bacteria were cultured and suspended using Middlebrook 7H9 Broth Base (Remel) as medium. The medium was prepared by suspending 4.7g of material in 900 ml demineralised water with 2 ml of glycerol. To ensure sterilisation, the suspension was autoclaved for 10 minutes at 121°C. After cooling to 50°C, the solution was decanted to 450 ml, to which 20 ml of BBL™ Middlebrook OADC Enrichment solution was added.

6.3 Original bacterial concentration

The concentration of *M. smegmatis* in the starting solution was unknown. To determine the original concentration, 50µl of each dilution were plated for culture and enumeration. The colonies formed on these plates could be counted (via CFU assay). Using the 10^5 dilution sample, the number of bacteria in the starting solution could be calculated according to the following relationship:

$$\frac{\#\ of\ colonies\ in\ enumerated\ sample}{50\mu l\ plated} = \frac{\#\ of\ colonies\ in\ original\ sample}{1000\mu l\ of\ 10^5\ dilution}$$

6.4 Testing methodology

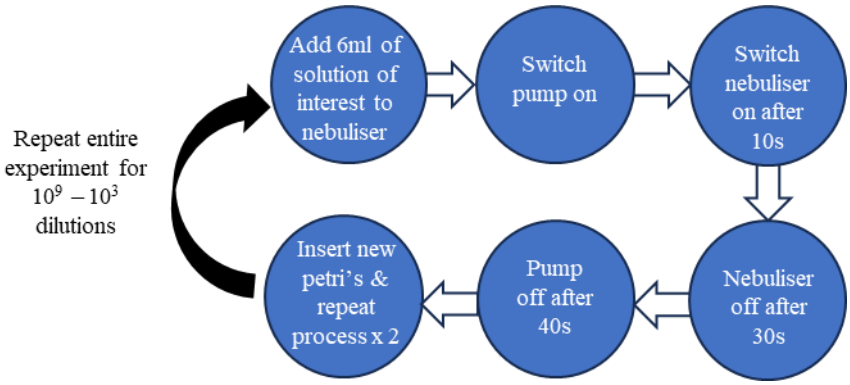

Figure 6-1: Experimental procedure for design validation test

Figure 6-1 describes the experimental procedure that was adhered to. The Mini CASS device and testing equipment were arranged as shown in Figure 6-2. The samples were tested in order of increasing concentration (with the first sample being 10^9 and the last being 10^3). This was done to minimise contamination between test runs. The nebuliser cup was filled to maximum capacity for each run (approximately 6 ml). The nebuliser was tested after each refill, before being connected to the Mini CASS inlet. The pump was run for 10 seconds prior to each run to purge the system of residual particles. The nebuliser was turned on after 30 seconds The actual experiment was conducted in the laboratory at the Centre for Lung Infection and Immunity as shown in Figure 6-3.

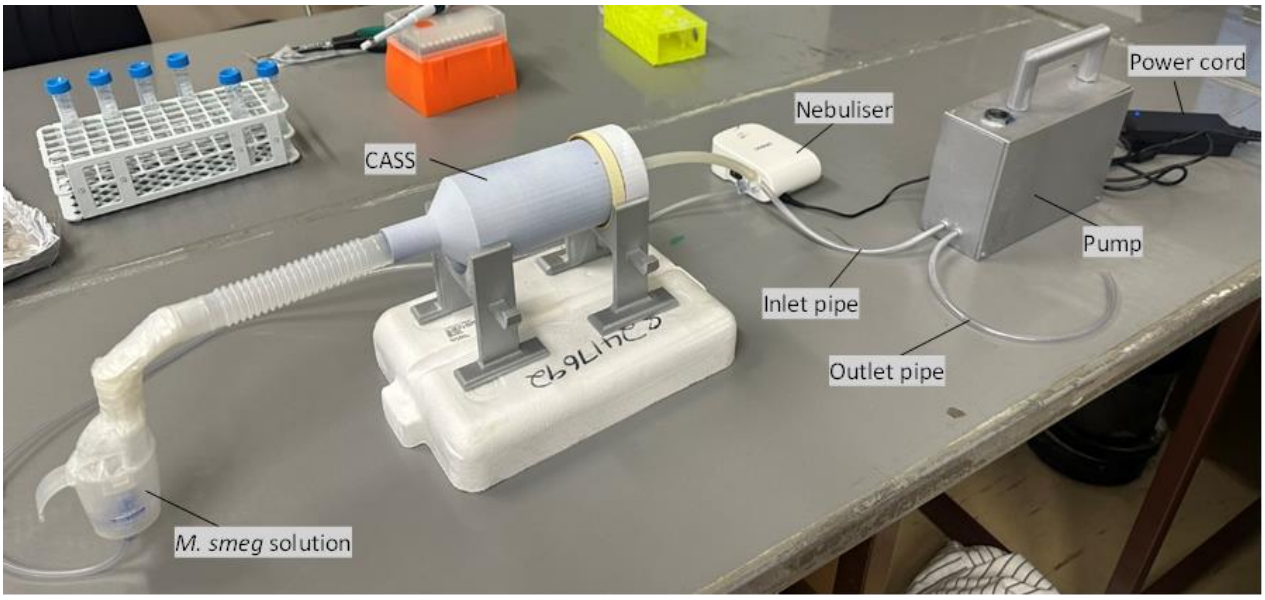

Figure 6-3: Actual Experimental Setup for Viability Testing

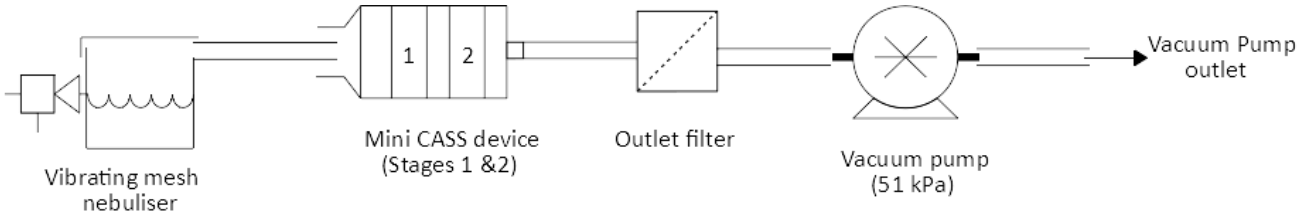

Figure 6-2: Viable cough aerosol sampling test setup

The aforementioned procedure would produce results in the form of colonies on each impaction plate. These could be enumerated to determine if primary & secondary aims were met, such as determining:

1. If the device can successfully collect bioaerosol in a viable state
2. The relationship between solution concentration (bacterial load) and colony formation when using the device
3. The lowest concentration at which the device can yield a successful sample by means of culture

The same test procedure shown in Figure 6-3 was used for the commercial Andersen impactor with the exception that this CASS device & pump were used in place of the Mini CASS device. This will provide a comparison for the new device in terms of aims 2 & 3 above. For the comparative tests, the standard 1m long pipe was used for both the Mini CASS and commercial CASS devices in order to confirm differences in results are not arising from the length of channel only. This test is shown in Figure 6-4 and Figure 6-5 below.

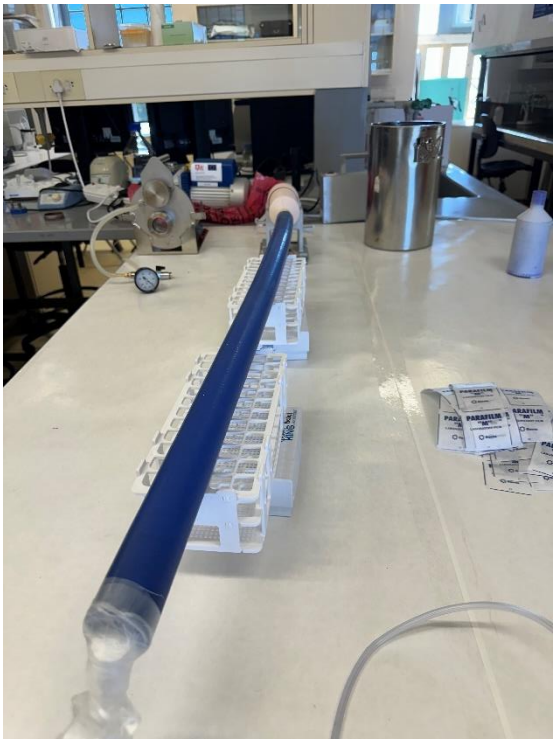

Figure 6-4: Mini CASS setup for comparative testing

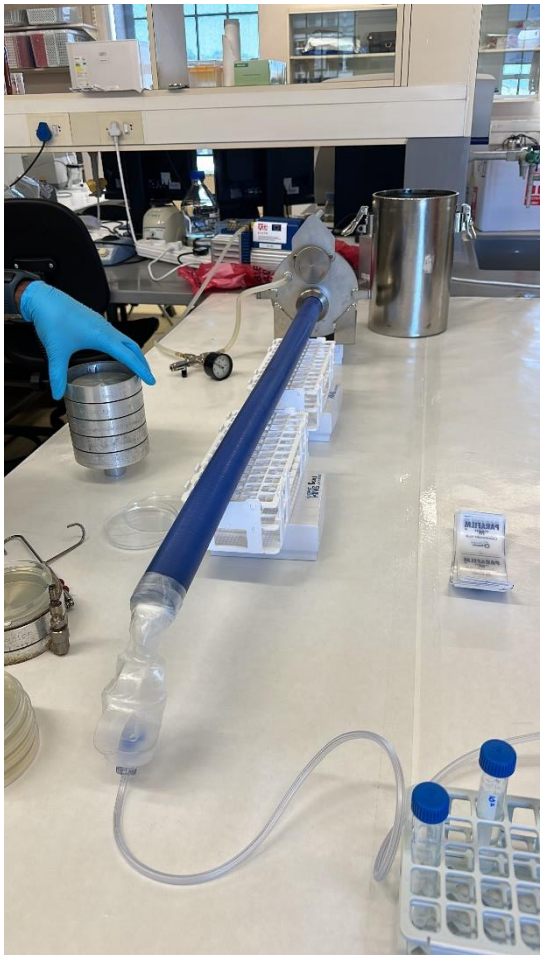

Figure 6-5: CASS setup for comparative testing

The Mini CASS device was connected to the pump by means of silicon tubing (inner diameter: 1.4cm, thickness 0.4 cm size). A filter cloth was also placed ahead of the pump, to collect any large aerosols. For testing, a single stage 8CFM diaphragm pump was used, the same which is used when doing field testing with the cascade impactor at UCT CLII.

Finally, the same procedure shown in Figure 6-1 was used to discern if the Mini CASS device could be used with the pump switched off. The only difference here was that the pump was not switched on at all. The rationale behind this was that if the device could be used without a pump it would reduce the overall size of the technology and reliance on electricity.

6.5 Test limitations

The test limitations for this study included that instead of *M.tb, M. smegmatis* was used in the culture experiments. While *M. smegmatis* may be one of the more similar bacterial strains to *M.tb*, it is much easier and quicker to grow. Furthermore, a pure culture was used in the tests when in reality other bacteria and viruses could land on the plate via cough. This also brings up the topic of *M.tb* being

outcompeted in terms of growth. This means that the success rate with regards to culturing and the magnitude of culture could appear more favourably when using this simulant.

The second consideration is the fact that the volumetric flowrate out of the nebuliser is only 8 LPM at most (experimentally tested via flowmeter), which is less than that of an actual cough (12 LPM).. Some issues with this may be that the degree of backflow in the device is lessened due to the flowrate used. This may need to be revisited in further testing. The solution to these issues would be to develop the test simulation to better emulate the cough of a person.

6.6 Experimental results

The plates were incubated in a 32°C oven and monitored every 12 hours until colonies were relatively distinct. After 72 hours the counts were conducted. Images were taken of the plates and the colonies were counted using the culture counting software ImageJ (National Institutes of Health) for improved accuracy and ease. Microsoft Excel was used to analyse results. The results describe the number of colonies found on each plate. A colony was defined as a distinct circular growth with an approximate radius of between 0.5 and 1mm.

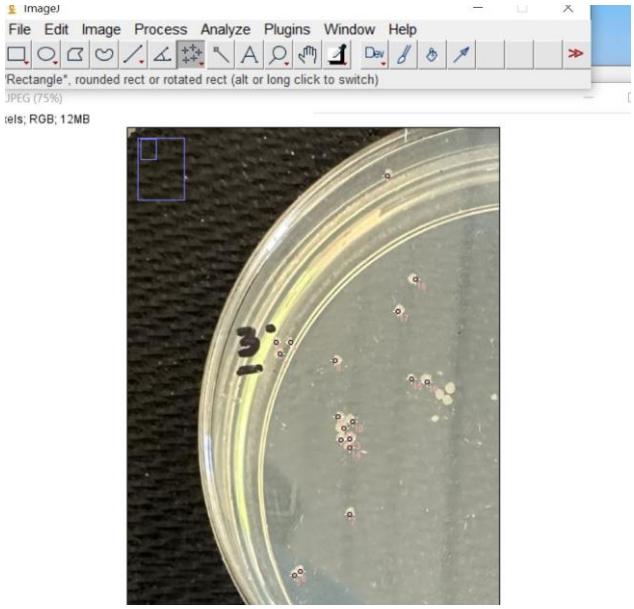

Figure 6-6: ImageJ for particle counting

Table 6-1: Colony counts for each concentration in viability testing of Mini CASS

Dilution	Stage 1 (CFU)	Stage 2 (CFU)
10^3	93 ± 7	50 ± 8
10^4	7 ± 2	3 ± 0.6
10^5	0	0.3 ±0.6
10^6	0	0
10^7	0	0
10^8	0	0
10^9	0	0

The results for the culturable cough aerosol tests can be found in Table 6-1 where the number of colony forming units (CFU's) were counted on each plate. The average of the 3 runs was used (with standard deviation given). The assumption was that each colony on a plate refers to a colony forming unit from one aerosol droplet. The limit of detection is thus 10^5 CFU/ml for stage 2 and 10^4 CFU/ml for stage 1.

6.6.1 Collection of bioaerosol in a viable state

The impaction plates from the viability test prove that *Mycobacterium smegmatis* was successfully cultured for the three solution of the highest concentrations (10^3, 10^4 and 10^5 dilutions). This can be seen in the photos of one set of plates shown in Figure 6-7. One set of plates (top row: stage 1, bottom row: stage 2) is shown as an exemplar for the sample. The columns correlate to the dilutions (left to right: 10^3, 10^4 and 10^5). No colonies grew at lower concentrations, even after 48 hours. Another aspect to note is the distinctive nozzle shape shown, especially for stage 1 where there are more bacteria concentrated in three discrete spaces, particularly in the centre. This can be taken as a confirmation that fluid streamlines are directly hitting the plate as they pass the nozzle, which shows that flow in the device is favourable. Based on enumeration of the 10^5 dilution streak plate, the stock concentration was $2x10^6$ CFU/ml.

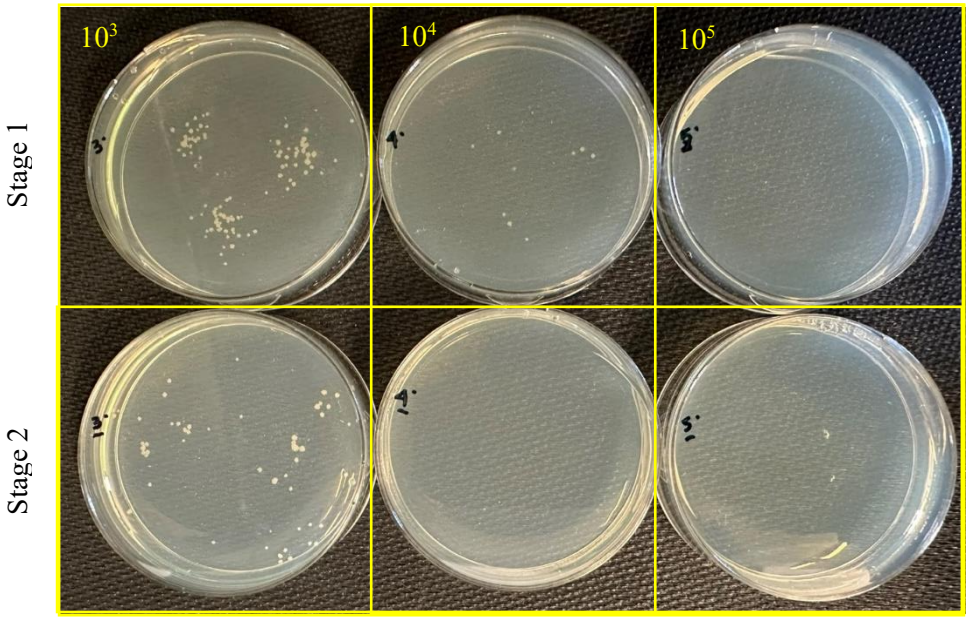

Figure 6-7: M. smegmatis cultured from Mini CASS sampling

Selected plates were also analysed using the Invitrogen™ EVOS™ XL Core Imaging System (Fisher Scientific). This aided in visualising the colonies. It was noted that there do exist limitations in the assumption of 1 colony: 1 CFU since there clearly exist many microbes in 1 colony as seen in Figure 6-8. This does not mean that the colony definitely did not start as one microbe but rather that there may

have been more than one in one aerosol droplet. This kind of assumption is unavoidable and ubiquitous in microbiological experimentation.

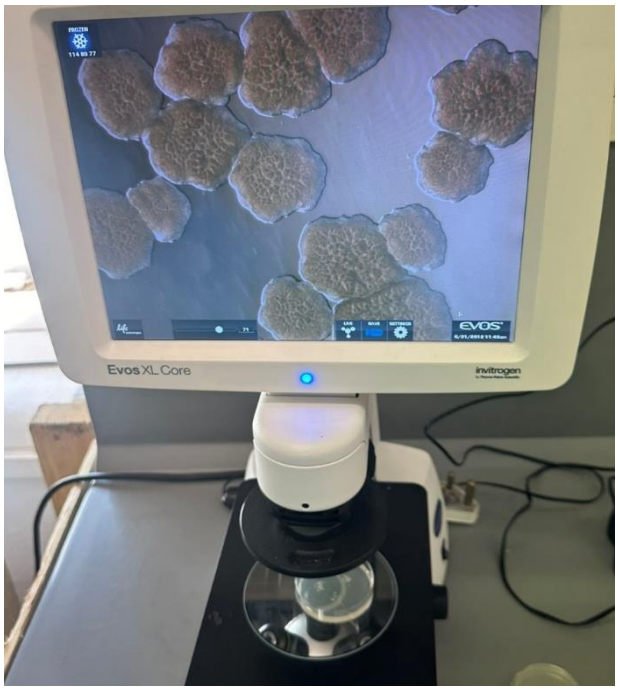

Figure 6-8: Colonies viewed using EVOS™ XL Core Imaging System (x80)

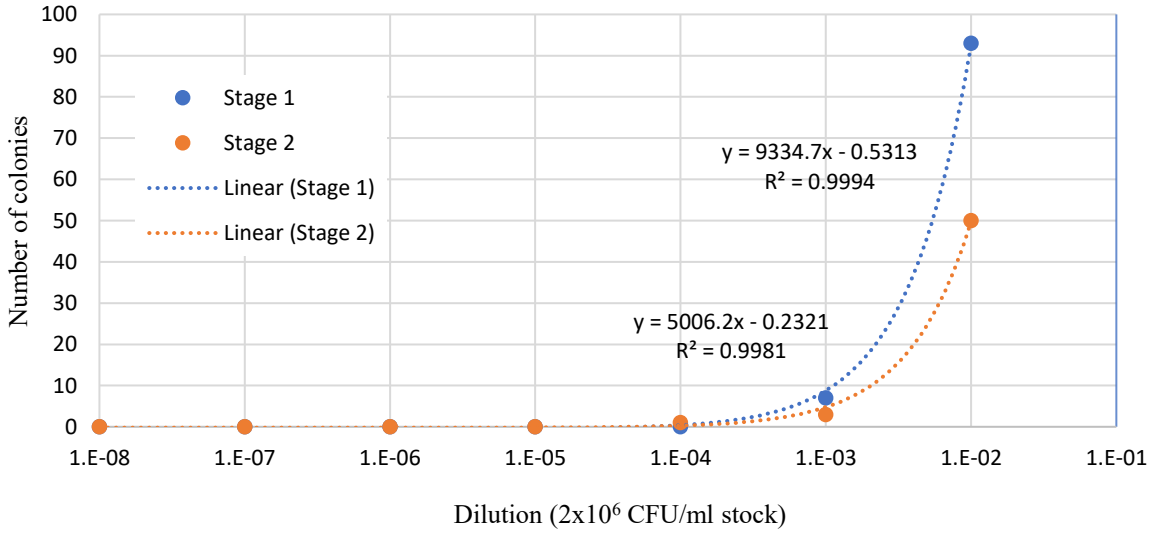

Figure 6-9: Concentration vs number of colonies for stages 1 & 2 in Culturable Cough Aerosol Tests

Figure 6-9 shows the correlation between the effective concentration of the *M. Smeg* solution and the number of CFU's which impact the plate. The trends show that as the solution concentration increases, so do the number of colonies produced. The results also provide an indication of the threshold of device in terms of successful bacterial capture. The colony counts indicate that the threshold concentration to

obtain any sort of results from the device is more than 200 colonies per ml. Assuming a 1:1 ratio of colonies to CFU, the threshold concentration can be taken as 200 CFU/ml.

6.6.2 Comparison of collection rates to current CASS

The next consideration was the comparison of how the commercial CASS device performed in the same type of test. The same test setup was used as described previously with a stock solution to be used for both CASS and Mini CASS devices. To minimise the effect of aspects other than the actual impaction cascade on effectivity the inlet pipe length was kept constant at 1m. 50µl of the 10^4 dilution solution was plated to enumerate the stock, which was found to have a concentration of 2174 CFU/ml.

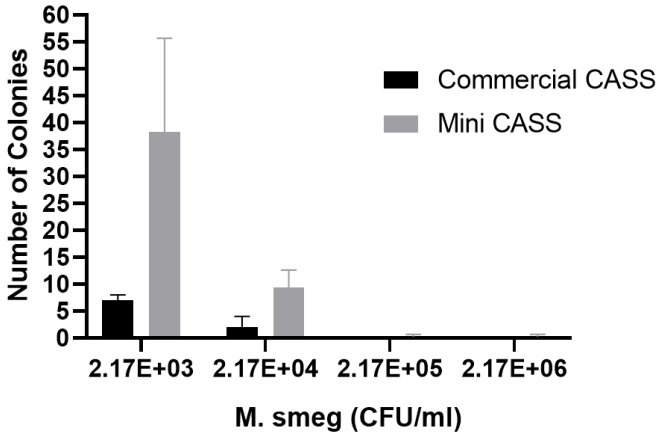

Figure 6-10: Number of colonies vs dilution for Stage 1 (Mini CASS vs Commercial CASS

Figure 6-10 shows the colony counts from the 1st stage of the Andersen impactor and Mini CASS devices corresponding to d_{50} values of 0.65 and 0.4µm respectively. The first stage was used as the comparison considering that it would contain the smallest particles, including 0.4µm. The colony counts indicate that the Mini CASS device outperformed the traditional device in both the 10^3 and 10^4 dilutions. In fact, the Mini CASS device collected almost 5 times as many particles than the commercial device did at the lowest dilution. This implies that the Mini CASS device performs almost 5 times better than the commercial device at collecting smaller particles at lower concentrations. This is a promising finding considering that CASS sampling would in reality entail fewer coughs and thus fewer particles in most cases.

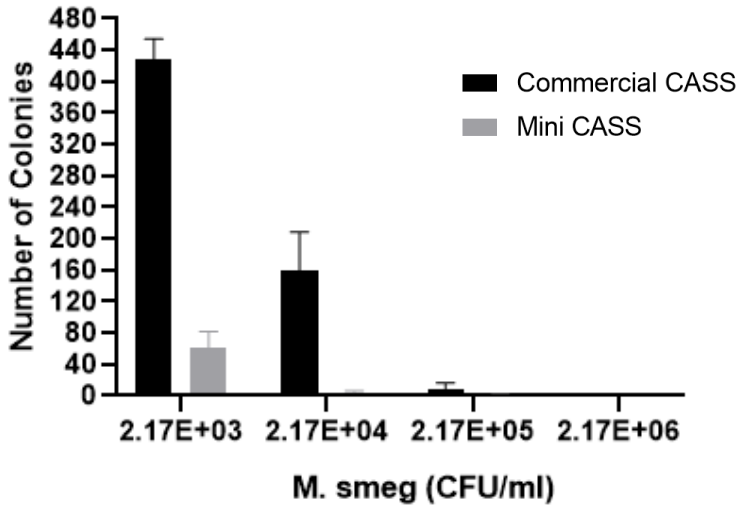

Figure 6-11: Number of colonies vs dilution for Stage 2 (Mini CASS vs Commercial CASS

Figure 6-11 shows the colony counts from the 4th stage of the Andersen impactor corresponding to a d_{50} of 2.1µm. This was chosen as the stage of comparison for stage 2 of Mini CASS considering this stage deals with particles of less than 2.1µm in diameter. The cut point of stage 2 is 2.6µm and thus this stage is the most comparable to commercial CASS. The colony counts indicate that Mini CASS device collected much fewer particles than the commercial CASS did, especially in the lowest solution concentrations. This outlines an issue in the collection capacity of the device when considering larger particles at low concentrations. This is interesting considering the findings associated with stage 1 of the device. Less than 3 colonies each were collected by the Mini CASS device in the lower dilution ranges, this is consistent with the trend for conventional CASS systems for the 10^3 dilution and higher.

The reasoning behind these findings could be due to many factors. Firstly, the nozzle verification for stage 2 was relatively weak in that the selectivity is low. Therefore the actual collection efficiency may not correlate very well with the (assumed) corresponding stage in the normal CASS device.

6.6.1 Effect of Vacuum Pump on Aerosol Collection

As stated previously the highest concentration of bacteria was used for this test, 10^3 dilution. The results from this run are shown with the data collected from the vacuum-on run for comparison. Bacteria were cultured but the yield is substantially lower without the vacuum pump turned on (<10%). It is also highly likely that with such a low yield at a higher bacterial concentration, there will be little to no culture from lower concentrations. Furthermore, as shown in Figure 6-12 there are colonies deposited on the corners of the petri dish from this run. This indicates that there is cross flow in the device and fluid streamlines are not directly impacting the plates as often as desired. That being said, since both plates experienced bacterial growth, the sample is travelling throughout the device. Hence this mode of use could be promising in certain applications – but the effective stage cut points must be determined as they are not known.

Table 6-2: Results for tests with and without vacuum pump

Vacuum	Stage 1 (CFU)	Stage 2 (CFU)
On	93	50
Off	2	4

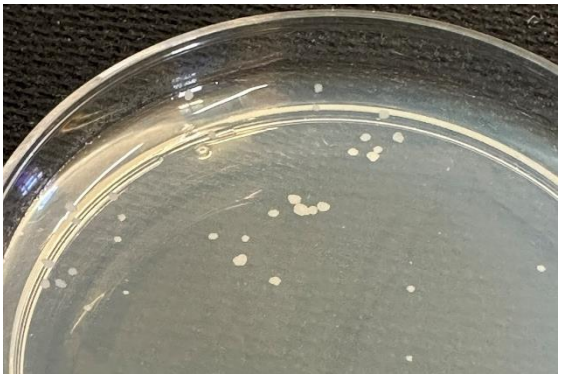

Figure 6-12: Colony deposition on edges of petri with no vacuum

7 Conclusions & Future Work

The aim of this research was to design, develop and test a miniaturised cough aerosol sampling system (Mini CASS) which can collect & size fractionate bioaerosols for diagnostic applications. The primary objectives decided at the start of the project were:

1. To develop a miniaturised cough aerosol sampling system that is portable & partly disposable for *M.tb* sample collection purposes.
2. To optimise the Mini CASS device designs by utilising computational fluid dynamics & evaluating various substrates for particle collection.
3. To test if the device successfully fractionates particles into two distinct size ranges reflecting degrees of infectivity.
4. To test if the device can collect viable and culturable mycobacteria. Furthermore, to compare the efficiency of this device against that of current CASS technology.

At the conclusion of the project, it was found that all objectives were met and the aim of the research was therefore achieved.

7.1 Design Methodology

A comprehensive literature review was conducted which contextualised the need for better sampling solutions for TB patients of interest with sputum scarcity. This highlighted the fact that while there do exist solutions for people who are sputum scarce, they are not optimised for use in a mass testing setting. The cough aerosol sampling system was selected as the technology of choice to be improved. The requirements for the new system included that the device had to collect culturable cough aerosol samples. Furthermore, it needed to fractionate the collected particles based on distinct diameters. It had to meet these requirements while being handheld, portable and partially disposable.

Ideation around possible solutions was conducted to determine the type of device which could be designed. It was decided that a miniaturised cough aerosol sampling system (Mini CASS) would be built. The device was created to provide an alternative to the commercial cough aerosol sampling systems which are bulky and heavy. It was also designed to fractionate particles based on specific levels of infectivity by collection on different stages.

7.2 Device Design, Modelling & Simulation

The design was compartmentalised into subsystems which each had different components and functionalities. These subsystems together make up the final Mini CASS device. Flow simulations and particle studies were conducted on the CAD model during the design and optimisation process. This allowed for analysis of the general flow throughout the device and theoretical collection efficiencies for each stage.

This final design was small enough to carry in two hands, with a total weight of less than 1kg. Furthermore it was designed to be used by the patient, not necessarily the technician. The final design incorporated a 3D printed impaction cascade with agar plates as impaction substrates. Other impaction substrates were also designed using PVA and various production methods. Upon testing, none of these substrates were able to culture *M.smeg* besides the PVA. This was also much less successful than agar, as such the gold standard (agar) was used in the impaction plates for the device. Connections in the cascade impactor were snap fit, designed for ease of assembly and disassembly by technicians. A vacuum pump built into a carrycase with a simply operated switch and a mask was designed with patient comfort in mind. The entire system can be assembled in under 2 minutes.

7.3 Design Verification

The verification of the design entailed evaluating the final prototype against the device requirements outlined in the initial conceptualisation of Mini CASS. The verification testing was primarily aimed at assessing the ability of the impaction cascade to fractionate particles according to their diameters. The size ranges of interest were chosen according to the aerosol sizes which correlate to being more or less likely to cause TB. The first range was from 10 to 5µm, which corresponded to stage 1 in the impaction cascade. Stage 2 was designed to collect particles with diameters between 5 and 0.5µm.

The physical test consisted of arranging the cascade impactor in 4 different modes, which included a control (no nozzle and impaction plates installed), stage 1 only (stage 1 nozzle and impaction plate), stage 2 only (stage 2 nozzle and impaction plate) and finally both stages with their respective impaction plates. Each test was repeated 5 times. Results from these tests were used to calculate the collection efficiencies for each stage. The overall collection efficiency was more than 50% for each particle range. Stage 1 was found to collect particles with 10µm>d >2.6µm. Stage 2 was found to collect particles with 2.6µm>d>0.3µm. These ranges, although varying from the design ones, are still linked to the initial ranges of infectivity as initially desired.

7.4 Design Validation

Validation of the device constituted lab testing to ensure that the compulsory needs criteria were met. The test was conducted by simulating a cough by means of nebulising *M. smeg* into the system, by means of 5 concentrations ranging from low to high. The primary purpose of this test was to determine the ability of the device to collect culturable aerosol particles. A stock solution of pure culture was prepared with 2 million CFU/ml. From this, nebulised solution, culture was only noticed on the three highest of the serial dilutions. The Mini CASS device fares better in detecting smaller particles at lower concentrations than it does with larger particle sizes. It collected 5 times as many particles as the commercial device was capable of collecting. This is an important aspect to consider in terms of proving infectious capability.

7.5 Evaluation of Outcomes

Table 7-1: Design requirements & outcomes

Requirement	Design Parameter	Acceptable threshold	Achieved value within acceptable limit?
1	Impaction plates which can successfully culture *M.tb*	< 3 colonies of *M. smegmatis* cultured on impaction substrate	Yes. More than 90 colonies cultured on a single agar plate. (Chapter 6)
2	Capture particles in desired particle size categories	> 50% collection efficiency per stage	Partially. Stage 1 collects particles between 5 & 10µm with 30-50% efficiency. Stage 2 collects particles between 5 and 0.5µm with 28-48% efficiency. Actual d_{50} values are 2.6 and 0.4µm.
3	Simple setup & operation – minimise setup time	Setup time < 5 minutes	Yes. 2 minutes required (sampled during testing)
4	Device size (bottle)	Diameter < 15cm, length < 20cm	Partially, device length is 21 cm (Chapter 6)
5	Total weight	< 1 kg	Yes (Appendix B)
6	Disposable parts & compartmentalized design	3D printed parts	Yes. All parts ahead of vacuum pump 3D printed. Pump can be sterilised for next use and reconnected.
7	3D printed parts	3D printed PLA (FDM)	Disposable parts are 3D printed.

The outcomes of the research can be evaluated according to the device requirements outlined early on in this research. This dissertation discussed the development and design of a miniaturised Cough Aerosol Sampling System (Mini CASS). The device met almost all of the requirements with some issues with requirement 2, where stage 2 did not exhibit the designed specificity. That being said, the device still exhibits an overall collection efficiency of more than 50% across all particle sizes of interest. This means that it can be utilised to at the very least collect cough aerosol samples of a known diameter, at known efficiencies. These samples could be cultured and further extended to understanding patient infectivity to some point.

While not completely ideal, the device has shown to be promising in the setting of sampling accessibility for sputum scarce tuberculosis patients. This was in the primary aim of the development of this technology. It has also shown to be much easier to use and assemble than the current CASS technology. Furthermore, the fractionation testing can be approached as more of a research tool whereas sample collection is somewhat of a more common issue. The device has proven to achieve the primary goal of

sample collection and being portable with a collection part shorter than 21 cm bottle and a carry case smaller than an average laptop. The device is lightweight with a total weight of approximately 1kg. Assembly during testing showed that the device is also easy to assemble. While there is much to do and test to reach a point where this could be used in an actual clinical set, taking approximately 2 minutes to set up.

Another aspect which was considered was the use of PVA in the device. Various material and material types were used to test the applicability of this material in TB sampling. The benefits of this would be the use of PVA in rPCR sampling, which would increase the throughput of TB sampling *and* diagnosis. Substrate test results were discouraging, with virtually no successful culture of *M. smeg* on the PVA substrates thus standard agar was used instead. Noting all these points, there does exist a baseline proof of concept on which improvements can be made.

7.6 Future Recommendations

In terms of future recommendations for design of the device, there would be value in revisiting the design of stage 2. This would be to refine the stage efficiency and outcomes, which is an important consideration to achieve better verification outcomes. Furthermore, the device was not tested on human subjects. This is an important step to take to validate the design further. Prior to this, the device could be tested with *Mycobacterium tuberculosis* cultures, but this requires biosafety clearances.

Other aspects of the research which could be expanded on include the use of such a device without the vacuum pump – which showed promise but was not entirely explored in this project. Research into other substrates could be conducted, specifically PVA. This material could be explored in more depth, specifically why the produced substrates did not show promise of being a suitable substrate for TB sample collection. In terms of material of construction, stakeholder consultation should be carried out to discern if one time use devices are indeed easier to handle than easily sanitised or partially disposable ones. Further, the substitution of certain parts could be considered, specifically of the mask part (replacement with KN95 mask).

Future work could include that the efficiency of each stage be bettered such that there is a higher level of confidence in the size ranges collected over the 2 stages. Furthermore, preclinical trials could be conducted with *M.tb* instead of simulants to evaluate its performance in tuberculosis sampling. Biosafety would be a concern here. Thereafter, clinical trials could be conducted using this device in a field testing setup. This evaluation could include a usability survey for the technician and user to compare the device to current CASS. Introducing the device to a real setting (e.g. active case finding tests at Brooklyn Chest) would also allow for the verification of its ability to collect viable bioaerosol in a less controlled environment (temperature, humidity, time). Thus, design improvements could be made to mitigate the effect of these factors on bacterial viability.

In terms of taking the device further into regulatory approval and commercialisation, firstly a patent would need to be filed on the design of the system. Furthermore, it would be beneficial to gain some backing from a governmental organisation as well as SAHPRA approval in order to roll a device such as this out on a national scale. This device could fall under a sample collection device and not a diagnostic. Simultaneously it may be of value to begin applying for FDA approval. Once this has been completed, it may be of value to approach the WHO as TB is a global issue and sample collection devices such as these could be helpful in many epidemics in resource poor settings.

8 References

Adams, S., Ehrlich, R., Baatjies, R., Van Zyl-Smit, R. N., Said-Hartley, Q., Dawson, R., & Dheda, K. (2015). Incidence of occupational latent tuberculosis infection in South African healthcare workers. *European Respiratory Journal*, *45*(5), 1364-1373. https://doi.org/10.1183/09031936.00138414

Akullian, A., Vandormael, A., Miller, J. C., Bershteyn, A., Wenger, E., Cuadros, D., Gareta, D., Bärnighausen, T., Herbst, K., & Tanser, F. (2021). Large age shifts in HIV-1 incidence patterns in KwaZulu-Natal, South Africa. *Proceedings of the National Academy of Sciences*, *118*(28), e2013164118. https://doi.org/10.1073/pnas.2013164118

Alsayed, S. S. R., & Gunosewoyo, H. (2023). Tuberculosis: Pathogenesis, Current Treatment Regimens and New Drug Targets. *International Journal of Molecular Sciences*, *24*(6), 5202. https://doi.org/10.3390/ijms24065202

Ayles, H., Mureithi, L., & Simwinga, M. (2022). The state of tuberculosis in South Africa: what does the first national tuberculosis prevalence survey teach us? *The Lancet Infectious Diseases*, *22*(8), 1094-1096. https://doi.org/10.1016/s1473-3099(22)00286-9

Brett, J. L., & Humble, M. W. The BACTEC TB system in the laboratory diagnosis of mycobacterial infection. (0028-8446 (Print)).

Bussi, C., & Gutierrez, M. G. (2019). Mycobacterium tuberculosisinfection of host cells in space and time. *FEMS Microbiology Reviews*, *43*(4), 341-361. https://doi.org/10.1093/femsre/fuz006

Cambau, E., & Drancourt, M. (2014). Steps towards the discovery of Mycobacterium tuberculosis by Robert Koch, 1882. *Clinical Microbiology and Infection*, *20*(3), 196-201. https://doi.org/10.1111/1469-0691.12555

Centre for Disease Control. (2019). *Transmission and Pathogenesis of Tuberculosis* Atlanta

Chen, P., Shi, M., Feng, G.-D., Liu, J.-Y., Wang, B.-J., Shi, X.-D., Ma, L., Liu, X.-D., Yang, Y.-N., Dai, W., Liu, T.-T., He, Y., Li, J.-G., Hao, X.-K., & Zhao, G. (2012). A Highly Efficient Ziehl-Neelsen Stain: Identifying Intracellular Mycobacterium tuberculosis and Improving Detection of Extracellular M. tuberculosis in Cerebrospinal Fluid. *Journal of Clinical Microbiology*, *50*(4), 1166-1170. https://doi.org/10.1128/jcm.05756-11

Chen, S., Gao, J., Yan, E., Wang, Y., Li, Y., Lu, H., Fan, L., Wang, D., & An, Q. (2021). A novel porous composite membrane of PHA/PVA via coupling of electrospinning and spin coating for antibacterial applications. *Materials Letters*, *301*, 130279. https://doi.org/https://doi.org/10.1016/j.matlet.2021.130279

Demokritou, P., Gupta, T., Ferguson, S., & Koutrakis, P. (2002). Development and Laboratory Performance Evaluation of a Personal Cascade Impactor. *Journal of the Air & Waste Management Association*, *52*(10), 1230-1237. https://doi.org/10.1080/10473289.2002.10470855

Esmail, A., Randall, P., Oelofse, S., Tomasicchio, M., Pooran, A., Meldau, R., Makambwa, E., Mottay, L., Jaumdally, S., Calligaro, G. A.-O., Meier, S., de Kock, M., Gumbo, T., Warren, R. M., & Dheda, K. A.-O. Comparison of two diagnostic intervention packages for community-based active case finding for tuberculosis: an open-label randomized controlled trial. (1546-170X (Electronic)).

Falzon, D., Zignol, M., Bastard, M., Floyd, K., & Kasaeva, T. (2023). The impact of the COVID-19 pandemic on the global tuberculosis epidemic. *Frontiers in Immunology*, *14*. https://doi.org/10.3389/fimmu.2023.1234785

Fennelly, K. P. (2020). Particle sizes of infectious aerosols: implications for infection control. *The Lancet Respiratory Medicine*, *8*(9), 914-924. https://doi.org/10.1016/s2213-2600(20)30323-4

Fennelly, K. P., Martyny, J. W., Fulton, K. E., Orme, I. M., Cave, D. M., & Heifets, L. B. (2004). Cough-generated aerosols of Mycobacterium tuberculosis: a new method to study infectiousness. *Am J Respir Crit Care Med*, *169*(5), 604-609. https://doi.org/10.1164/rccm.200308-1101OC

Finlay, W. (2001). *The Mechanics of Inhaled Pharmaceutical Aerosols*.

Gao, N., & Niu, J. (2006). Transient CFD simulation of the respiration process and inter-person exposure assessment. *Building and Environment*, *41*(9), 1214-1222. https://doi.org/10.1016/j.buildenv.2005.05.014

Golovin, M., & Putnam, A. (1962). Inertial impaction on single elements. *Industrial & Engineering Chemistry Fundamentals*, *1*(4), 264-273.

Grinshpun, S. A., Mainelis, G., Trunov, M., Górny, R. L., Sivasubramani, S. K., Adhikari, A., & Reponen, T. (2005). Collection of airborne spores by circular single-stage impactors with small jet-to-plate distance. *Journal of Aerosol Science*, *36*(5), 575-591. https://doi.org/https://doi.org/10.1016/j.jaerosci.2004.06.078

Gussman, R. A. (1969). On the Aerosol Particle Slip Correction Factor. *Journal of Applied Meteorology (1962-1982)*, *8*(6), 999-1001. http://www.jstor.org/stable/26174715

Jones-López, E. C., Namugga, O., Mumbowa, F., Ssebidandi, M., Mbabazi, O., Moine, S., Mboowa, G., Fox, M. P., Reilly, N., Ayakaka, I., Kim, S., Okwera, A., Joloba, M., & Fennelly, K. P. (2013). Cough Aerosols of Mycobacterium tuberculosis Predict New Infection. A Household Contact Study. *American Journal of Respiratory and Critical Care Medicine*, *187*(9), 1007-1015. https://doi.org/10.1164/rccm.201208-1422oc

Kaneda, Y., Ishihara, T., Morishita, K., Yokokawa, M., & Uno, A. (2021). Statistics of local Reynolds number in box turbulence: ratio of inertial to viscous forces. *Journal of Fluid Mechanics*, *929*. https://doi.org/10.1017/jfm.2021.806

Kanoğlu, M., & Çengel, Y. A. (2020). APPENDIX 1: Property Tables (SI Units). In (1st Edition ed.). McGraw-Hill Education. https://www.accessengineeringlibrary.com/content/book/9781260459098/back-matter/appendix1

Kothandaraman, C. P., & Rudramoorthy, R. (2013). 10.2 Turbulent Flow. In *Fluid Mechanics and Machinery (3rd Edition)* (pp. 496). New Academic Science. https://app.knovel.com/hotlink/pdf/id:kt011NPQ51/fluid-mechanics-machinery/turbulent-flow

Kwon, S. B., Kim, M. C., & Lee, K. W. (2002). Effects of jet configuration on the performance of multi-nozzle impactors. *Journal of Aerosol Science*, *33*(6), 859-869. https://doi.org/https://doi.org/10.1016/S0021-8502(02)00040-X

Lee, S. H. (2016). Tuberculosis Infection and Latent Tuberculosis. *Tuberculosis and Respiratory Diseases*, *79*(4), 201. https://doi.org/10.4046/trd.2016.79.4.201

Maison, D. P. (2022). Tuberculosis pathophysiology and anti-VEGF intervention. *Journal of Clinical Tuberculosis and Other Mycobacterial Diseases*, *27*, 100300. https://doi.org/10.1016/j.jctube.2022.100300

Mamun, A., Blachowicz, T., & Sabantina, L. (2021). Electrospun Nanofiber Mats for Filtering Applications—Technology, Structure and Materials. *Polymers*, *13*(9), 1368. https://doi.org/10.3390/polym13091368

Marple, V. A., & Liu, B. Y. H. (1974). Characteristics of laminar jet impactors. *Environmental Science & Technology*, *8*(7), 648-654. https://doi.org/10.1021/es60092a003

Marple, V. A., Liu, B. Y. H., & Whitby, K. T. (1973). *Fluid mechanics of the laminar flow aerosol impactor*. https://digital.library.unt.edu/ark:/67531/metadc1034504/m1/1/

Marple, V. A., & Willeke, K. (1976). Impactor design. *Atmospheric Environment (1967)*, *10*(10), 891-896. https://doi.org/https://doi.org/10.1016/0004-6981(76)90144-X

McCreesh, N., & White, R. G. (2018). An explanation for the low proportion of tuberculosis that results from transmission between household and known social contacts. *Scientific Reports*, *8*(1). https://doi.org/10.1038/s41598-018-23797-2

Melsew, Y. A., Gambhir, M., Cheng, A. C., Mcbryde, E. S., Denholm, J. T., Tay, E. L., & Trauer, J. M. (2019). The role of super-spreading events in Mycobacterium tuberculosis transmission: evidence from contact tracing. *BMC Infectious Diseases*, *19*(1). https://doi.org/10.1186/s12879-019-3870-1

Mugenyi, N., Ssewante, N., Baruch Baluku, J., Bongomin, F., Mukenya Irene, M., Andama, A., & Byakika-Kibwika, P. (2024). Innovative laboratory methods for improved tuberculosis diagnosis and drug-susceptibility testing. *Frontiers in Tuberculosis*, *1*. https://doi.org/10.3389/ftubr.2023.1295979

Nakayama, Y. (2000). 10.4.1.2 Froude Number. In *Introduction to Fluid Mechanics (2nd Edition)* (pp. 208). Elsevier. https://app.knovel.com/hotlink/pdf/id:kt011PHBIP/introduction-fluid-mechanics/froude-number

Park, J.-C., Ito, T., Kim, K.-O., Kim, K.-W., Kim, B.-S., Khil, M.-S., Kim, H.-Y., & Kim, I.-S. (2010). Electrospun poly(vinyl alcohol) nanofibers: effects of degree of hydrolysis and enhanced water stability. *Polymer Journal*, *42*(3), 273-276. https://doi.org/10.1038/pj.2009.340

Patterson, B., Dinkele, R., Gessner, S., Morrowid, C., Kamariza, M., Bertozzi, C., Kamholz, A., Bryden, W., Call, C., Warner, D., & Wood, R. (2020). Sensitivity optimisation of tuberculosis bioaerosol sampling. *PloS one*, *15*. https://doi.org/10.1371/journal.pone.0238193

Patterson, B., Morrow, C., Singh, V., Moosa, A., Gqada, M., Woodward, J., Mizrahi, V., Bryden, W., Call, C., Patel, S., Warner, D., & Wood, R. (2018). Detection of Mycobacterium tuberculosis bacilli in bio-aerosols from untreated TB patients. *Gates Open Research*, *1*, 11. https://doi.org/10.12688/gatesopenres.12758.2

Peter, J. G., Theron, G., Singh, N., Singh, A., & Dheda, K. (2014). Sputum induction to aid diagnosis of smear-negative or sputum-scarce tuberculosis in adults in HIV-endemic settings. *European Respiratory Journal*, *43*(1), 185-194. https://doi.org/10.1183/09031936.00198012

Piccazzo, R., Paparo, F., & Garlaschi, G. (2014). Diagnostic Accuracy of Chest Radiography for the Diagnosis of Tuberculosis (TB) and Its Role in the Detection of Latent TB Infection: a Systematic Review. *The Journal of Rheumatology Supplement*, *91*(0), 32-40. https://doi.org/10.3899/jrheum.140100

Qiao, D., Tu, W., Zhong, L., Wang, Z., Zhang, B., & Jiang, F. (2019). Microstructure and Mechanical/Hydrophilic Features of Agar-Based Films Incorporated with Konjac Glucomannan. *Polymers*, *11*(12), 1952. https://doi.org/10.3390/polym11121952

Romay, F. J., & García-Ruiz, E. (2023). Design of Round-Nozzle Inertial Impactors Review with Updated Design Parameters. *Aerosol and Air Quality Research*, *23*(3), 220436. https://doi.org/10.4209/aaqr.220436

Rufino de Sousa, N., Sandström, N., Shen, L., Håkansson, K., Vezozzo, R., Udekwu, K., Croda, J., & Rothfuchs, A. (2019). A fieldable electrostatic air sampler enabling tuberculosis detection in bioaerosols. *Tuberculosis*, *120*, 101896. https://doi.org/10.1016/j.tube.2019.101896

Sakamoto, K. (2012). The Pathology of Mycobacterium tuberculosis Infection. *Veterinary Pathology*, *49*(3), 423-439. https://doi.org/10.1177/0300985811429313

Sakula, A. (1983). BCG: who were Calmette and Guerin? *Thorax*, *38*(11), 806-812. https://doi.org/10.1136/thx.38.11.806

Sakundarno, M., Nurjazuli, N., Jati, S. P., Sariningdyah, R., Purwadi, S., Alisjahbana, B., & Van Der Werf, M. J. (2009). Insufficient quality of sputum submitted for tuberculosis diagnosis and associated factors, in Klaten district, Indonesia. *BMC Pulmonary Medicine*, *9*(1), 16. https://doi.org/10.1186/1471-2466-9-16

Shah, W. (2016). To determine diagnostic accuracy of gene xpert and sputum Ziehl-Neelsen staining taking sputum culture as gold standard. *European Respiratory Journal*, *48*(suppl 60). https://doi.org/10.1183/13993003.congress-2016.PA2779

Silva Miranda, M., Breiman, A., Allain, S., Deknuydt, F., & Altare, F. (2012). The Tuberculous Granuloma: An Unsuccessful Host Defence Mechanism Providing a Safety Shelter for the Bacteria? *Clinical and Developmental Immunology*, *2012*, 1-14. https://doi.org/10.1155/2012/139127

Snieszko, S. F. (1974). The effects of environmental stress on outbreaks of infectious diseases of fishes. *Journal of Fish Biology*, *6*(2), 197-208. https://pubs.usgs.gov/publication/1014180

South African Department of Health. (2023). *TB Screening and Testing Standard Operating Procedure*. Retrieved from https://www.westerncape.gov.za/assets/departments/health/FP/tutt_circular_annexure_1_-_screening_testing_sop.pdf

Stein, R. A. (2011). Super-spreaders in infectious diseases. *International Journal of Infectious Diseases*, *15*(8), e510-e513. https://doi.org/10.1016/j.ijid.2010.06.020

Storla, D. G., Yimer, S., & Bjune, G. A. (2008). A systematic review of delay in the diagnosis and treatment of tuberculosis. *BMC Public Health*, *8*(1), 15. https://doi.org/10.1186/1471-2458-8-15

Sutthiwanjampa, C., Hong, S., Kim, W. J., Kang, S. H., & Park, H. (2023). Hydrophilic Modification Strategies to Enhance the Surface Biocompatibility of Poly(dimethylsiloxane)-Based Biomaterials for Medical Applications. *Advanced Materials Interfaces*, *10*(12), 2202333. https://doi.org/10.1002/admi.202202333

Svarovsy, L., & Thew, M. T. (1992). Hydrocyclones. *Fluid Mechanics and Its Applications*. https://doi.org/10.1007/978-94-015-7981-0

Teo, A. K. J., Maclean, E. L.-H., & Fox, G. J. (2024). Subclinical tuberculosis: a meta-analysis of prevalence and scoping review of definitions, prevalence and clinical characteristics. *European Respiratory Review*, *33*(172), 230208. https://doi.org/10.1183/16000617.0208-2023

Theron, G. A.-O., Limberis, J. A.-O., Venter, R. A.-O., Smith, L., Pietersen, E. A.-O., Esmail, A., Calligaro, G. A.-O., Te Riele, J., de Kock, M., van Helden, P., Gumbo, T., Clark, T. A.-O., Fennelly, K., Warren, R., & Dheda, K. A.-O. Bacterial and host determinants of cough aerosol culture positivity in patients with drug-resistant versus drug-susceptible tuberculosis. (1546-170X (Electronic)).

Van Cleeff, M., Kivihya-Ndugga, L., Meme, H., Odhiambo, J., & Klatser, P. (2005). The role and performance of chest X-ray for the diagnosis of tuberculosis: A cost-effectiveness analysis in Nairobi, Kenya. *BMC Infectious Diseases*, *5*(1). https://doi.org/10.1186/1471-2334-5-111

van Seventer, J. M., & Hochberg, N. S. (2017). Principles of Infectious Diseases: Transmission, Diagnosis, Prevention,

and Control. In *International Encyclopedia of Public Health* (2 ed., Vol. 6, pp. 22-26).

Vincent, J. H. (1995). 4.6 Impaction. In *Aerosol Science for Industrial Hygienists*. Elsevier. https://app.knovel.com/hotlink/pdf/id:kt00BY55S3/aerosol-science-industrial/impaction

Wahi, B. N., & Liu, B. Y. (1971). The mobility of polystyrene latex particles in the transition and the free molecular regimes. *Journal of Colloid and Interface Science*, *37*(2), 374-381.

Wang, Y., Ma, Z., Liu, Z., Dong, X., Shu, W., Wei, M., Cui, J., Shu, W., Li, R., Jing, W., Shi, J., Wang, B., Shen, D., Qin, C., Shao, R., Wan, Z., Wu, J., Luo, L., Huang, L., . . . Pang, Y. (2025). Tongue swab-based molecular diagnostics for pulmonary tuberculosis and drug resistance in adults: A prospective multicenter diagnostic accuracy study. *Journal of Infection*, *91*(1), 106517. https://doi.org/https://doi.org/10.1016/j.jinf.2025.106517

Williams, C. M., Abdulwhhab, M., Birring, S. S., De Kock, E., Garton, N. J., Townsend, E., Pareek, M., Al-Taie, A., Pan, J., Ganatra, R., Stoltz, A. C., Haldar, P., & Barer, M. R. (2020). Exhaled Mycobacterium tuberculosis output and detection of subclinical disease by face-mask sampling: prospective observational studies. *The Lancet Infectious Diseases*, *20*(5), 607-617. https://doi.org/10.1016/s1473-3099(19)30707-8

World Health Organisation. (2022). *Global Tuberculosis Report 2022*.

Wurie, F. B., Lawn, S. D., Booth, H., Sonnenberg, P., & Hayward, A. C. (2016). Bioaerosol production by patients with tuberculosis during normal tidal breathing: implications for transmission risk. *Thorax.*, *71*(6), 549-554. https://doi.org/10.1136/thoraxjnl-2015-207295

Yock, P. G. (2015). *Biodesign*. Cambridge University Press.

9 Appendices

9.1 Appendix A: Flow Simulations

Flow simulation setup & analysis can be seen in the images below

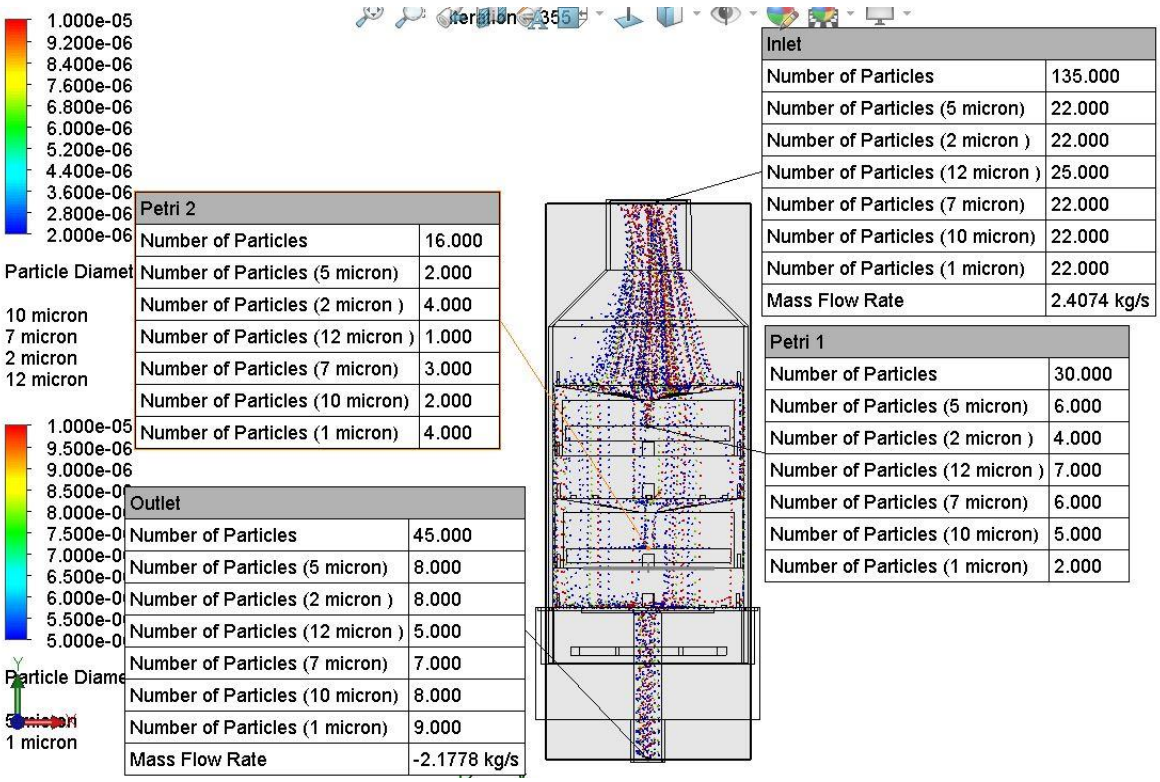

Petri 2	
Number of Particles	16.000
Number of Particles (5 micron)	2.000
Number of Particles (2 micron)	4.000
Number of Particles (12 micron)	1.000
Number of Particles (7 micron)	3.000
Number of Particles (10 micron)	2.000
Number of Particles (1 micron)	4.000

Outlet	
Number of Particles	45.000
Number of Particles (5 micron)	8.000
Number of Particles (2 micron)	8.000
Number of Particles (12 micron)	5.000
Number of Particles (7 micron)	7.000
Number of Particles (10 micron)	8.000
Number of Particles (1 micron)	9.000
Mass Flow Rate	-2.1778 kg/s

Inlet	
Number of Particles	135.000
Number of Particles (5 micron)	22.000
Number of Particles (2 micron)	22.000
Number of Particles (12 micron)	25.000
Number of Particles (7 micron)	22.000
Number of Particles (10 micron)	22.000
Number of Particles (1 micron)	22.000
Mass Flow Rate	2.4074 kg/s

Petri 1	
Number of Particles	30.000
Number of Particles (5 micron)	6.000
Number of Particles (2 micron)	4.000
Number of Particles (12 micron)	7.000
Number of Particles (7 micron)	6.000
Number of Particles (10 micron)	5.000
Number of Particles (1 micron)	2.000

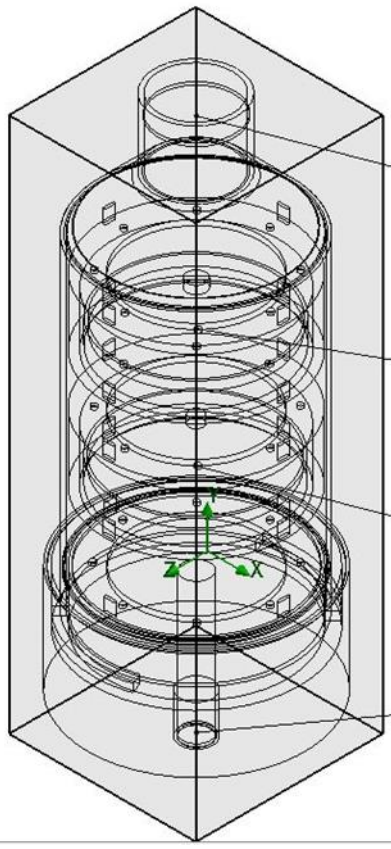

Inlet	
Number of Particles	38
Number of Particles (5 micron)	19
Number of Particles (10 micron)	19
Mass Flow Rate	0.0118 kg/s

Petri 1	
Number of Particles	16
Number of Particles (5 micron)	4
Number of Particles (10 micron)	12

Petri 2	
Number of Particles	0
Number of Particles (5 micron)	0
Number of Particles (10 micron)	0

Surface Parameters 4	
Number of Particles	1
Number of Particles (5 micron)	1
Number of Particles (10 micron)	0
Mass Flow Rate	-0.0016 kg/s

9.2 Appendix B: Device measurements

The weight of the major equipment is approximately 1kg as shown below.

Figure 9-1: Bottle weight

Figure 9-2: Pump weight

9.3 Appendix C: *FMEA*

FMEA Ranking Explanations

Ranking	Definition	Use and Design Clinical Effects; Process End Effects
5	Catastrophic	Serious injury (irreversible) or death of the patient or user; very severe negative effect on the environment.
4	Critical	Serious injury (reversible) to the patient or user; severe negative effect on the environment. Note: Any labeling issues that could lead to a field action must be ranked at a minimum of 4.
3	Moderate	Moderate injury to the patient or user; moderate negative effect on the environment. Decline of product performance or user confidence in the product/company (e.g. customer is very annoyed or dissatisfied).
2	Minor	Minor injury to the patient or user; minor negative effect on the environment. Slight decline of product performance or user confidence in the product/company (e.g. customer slightly annoyed or inconvenienced).
1	Negligible/ Cosmetic	No/virtually no injury to the patient or user; no/virtually no negative effect on the environment. No impact on product performance or user confidence in the product/company; user may or may not even notice the failure.

Ranking	Definition	Frequency
5	Up to 1 in 20 (5 %)	Very High
4	< 1 in 20 to > 1 in 400 (0.25 to 5 %)	High
3	< 1 in 400 to > 1 in 15,000	Moderate
2	< 1 in 15,000 to > 1 in 150,000	Low
1	< 1 in 150,000	Remote

Ranking	Definition	Design
5	Very High	Very unlikely that occurrence of failure will be detected – not seen or effect not seen
4	High	Low chance that occurrence of failure will be detected – not obvious or effect not obvious
3	Moderate	Moderate chance that occurrence of failure will be detected
2	Low	High chance that occurrence of failure will be detected – either obvious or effect obvious
1	Remote	Very likely that occurrence of failure will be detected

Product / Project: CASS	Date:	Revision:	Approved by / Date:
	12-Nov-22	1.0	Approved by / Date:
			Approved by / Date:

Comments:	> 60	Unacceptable, mitigation mandatory
	24 to 59	Mitigation required
	1 to 23	No Mitigation required

ID No.	HAZARD	POTENTIAL CAUSES	POTENTIAL EFFECTS	SEV	OCC	DET	RPN	Recommended Action(s)	SEV	OCC	DET	RPN	RECORD OF MITIGATION
Face Mask Component													
1	User error while wearing mask (mask not positioned correctly)	Improper instruction by technician.	Positive TB case goes undetected	4	3	4	**48**	provide clear instruction set with each mask purchase	4	2	2	**16**	Protocol document
2		Patient doesn't listen to technicians instruction		4	3	3	**36**	technician must monitor user	4	2	1	**8**	Protocol document
3	User hyperventilates	User is claustrophobic	User would experience discomfort	3	2	1	**6**	screen for claustrophobia and add disclaimer to accompanying mask documentation	3	2	1	**6**	Protocol document
4			User may forfeit the test	4	2	1	**8**	ask user to try mask on again after a break	3	2	1	**6**	Protocol document
5	Sharp edges of mask	Mask broken/faulty	User gets cut	3	2	4	**24**	add neoprene strips to all edges, file edges down	3	1	1	**3**	Design change
6	Electrocution	Exposed wire ends from a broken box	User gets shocked	3	2	4	**24**	use insulated wiring, add another layer of rubber insulation	3	1	4	**12**	Design change
7	Mask overheating and melting	Electrical shorting & mask left on for too long	User may be at risk of burning	2	2	3	**12**	technician must monitor when mask is on or off	2	1	3	**6**	Protocol document
8	Plastic/Neoprene Allergen	Allergic reaction	User develops rash/anaphalaxis	4	2	4	**32**	screen for allergies beforehand, have anti-histamine ready	4	1	1	**4**	Protocol document
9	Mask breaks	mask is dropped	Contamination of area with infectious bacterial material	3	2	1	**6**	quality check beforehand, carry out test in closed area	3	2	1	**6**	Protocol document, Test results
10		Faulty printed mask		3	1	5	**15**	quality check beforehand, carry out test in closed area	3	1	1	**3**	Protocol document, Test results
11		strap breaks		3	1	1	**3**	use a strong material for strap	3	1	1	**3**	Design change
ID No.	**HAZARD**	**POTENTIAL CAUSES**	**POTENTIAL EFFECTS**	**SEV**	**OCC**	**DET**	**RPN**	**Recommended Action(s)**	**SEV**	**OCC**	**DET**	**RPN**	**RECORD OF MITIGATION**

Sample Collection Component													
12	Fan falls onto mouth	Faulty screws break/come loose	Physical injury to user	2	1	5	**10**	use quality screws, technician should check mask before use	2	1	4	**8**	Protocol Document
13		Fan bracket breaks	Physical injury to user	2	2	5	**20**	make sure bracket is thick enough	2	1	5	**10**	Protocol document
14	Agar leaks from cascade	CASS dropped & cracked	Sample missing, failed diagnosis	4	1	5	**20**	ensure agar is is positioned properly before use	4	1	1	**4**	Quality Test, Protocol document
15	Choking/ingestion	User ingests PVA	Is non-toxic, but could get stuck in	3	1	2	**6**	Ensure PVA is fixed in place, test that it does not fall out if mask is turned upside down	3	1	1	**3**	Design change, testing
Power source													
18	Chemical Hazard	Battery leakage	Chemical burns	4	1	5	**20**	create battery enclosure	3	1	1	**3**	Quality Test
19	Electrical Hazard	Switch malfunction	Shock					co					
16	Pump failure	Electrical issue	May affect diagnosis	3	2	5	**30**	quality check fan beforehand	3	1	5	**15**	Quality Test
Wiring													
20	Choking hazard	Tubing gets wrapped around neck	Physical harm	4	1	1	**4**	show user how to position mask	3	1	1	**3**	Protocol Document
21	Electrical disconnection	Wire gets cut/wet	Device failure	3	2	5	**30**	Use two layers of insulation	2	1	1	**2**	Design change

9.4 Appendix D: Raw Particle Count Data

The table below shows the raw particle count data from the Lighthouse particle counter

Name	*0,3 µm*	*0,5 µm*	*1,0 µm*	*5,0 µm*	*10,0 µm*	*25,0 µm*
			no stages			
LOC001	1039728	933870	784214	94105	13611	41
LOC001	1288978	1149797	970675	104839	16302	58
LOC001	1271006	1141816	976264	155653	34928	47
LOC001	1316118	1186319	1020475	152453	29581	13
LOC001	1376611	1237863	1059028	163470	34556	88
mean	1258488	1129933	962131	134104	25796	49
std dev	128663	115979	105736	32093	10162	27
% std dev	10	10	11	24	39	55
			stage 2			
LOC001	1256875	1154679	1019774	187797	43544	57
LOC001	1257359	1157093	1022892	196991	48579	177
LOC001	1135048	1041151	909984	161403	38945	124
LOC001	1282622	1180003	1034140	195584	41329	104
LOC001	1212587	1115900	978249	200049	47661	169
mean	1228898	1129765	993008	188365	44012	126
std dev	58208	54626	51020	15735	4101	49
% std dev	5	5	5	8	9	39
# particles retained (from control)	29590	168	-30877	-54261	-18216	-77
% particles retained (from control)	2	0	-3	-40	-71	-155
			stage 1			
LOC001	1009042	915355	777044	119633	20606	62
LOC001	897221	798166	649062	63511	7588	3
LOC001	917479	825912	699339	114624	22513	5
LOC001	915667	819477	683887	85432	12942	33
LOC001	965332	865061	721073	93000	14572	26
mean	940948	827154	688340	89142	14404	17
std dev	45644	46264	47565	22796	6024	24
% std dev	5	6	7	26	42	144
#particles retained (from control)	317540	302779	273791	44962	11392	33

%particles retained (from control)	25	27	28	34	44	66
			Both stages			
LOC001	601698	525039	426535	31839	2271	1
LOC001	570013	493439	388377	22607	1849	17
LOC001	561739	488465	387273	24223	1902	5
LOC001	619237	540772	433887	26255	1964	15
LOC001	609155	527349	417313	24791	1808	5
mean	592368	515013	410677	25943	1959	9
std dev	25143	22839	21675	3545	184	7
%std dev	4	4	5	14	9	81
#particles retained (from control)	666120	614920	551454	108161	23837	41
%particles retained (from control)	52.9	54.4	57.3	80.7	92.4	82.6

9.5 Appendix E: Ethics Approval

UNIVERSITY OF CAPE TOWN
Faculty of Health Sciences
Human Research Ethics Committee

E52 Room 46 Old Main Building
Groote Schuur Hospital
Observatory 7925
Email: hrec-submissions@uct.ac.za
Website: www.health.uct.ac.za/fhs/research/humanethics/forms

15 March 2024

HREC REF: 192/2024

Prof S Sivarasu
Division of Biomedical Engineering
Department of Human Biology
PI Email: Sudesh.sivarasu@uct.ac.za
Student Email: ismrae003@myuct.ac.za

Dear Prof Sivarasu

PROJECT TITLE: MINI CASS - A NOVEL COUGH AEROSOL & INFECTIVITY SAMPLING DEVICE FOR SPUTUM-SCARCE INDIVIDUALS WITH TUBERCULOSIS (MSC IN BIOMEDICAL ENGINEERING CANDIDATE RA'EESAH ISMAIL)

Thank you for your request to review your proposal submitted to the Faculty of Health Sciences Human Research Ethics Committee.

The HREC has reviewed your proposal and confirms that no ethics is required for the above-mentioned study.

We note that this project is a proof of concept work that will be carried out using a lab strain of Mycobacterium smegmatis and Escherichia coli both of which are non-pathogenic.

The HREC acknowledges that the following MSc Candidate Ra'eesah Ismail is also involved in this project.

Please quote the HREC reference number 192/2024 in all your correspondence.

Yours sincerely

PROFESSOR MARC BLOCKMAN
CHAIRPERSON, FACULTY OF HEALTH SCIENCES HUMAN RESEARCH ETHICS COMMITTEE